

Accurate Cross-Layer Modelling and Evaluation of
IEEE 802.11e using a Differentiated p -Persistent
CSMA Protocol

Salim H. S. Abukharis

Submitted in accordance with the requirements for the degree
of Doctor of Philosophy

University of Sheffield

Department of Electronic and Electrical Engineering

June 2013

The candidate confirms that the work submitted is his own and that
appropriate credit has been given where reference has been made to
the work of others

Acknowledgements

I would like to thank Professor Timothy O'Farrell for his help, guidance and encouragement throughout my PhD study. Having a supervisor who is keen, encouraging and friendly has been a great asset in completing my thesis.

Special thanks go to thank Dr. Richard Mackenzie from BT for his continued help and co-operation. His detailed responses and feedback to my emails helped save me valuable time in the development of my thesis, and for that I am very grateful.

I am also grateful to the Ministry of Higher Education in Libya for their financial support.

I would like to thank all my fellow students, at both Swansea University and the University of Sheffield.

I would like to thank my wife and my sons, Hamouda, Muad and Malik, and all my family in Libya for their constant support, encouragement and love.

Above, all I thank God for giving me the encouragement, patience and power all the way through my life.

Abstract

With the extensive deployment of 802.11 wireless local area networks (WLANs) and the need for better quality of service (QoS), the 802.11e MAC with service differentiation was developed. In practical WLAN deployments, the capture effect has been shown to enhance the throughput performance of the network. Analysing the effect of fading and near-far effect on the performance of 802.11 is a fundamental consideration in practical situations since the wireless channels are error-prone. Developing an accurate closed form solution of the throughput/delay is a crucial task for the network planning and design. This thesis develops a physical/medium-access-control (PHY/MAC) cross-layer model to characterise the throughput and delay performance of WLANs in error-prone wireless environments. The developed model incorporates the capture effect and channel errors from the PHY-layer perspective, while from the MAC perspective the approach considers the QoS differentiated p -persistent CSMA protocol. This research develops PHY/MAC models that accurately calculate the saturated and non-saturated throughput/delay of p -persistent CSMA protocol with multiple traffic types which can be used to model 802.11e. The developed model expresses the saturated and non-saturated throughput/delay as a function of the number of terminals, packet error rates and capture threshold. The work shows that the PHY layer effects have a significant impact on the throughput/delay performance of WLANs and their dimensioning.

The anomaly effect also has a significant impact on performance of 802.11 WLANs which affects the calculation of the network capacity during the network planning phase. This research develops an adaptive QoS differentiated p -persistent CSMA protocol with multirate capability that can be used to resolve the *performance anomaly* of 802.11 DCF and 802.11e EDCA. The developed models can be applied to the QoS differentiated systems such as

802.11e EDCA with significantly less complexity than Markovian models. The adaptive protocol improves the network capacity which leads to more efficient network deployments in terms of capacity, spectral efficiency and energy consumption.

Table of Contents

Chapter 1: Introduction.....	1
1.1 Problem Definition.....	2
1.2 Thesis Objectives.....	3
1.3 Areas of Novelty and Originality.....	4
1.4 Thesis Structure.....	6
Chapter 2: Background and Literature review.....	8
2.1 Introduction.....	8
2.2 PHY Layer Overview.....	10
2.2.1 IEEE 802.11g System Overview.....	10
2.2.1.1 Principles of OFDM.....	12
2.2.2 IEEE 802.11n Overview.....	14
2.2.2.1 MIMO SYSTEMS.....	15
2.2.2.2 MIMO-OFDM.....	15
2.4 IEEE 802.11 MAC and IEEE 802.11e Overview.....	19
2.4.1 IEEE 802.11 MAC.....	19
2.4.2 IEEE 802.11e.....	20
2.4.3 EDCA protocol.....	21
2.5 Persistent CSMA protocol.....	23
2.6 Literature review.....	26
2.6.1 PHY/MAC Modelling.....	29
2.6.2 Multirate Modelling.....	35
2.7 Summary.....	37
Chapter 3: Saturated Throughput and Delay Analysis of p -persistent CSMA.....	39
3.1 System Model of p -persistent CSMA.....	40

3.2	Capture Model.....	41
3.3	Simulation Modelling of p -persistent CSMA protocol with PHY layer effects.....	45
3.4	p -Persistent CSMA protocol Throughput	48
3.4.1	Basic analysis of differentiated p -persistent CSMA protocol.....	48
3.4.2	Throughput analysis of p -persistent CSMA with PHY layer effects	51
3.5	Delay analysis of p -persistent CSMA protocol.....	53
3.5.1	Delay analysis of basic p -persistent CSMA protocol.....	53
3.5.2	Delay analysis of p -persistent CSMA with PHY layer effects.....	54
3.6	Numerical Results and Discussion.....	55
3.6.1	Throughput Results.....	55
3.6.2	Delay Results	62
3.7	WLAN Planning.....	64
3.8	Conclusions.....	65
Chapter 4: Non-Saturated Throughput and Delay Analysis of p -persistent CSMA.....		67
4.1	System Model of p -persistent CSMA protocol.....	68
4.2	Throughput analysis.....	69
4.2.1	Basic p -persistent CSMA.....	69
4.2.2	p -persistent CSMA with PHY layer effects.....	75
4.3	Delay Analysis of p -persistent CSMA with PHY Effects.....	79
4.4	Numerical results and discussion.....	83
4.4.1	Throughput Results.....	83
4.5	Delay Results	95
4.6	Adaptive p -persistent CSMA protocol.....	97
4.6.1	Limitations and Complexity of the Adaptive Protocol.....	101
4.7	WLAN Planning.....	101
4.7	Conclusions.....	102

Chapter 5: Modelling p -persistent CSMA protocol with Multirate Capability and PHY Layer Effects.....	104
5.1 System Model for p -persistent CSMA with Multirate.....	104
5.2 Throughput analysis of p -persistent CSMA with multirate.....	106
5.2.1 Basic p -persistent CSMA with Multirate.....	106
5.2.2 Multirate p -persistent CSMA with PHY layers effects.....	111
5.3 Delay analysis of p -persistent CSMA with Multirate.....	113
5.3.1 Basic p -persistent CSMA with Multirate.....	114
5.3.2 Multirate p -persistent CSMA with PHY Layer Effects.....	114
5.4 Adaptive Multirate p -persistent CSMA Protocol.....	115
5.5 Simulation Setup.....	118
5.6 Results and Discussions.....	118
5.6.1 Throughput Results.....	118
5.6.2 Delay Results.....	127
5.6.3 Adaptive Protocol Results.....	130
5.7 Enhanced Multirate Model.....	134
5.7.1 Model Description.....	134
5.7.2 Basic Throughput Analysis.....	135
5.7.3 Basic Delay Analysis	139
5.7.4 Throughput Analysis with PHY Effects.....	139
5.7.5 Delay analysis with PHY Effects.....	142
5.7.6 Results and Discussions.....	142
5.7.6 Adaptive Protocol Results for Enhanced Protocol.....	146
5.8 WLAN Planning.....	147
5.8 Conclusions.....	148
Chapter 6: Conclusions and Future Work.....	150
6.2 Summery and Discussion.....	151

6.3	Areas of Novelty and Originality.....	154
6.4	Final conclusions.....	155
6.5	Recommendations for Future Work.....	156
	Appendix A.....	158
	References.....	159

List of Tables

Table 2-1 : IEEE 802.11a/g Transmission Modes.....	12
Table 2-2: Channels between transmitting and receiving antennas.....	16
Table 2-3: The received signals at the two receive antennas.....	16
Table 3-1: p-persistent CSMA parameters	45
Table 3-2: MCS indexes for 2x2 IEEE 802.11g/n WLANs	47
Table 4-1: p-persistent CSMA parameters	84
Table 5-1: System simulation parameters of 802.11b/n	120

List of Figures

Figure 2-1 A schematic of the OFDM transmitter.....	14
Figure 2-2: Two-branch transmit diversity scheme with two receivers.....	17
Figure 2-3: STBC MIMO-OFDM (2×2) transmitter.....	19
Figure 2-4 : Transmission queues of EDCA.....	23
Figure 2-5: Non-persistent CSMA protocol.....	24
Figure 2-6: 1-persistent CSMA protocol.....	25
Figure 2-7: p-persistent CSMA protocol.....	26
Figure 3-1: Channel state cycle for saturated case.....	41
Figure 3-2: Capture probability as a function of colliding stations at different threshold (z) values. ..	44
Figure 3-3a: PER versus SNR for IEEE 802.11g in multipath channel	47
Figure 3-3b: PER versus SNR for IEEE 802.11n in multipath channel	48
Figure 3-4: Total throughput vs. number of stations with SNR as a parameter with $p_1=0.05$	56
Figure 3-5: Normalised throughput vs p_1 for 5 stations per traffic type comparing capture with basic mode.....	57
Figure 3-6: Throughput per access categories vs. number of stations with SNR as a parameter for capture threshold $z=5$ dB and $p_1=0.05$	58
Figure 3-7: Total saturated throughput vs. number of contending stations with capture threshold z as a parameter for SNR=8 dB and $p_1=0.05$	60
Figure 3-8: Saturated throughput vs. SNR for 802.11n and 802.11a/g with z as a parameter: 2 AC categories with $M_1=M_2=10$	61
Figure 3 9: Average Delay vs p_1 for 5 stations per traffic type with $z=5$ dB.....	63
Figure 3-10: Average delay vs number of stations with SNR as a parameter and $p_1=0.05$ and capture threshold $z =5$ dB.....	64
Figure 3-11: Saturated throughput per user as a function of number of user per traffic type with capture effect.....	65
Figure 4-1: p -persistent CSMA Channel state cycle for saturated case.....	69
Figure 4-2: Throughput with heterogeneous priorities at data rate 26 Mbit/s.....	84
Figure 4-3: Total throughput with heterogeneous traffic loads versus p values.....	85
Figure 4-4: Throughput versus offered load for 2 traffic types with heterogeneous priorities. $z=5$ dB, $p_1=0.1$, $p_2=0.05$ and $G_{r_1}=G_{r_2}=0.5$	86

Figure 4-5: Throughput versus offered load for 2 traffic types with heterogeneous offered loads. $z=5$ dB, $p_1=p_2=0.1$, $Gr_1=0.75$ and $Gr_2=0.25$	87
Figure 4-6a: Total throughput of 2 traffic types versus number of stations for varying of the offered load with $z=5$ dB, $p_1=p_2=0.1$, $Gr_1=0.75$ and $Gr_2=0.25$	88
Figure 4-6b: total throughput of 2 traffic types gain versus number of stations the with $z=5$ dB, $p_1=p_2=0.1$, $Gr_1=0.75$ and $Gr_2=0.25$	89
Figure 4-7a: Total throughput of 4 traffic types versus number of stations for varying of the offered load with $z=5$ dB, $p=[0.1, .1, .1 .1]$ and $Gr=[8/15, 4/15, 2/15, 1/15]$	89
Figure 4-7b: Total throughput gain of 4 traffic versus number of stations the percentage types with $z=5$ dB, $p=[0.1, 0.1, 0.1, 0.1]$ and $Gr=[8/15, 4/15, 2/15, 1/15]$	90
Figure 4-8: Throughput versus offered load for 4 traffic types with heterogeneous priorities. $z=5$ dB, $p=[0.1, 0.05, 0.025, .0125]$, and $Gr=[0.25, 0.25, 0.25, 0.25]$	91
Figure 4-9: Throughput versus offered load for 4 traffic types with heterogeneous offered loads. $z=5$ dB, $p=[0.1, 0.1, 0.1, 0.1]$ and $Gr=[8/15, 4/15, 2/15, 1/15]$	92
Figure 4-10 a: Non-saturated throughput of 4ACs vs.SNR for 802.11a/g with with $p=[0.1, 0.1, 0.1, 0.1]$ and $Gr=[8/15, 4/15, 2/15, 1/15]$	93
Figure 4-10b: Non-saturated throughput of 4ACs vs.SNR for 802.11a/g with with $p=[0.1, 0.1, 0.1, 0.1]$, $Gr=[8/15, 4/15, 2/15, 1/15]$ and $z=5$ dB.....	93
Figure 4-11a: Non-saturated throughput of 4ACs vs.SNR for 802.11n with $p=[0.1, 0.1, 0.1, 0.1]$ and $Gr=[8/15, 4/15, 2/15, 1/15]$	94
Figure 4-11 b: Non-saturated throughput of 4ACs vs.SNR for 802.11a/g with with $p=[0.1, 0.1, 0.1, 0.1]$, $Gr=[8/15, 4/15, 2/15, 1/15]$ and $z=5$ dB.....	94
Figure 4-12 : Normalised delay for 4 traffic types with heterogeneous traffic loads $Gr=[8/15, 4/15, 2/15, 1/15]$ and $p=[0.1, 0.1, 0.1, 0.1]$ with AC1 & AC2 have SNR=7dB.....	96
Figure 4-13: Normalised delay with heterogeneous traffic loads $Gr=[8/15, 4/15, 2/15, 1/15]$ and $p=[0.1, 0.1, 0.1, 0.1]$ at SNR=7 and 8 dB and $z=5$ dB.....	96
Figure 4-14: Throughput performance of the adaptive protocol with heterogonous loads $Gr=[0.25, 0.75]$, $p=[0.1, 0.05]$ and PER=0.....	100
Figure 4-15: Throughput performance of the adaptive protocol with heterogonous loads $Gr=[0.25, 0.75]$, $p=[0.1, 0.05]$ and PER=0.3.....	100
Figure 4-16: Non-saturated throughput per user as a function of number of users per traffic type with capture effect	102
Figure 5-1: Channel state cycle for saturated case with multirate	105
Figure 5-2a: Saturated throughput per group and traffic type of 802.11DCF and p-persistent CSMA respectively for 802.11b stations.....	120

Figure5 -2b: Saturated throughput per group and traffic type of 802.11DCF and p -persistent CSMA respectively for 802.11n stations.....	121
Figure 5-3: Throughput of stations transmitting at different data rates for 802.11n with different priorities.....	122
Figure 5-4 Throughput for stations of 4 traffic types with single rate and multirate scenarios and channel errors effect.....	123
Figure 5-5a: Throughput versus number of stations for 4 traffic types with single rate and multirate scenarios, $p_1=0.5$ and $z=5$ dB.....	125
Figure 5-5b: Total throughput versus number of stations for 4 traffic types with single rate and multirate scenarios, $p_1=0.5$ and $z=5$ dB	125
Figure 5-6: Total throughput versus number of stations for 4 traffic types with $p_1=0.5$, PER =0.06 and capture threshold z as parameter at different data rates	126
Figure 5-7 : Delay of stations for 4 ACs with single rate and multirate scenarios, $p_1=0.5$	127
Figure 5-8 Average delay of stations of 4 traffic types transmitting at different data rates.....	128
Figure 5-9 Average delay versus number of stations for 4 traffic types with $p_1=.05$ and $z=5$ dB at different data rates.....	129
Figure 5-10: Average delay versus number of stations for 4 traffic types with $p_1=0.5$, PER=0.06 and capture threshold z as parameter at different data rates	129
Figure 5 11: Throughput performance of the adaptive protocol for 2 access categories with 5 stations each and $p_1=0.03$ at different data rates.....	131
Figure 5-12: Average delay performance of the adaptive protocol for 2 access categories with 5 stations each and $p_1=0.03$ at different data rates.....	131
Figure 5-13: Throughput performance of the adaptive protocol for 5 station per 2 access with $p_1=0.03$ and α as a parameter.....	133
Figure 5-14: Average delay performance of the adaptive protocol for 5 stations per access category with $p_1=0.03$ and φ as a parameter.....	133
Figure 5-15: Channel state cycle for saturated case with multirate per station.....	135
Figure 5-16: Throughput of stations of 2 traffic types with 2 groups each transmitting at different data rates for 802.11n with different priorities and $p_1=0.03$	143
Figure 5-17: Average delay of stations of 2 traffic types with 2 groups each transmitting at different data rates for 802.11n with different priorities and $p_1=0.03$	144
Figure 5-18: Total throughput versus number of stations for 2 traffic types with 2 groups each and $p_1=0.5$, $z=5$ dB and PER as parameter at different data rates.....	145
Figure 5-19: Average delay versus number of stations for 2 traffic types with 2 groups each and $p_1=0.5$, $z=5$ dB and PER as parameter at different data rates.....	145

Figure 5-20: Throughput performance of the adaptive protocol for 2 AC with 5 station per group with $p_1=0.03$147

Figure 5-21: Saturated throughput per user as a function of number of user per traffic type with adaptive protocol.....148

List of Abbreviations

AC	Access Category
ACK	Acknowledgment
AIFS	Arbitration Interframe Space
AP	Access Point
BSS	Basic Service Set
BK	Background
BE	Best Efort
CS	Carrier Sense
CSMA	Carrier sense multiple access
CSMA/CA	Carrier sense multiple access with collision avoidance
CTS	Clear-To-Send
CW	Contention Window
D/A	Digital to Analogue Converter
DCF	Distributed Coordination Function
DIFS	DCF Interframe Space
EDCA	Enhanced Distribution Channel Access
ESS	Extended Service Set
EIFS	Extended Interfarme Space
GI	Guard Interval
HCF	Hybrid Coordination Function
HCCA	HCF Controlled Channel Access

IBSS	Independent Basic Service Set
IFFT	Inverse Fourier Fast Transform
IDFT	Inverse Discrete Fourier Transform
IPTV	Internet Protocol Television
ISI	Intersymbol Interference
S/P	Serial to Parallel converter
MAC	Medium Access Control
Mbit/s	Megabit(s) Per second
MIMO	Multiple-Input/Multiple-Output
MSDU	MAC Service Data Unit
OFDM	Orthogonal Frequency Division Multiplexing
PCF	Point Coordination Function
PER	Packet Error Rate
PHY	Physical Layer
PSK	Phase Shift Keying
QAM	Quadrature Amplitude Modulation
RF	Radio Frequency
RTS	Request-To-Send
s	Second
SIFS	Short Interframe Space
STBC	Space-Time Block Coding
TXOP	Transmit/Transmission Opportunity
VI	Video
VO	Voice

WLAN

Wireless Local Area Network

μ s

Microsecond(s)

List of Symbols

a	Timeslot length
b	Fraction of T that is useful data
b_1	Fraction of T_1 that is useful data (For type 1 transmissions)
$b_{1,1}$	Fraction of $T_{1,1}$ that is useful data (For group 1 of traffic type 1 transmissions)
B	Duration of a busy period
B^j	Duration of the j th busy subperiod
B_{phy}	Duration of the j th busy subperiod with PHY layer effects
CW	Contention window size
\bar{D}_1	Average delay for a type 1 packet
$\bar{D}_{1,phy}$	Average delay for a type 1 packet with PHY layer effects
$\bar{D}_{1,1}$	Average delay for a type 1 group1 packet
$\bar{D}_{1,1,phy}$	Average delay for a type 1 group1 with PHY layer effects
g_d	Offered load per timeslot for a type d station
g_1	Offered load per timeslot for a type 1 station
G	Normalised offered load in the system
Gr_d	Fraction of G that is for type d stations
I	Duration of an idle period
j	Index for busy subperiods in a busy period
J	Number of busy subperiods in a busy period
k	Index for timeslot boundaries
M_d	Number of type d stations in the system
M_1	Number of type 1 stations in the system

$M_{1,1}$	Number of type 1 group 1 stations in the system
$M_{1,\vartheta}$	Number of type 1 group ϑ stations in the system
$M_{d,\vartheta}$	Number of type d group ϑ stations in the system
$N_{0,1}^j$	Number of type 1 stations that accumulate a packet during B^j
$N_{k,d}^j$	Number of type d stations that accumulate a packet during X^j
p_1	Probability of transmitting a type 1 packet at the start of the timeslot
p_d	Probability of transmitting a type d packet at the start of the timeslot
p_l	Zero mean local power
p_0	Power of the wanted packet
p_i	Power of interfering packet i
p_s	Instantaneous power
P_{e1}	Probability of external collisions
P_{i1}	Probability of internal collisions
P_e^1	Type 1 packet probability error
P_e^d	Type d packet probability error
q_β	The probability that one out of β packets is captured by the AP
R	Deferral time in busy subperiod B
R^j	Deferral time in the j th busy subperiod B^j
R_d^j	Deferral time in busy subperiod B when only considering type d stations
R^{j*}	Deferral time in the j th busy subperiod B^j when considering all stations except for one type 1 station
S	Normalised total system throughput
S_1	Normalised type 1 throughput
S_{1abs}	Absolute type 1 throughput
$S_{1,1}$	Normalised type 1 group 1,1 throughput
$S_{1,\vartheta}$	Normalised type 1 group ϑ throughput

S_{phy}	Normalised total system throughput with PHY layer effects
$S_{1,phy}$	Normalised type 1 throughput with PHY layer effects
T	Transmission time in busy subperiod B
T_c	Time for a collided transmission in busy subperiod B
$T_{c,1}$	Time for a collided transmission for type 1 in busy subperiod B
$T_{c,d}$	Time for a collided transmission for type d in busy subperiod B
$T_{c,cap}$	Time for the total collided transmission in busy subperiod B with capture
$T_{c,1,1}$	Time for a collided transmission for type 1 group 1 in busy subperiod B
$T_{c,1,\vartheta}$	Time for a collided transmission for type 1 group ϑ in busy subperiod B
T_1	Packet duration of type 1
$T_{1,1}$	Packet duration of type 1 group 1
T_{max}	Maximum packet duration in the system
$T_{d,\vartheta}$	Packet duration of type d group ϑ
T_f	Time for a failure due to packet error rates
$T_{s,d}$	Time for a successful transmission for type d in busy subperiod B
T_s	Time for a successful transmission in busy subperiod B
$T_{s,1}$	Time for a successful transmission for type d in busy subperiod B
$T_{s,phy}$	Time for a successful transmission in busy subperiod B with PHY layer effects
$T_{s,1,\vartheta}$	Time for a successful transmission for type 1 group ϑ in busy subperiod B
$T_{s,1,1}$	Time for a successful transmission for type 1 group 1 in busy subperiod B
U	Time spent on successful transmissions during a busy subperiod
U_1	Time spent on successful type 1 transmissions during a busy subperiod
U_d	Time spent on successful type d transmissions during a busy subperiod

$U_{1,1}$	Time spent on successful type 1 group1 transmissions during a busy Subperiod
U_d^j	Time spent on successful type d transmissions during the j th busy subperiod
U_1^j	Time spent on successful type 1 transmissions during the j th busy subperiod
$U_{1,phy}^j$	Time spent on successful type 1 transmissions during the j th busy subperiod with PHY layer effects
$U_{1,1,phy}$	Time spent on successful type 1 group1 transmissions during a busy subperiod with PHY layer effects
X_j	Packet accumulation time for the j th busy subperiod to occur
z	Capture threshold
φ	Scaling factor
β	Total number of the stations in the system
γ	Path loss exponent
ϑ	Group number index

Chapter 1

Introduction

In the last decade there has been a wide spread deployment of IEEE 802.11 Wireless Local Area Networks (WLANs) which has resulted in an increased demand for various wireless services supporting data, voice, and video which require better quality of service (QoS). In order to meet this demand, the 802.11e medium access control (MAC) with service differentiation has been introduced [1]. The MAC protocol used in IEEE 802.11 WLANs is called distributed coordination function (DCF) [2]. It is a random access scheme based on the carrier sense multiple access with collision avoidance (CSMA/CA) protocol.

Since 2000 over 5 billion WLAN (Wi-Fi) enabled devices have been shipped. The number of devices shipped in 2012 exceeded 1.5 billion alone and is expected to exceed 1.9 billion in 2014. This growth is across many markets, including mobile handsets, laptops, media tablets, printers and TVs [3]. The rapid increase in the demand of WLAN enabled devices made the installers typically focus on ensuring the coverage, rather than the capacity or quality of service. Thus, WLAN users usually experience significant performance and reliability issues. WLAN deployment is considered more complicated than wired network deployment due to the use of radio frequency (RF) links. Each location has its own RF characteristics and thus unexpected radio interference needs to be mitigated. In general, in order to deploy WLANs, five key issues need to be addressed: coverage, capacity, security, mobility and QoS [4].

Many research studies have focused on improving the throughput and delay performance of wireless networks in the context of IEEE 802.11 WLAN. Bianchi in [5] provided an analytical model of saturation throughput performance of IEEE 802.11 that applies to DCF. Since the throughput is considered to be the key factor for efficient WLAN design and planning, this motivated many researchers to develop more accurate approaches to calculate the throughput of WLANs.

1.1 Problem Definition

In wireless networks, a packet collision does not necessarily mean all the simultaneously transmitted packets are being destroyed. Depending on the relative signal power and the arrival time of the involved packets in the collision, some of these packets can be received successfully if the received power to interference ratio is greater than a certain value, called a threshold. This phenomenon is called the capture effect. In practical WLAN deployments, the capture effect has been shown to enhance the performance of the system throughput and delay performance.

In general, higher capacity WLANs come at the expense of less coverage area of the access point (AP). One of the key parameters that determine the capacity is the minimum association rate between the AP and the stations. The minimum association rate is set to prevent edge users from associating with an AP at low data rates, which results in low overall network capacity. This phenomenon is known as the *performance anomaly*. The minimum association rate is one of the main parameters that determine the number of APs required from the capacity standpoint. These two phenomena are discussed in more detail in chapter 2.

The vast majority of existing studies that have investigated the capture effect and minimum associated rate consider the 802.11 DCF. Very few studies consider the 802.11e due to the analytical complexity of the Markov chain approach. There is an urgent need for a new

analytical approach to modelling 802.11e which is both computationally efficient and accurate. In order to efficiently design and deploy WLANs the throughput/delay performance should be calculated accurately in a realistic environment. To the best of our knowledge none of the previous studies have investigated the combined packet error rate and capture effects for QoS differentiated WLANs in both saturated and non-saturated networks. Similarly, modelling the multirate capability of the WLANs has not been considered by any previous studies for the case of QoS differentiation.

1.2 Thesis Objectives

In this thesis the primary aim is to develop a more realistic model that calculates the throughput and delay of a QoS differentiated p -persistent CSMA protocol that can be applied to the evaluation of 802.11e EDCA. This is achieved by including the PHY layer effects in terms of packet error rates and capture effect. In other words, a cross-layer, MAC/PHY approach is developed to evaluate both the saturated and non-saturated throughput/delay performance of p -persistent CSMA protocol with QoS differentiations. The second aim of this thesis is to model the multirate capability of 802.11 WLANs and provide a mechanism to resolve the anomaly issue which significantly reduces the network performance. This modelling is based on the p -persistent CSMA protocol with differentiated QoS. The anomaly issue is also investigated in the presence of PHY layer effects. A cross-layer approach is also developed to evaluate the saturated throughput/delay of the QoS differentiated p -persistent CSMA protocol with multirate capability as a means of accurately modelling 802.11 WLANs.

The overall goal of this study is to develop more realistic models (PHY/MAC) that can be used to evaluate the QoS differentiated p -persistent CSMA protocol that can be applied in 802.11e which leads to more efficient WLAN planning and deployment in terms of the

network capacity, coverage and energy efficiency. In order to achieve this major goal, 4 measurable objectives, listed below, have been identified.

1. Creating an analytical closed form solution to model a PHY/MAC cross-layer approach that can accurately calculate saturated throughput/delay of the QoS differentiated p -persistent CSMA protocol
2. Developing an analytical closed form solution to model a PHY/MAC cross-layer approach which accurately calculates non-saturated throughput/delay of the QoS differentiated p -persistent CSMA protocol.
3. Modelling and analysing the saturated throughput/delay of QoS differentiated p -persistent CSMA protocol with multirate capability which quantifies the anomaly issue in WLANs. Developing the PHY/MAC cross-layer approach for the case of multirate.
4. Introducing the p -persistent CSMA protocol as a solution for the anomaly issue in the QoS differentiated WLANs.

1.3 Areas of Novelty and Originality

The primary goal of this research work was to develop more realistic models of the throughput and delay of the 802.11e EDCA protocol using the p -persistent CSMA protocol and can be applied. The throughput and delay are the most important elements for efficient WLAN planning and design. The work in this thesis shows the QoS differentiated p -persistent CSMA can be effectively used to mitigate the anomaly performance of WLANs. To conclude this chapter, the areas of original work within this research are listed below:

1. The straightforward time-domain analysis of the new PHY/MAC cross-layer approach, which calculates the saturated throughput/delay of p -persistent CSMA

allows for accurate characterisation of the network performance in a practical environment. This approach can be applied to systems with a QoS differentiation such as 802.11e EDCA networks by use of a fixed window size with less complexity than the Markovian models.

2. The numerical results of the analytical approach stated in 1 were validated by developing a MATLAB simulator. The results showed an excellent agreement between the simulation and the analytical models.
3. The new non-saturated form of p -persistent CSMA analysis with PHY layer effects enables the accurate evaluation of the throughput/delay performance of a non-saturated network with heterogeneous priorities and heterogeneous loads accurately in a realistic environment. This is the first time-domain analysis of a QoS differentiated p -persistent CSMA with PHY layer effects.
4. The new saturated form of a QoS differentiated p -persistent CSMA analysis with multirate capability allows for evaluating the *performance anomaly* of WLANs.
5. The multirate model was extended to include the PHY layer effects which allows for evaluating the anomaly performance accurately and in a realistic environment.
6. The multirate model was improved to a more general model where each station can have its own transmission rate regardless of its traffic type. This model was then extended to include the PHY layer effects.
7. An adaptive p -persistent CSMA protocol was introduced as a solution to the anomaly issue in the QoS differentiated WLANs. The protocol effectively mitigated the anomaly issue and improves the performance of the high priority traffic type. The adaptive protocol also enhances the network capacity and leads to more efficient network planning and deployment.

1.4 Thesis Structure

This section provides an overview of the content of the thesis. In chapter 2, a review of the PHY and MAC protocols relevant to the thesis is given. This includes 802.11g, 802.11n, 802.11 DCF, 802.11e EDCA. The persistent CSMA protocol is also discussed. A literature review of the relevant research is provided. This includes PHY/MAC cross-layer approaches for both saturated and non-saturated cases that have been developed recently and studies that have been investigated and modelled the anomaly issue in WLANs. This section emphasises the necessity of the research done in this thesis.

Chapter 3 provides a cross-layer investigation of the saturated throughput and delay of QoS differentiated systems. This is based on the p -persistent CSMA protocol. The PHY layer effects include the packet error rates and capture effect. In this chapter it is demonstrated how the accuracy of calculating the system throughput/delay performance is improved by including the PHY layer effects.

Chapter 4 develops the model presented in chapter 3 into a more realistic and challenging model by considering the non-saturated throughput and delay for QoS differentiated p -persistent CSMA protocol. In this chapter a cross-layer approach is also presented to evaluate the system throughput and delay performance with packet error rates and the capture effect. An adaptive protocol is presented to alleviate the packet error rate effect for the case of single rate (i.e. no link-adaptation mechanism). A network planning case is also demonstrated.

Chapter 5 investigates the *performance anomaly* issue in WLANs. A saturated form of analysis for the QoS differentiated p -persistent CSMA with multirate capability is derived. The PHY layer effects in terms of packet error rates and capture effect is also incorporated into the analysis. In this chapter the p -persistent CSMA protocol is introduced as a solution to the anomaly issue by replacing EDCA.

Finally, in chapter 6 a summary of the work covered in this thesis is presented and the main conclusions are provided. This chapter also outlines some potential areas for future work based on the results provided in the thesis.

Chapter 2

Background and Literature Review

2.1 Introduction

IEEE 802.11 wireless local area networks (WLANs) [2] have been widely deployed for Internet access. The legacy 802.11a/g standards can support up to 54 Mbit/s data rate [6]. In order to meet the increased demand of multimedia services such as streaming video and IP telephony, IEEE 802.11n was proposed as an amendment to the previous 802.11 standard to improve network throughput, aiming to provide data transmission rates of up to 600 Mbit/s. The version 9.0 draft specification was approved in March 2009 and it contains substantial enhancements for both the physical (PHY) and medium access control (MAC) layers for high throughput, efficiency and robustness [7]. The 802.11n, based on the Multiple Input Multiple Output - Orthogonal Frequency Division Multiplexing (MIMO-OFDM) technique, which employs multiplexing technique to transmit two or more data streams simultaneously. MIMO is a signal processing technique for transmitting multiple data streams through multiple antennas to improve the spectral efficiency, achieving higher data rate, and range extension. The increase in 802.11n physical layer rates and Internet connection speeds has led to many multimedia applications with different quality of service (QoS) requirements. Many video applications are now available such as YouTube, video conferencing and Internet Protocol Television (IPTV) in standard and high definition. Amendment 802.11e addressed

the need for improved quality of service (QoS) over these, previously best effort, networks [1]. The IEEE 802.11 scheme specifies a physical layer and a medium access control (MAC) protocol for channel access [2]. The IEEE 802.11 standard supports two services: Distributed coordination function (DCF) and point coordination function (PCF). In the DCF, wireless stations have to contend for to gain access to the channel at every attempt to transmit a packet. In the PCF (optional) mode, gaining the access to the channel is controlled by the Access Point (AP), polling the stations to access the medium, thus eliminating the need for contentions. The MAC layer enhancements specified includes enhanced distributed channel access (EDCA) which provides service differentiation, thus allowing for traffic with different QoS requirements to gain differential treatment. The EDCA parameters can be adjusted which can allow for the system throughput to be maximised and also for a desired level of service differentiation to be achieved.

This chapter provides the relevant background information required for the reader to gain a good understanding of the work carried out in this thesis. The background section provides an overview of IEEE 802.11g/n, an overview of IEEE 802.11/802.11e contention based access and persistent CSMA protocols. The section which follows the background is a literature review which is divided into three main parts. The first part of the literature review presents a broad review of the research carried out in the field of modelling 802.11 DCF and 802.11e EDCA. The other two parts are more focused on the areas of research the work in this thesis is based upon. These are used to highlight the gaps in the existing research that have motivated the work presented in this thesis. The second part focuses on the saturated and non-saturated throughput/delay analysis of WLANs in the presence of PHY layer effects. The third part focuses on the performance anomaly in WLANs and clearly shows a lack of modelling on this issue in a QoS differentiated systems such as 802.11e.

This chapter is organized as follows: Sections 2.2 and 2.3 of this chapter give an overview of the IEEE 802.11g and 802.11n WLAN physical layer, respectively. An overview of the 802.11e MAC is presented in section 2.3. The p -persistent CSMA protocol is discussed in section 2.5. An extensive literature review is presented in section 2.6 to highlight the gaps in the research that have motivated the work carried out in this thesis. Finally, Section 2.7 presents the conclusions that are reached in this chapter.

2.2 PHY Layer Overview

In this section, the IEEE 802.11g/n system overview is presented and the principles of OFDM and MIMO-OFDM are discussed.

2.2.1 IEEE 802.11g System Overview

IEEE 802.11g is an enhancement of the 802.11b standard [6], allowing transmission rates up to 54 Mbps over the 2.4 GHz ISM band by using the same baseband radio modulation as in 802.11a (i.e. COFDM). 802.11g uses three non-overlapping frequency channels which is the same as in 802.11b.

A wireless LAN can operate in one of two modes, an Ad-Hoc mode and an infrastructure mode. The Ad-Hoc mode is also called the peer-to-peer mode or an Independent Basic Service Set (IBSS). It requires a minimum of two PCs equipped with wireless adapter cards to form a peer-to-peer network, enabling the PCs to share resources. This type of network requires no access point, administration or pre-configuration. Ad-Hoc networks are most useful for a group of devices that only need to communicate with each other [8].

The infrastructure mode is the most common type of WLAN configuration. A WLAN operating in the infrastructure mode generally consists of at least one access point (AP) connected to the wired network infrastructure and a set of wireless end-stations. This configuration is called a Basic Service Set (BSS). An Extended Service Set (ESS) consists of

two or more BSSs forming a single sub-network. The access points allow wireless clients to join a wired network almost as if connected directly by cable. Some access points can act as routers or firewalls, which is often the case in home networks. The infrastructure mode is an easy way to add wireless devices to an existing network [8] because it keeps complexity and costs low.

The 802.11a/g physical layer is based on the use of COFDM [6, 9] and the OFDM modulation is implemented by means of an inverse fast Fourier transform (IFFT) [10, 11]. In the 802.11g specification, the guard interval is set to $0.8 \mu\text{s}$ and the OFDM symbol (i.e. guard interval and data payload) duration is set to $4 \mu\text{s}$ with sub-carrier spacing at 312.5 KHz. The OFDM waveform is sampled at a rate of $f_s = 20 \text{ MHz}$, resulting in a sampled symbol length of $L=80$ samples. Out of 64 possible sub-carriers, within an IFFT window length only 52 sub-carriers are used; 48 sub-carriers for data transmission and 4 sub-carriers for pilot symbols. The remaining unused sub-carriers are zero-padded in order to perform fast Fourier transform (FFT) at the receiver. The convolutional channel encoder uses the industry-standard generator polynomial [133,171] with a constraint length of 7 and a base coding rate of 1/2. Optional coding rates of 2/3 and 3/4 are obtained by puncturing [6]. Various combinations of coding rate and modulation order are specified to facilitate 8 different modes of transmission; these eight modes are summarised in Table 2-1.

Table 2-1 IEEE 802.11a/g Transmission Modes

Mode	Modulation Scheme	Coding Rate	Data Rate
1	BPSK	1/2	6 Mb/s
2	BPSK	3/4	9 Mb/s
3	QPSK	1/2	12 Mb/s
4	QPSK	3/4	18 Mb/s
5	16QAM	1/2	24 Mb/s
6	16QAM	3/4	36 Mb/s
7	64QAM	2/3	48 Mb/s
8	64QAM	3/4	54 Mb/s

2.2.1.1 Principles of OFDM

OFDM signalling schemes have been widely used in both wired and wireless telecommunications technologies. This increasing use of OFDM is due to the fact that it is an efficient scheme for transmission in a frequency-selective fading channel without requiring the use of complex equalization techniques [10,12].

Unlike conventional multi-carrier communication schemes where the spectrum of each sub-carrier is non-overlapping and bandpass filtering is used to extract the frequency of interest, in OFDM the frequency spacing between sub-carriers is selected such that the sub-carriers are mathematically orthogonal to each other. The spectra of sub-carriers overlap each other but individual sub-carriers can be extracted by baseband processing. This overlapping spectral property of OFDM makes it more spectrally efficient than the conventional multi-carrier communication schemes that do not use overlapping.

A baseband OFDM symbol can be generated in the digital domain before modulating a radio frequency carrier for transmission. To generate a baseband OFDM symbol, a series of digitized data symbol-streams are obtained from a suitable bit-to-symbol mapping constellation scheme, such as phase shift keying (PSK) or quadrature amplitude modulation (QAM). These data symbols are then converted from serial-to-parallel (S/P) before modulating the sub-carriers. Sub-carriers are sampled at a sampling rate of N/T_{sym} , where N is the number of sub-carriers and T_{sym} is the OFDM symbol duration. The frequency separation between two adjacent sub-carriers is $2\pi/N$. Finally, the samples from each sub-carrier are summed together to form an OFDM symbol. An OFDM symbol generated by an N -subcarrier OFDM system consists of N samples and the m -th sample of an OFDM symbol is given by (2-1) as in [12,13].

$$x_m = \sum_{n=0}^{N-1} X_n \exp\left\{-j \frac{2\pi mn}{N}\right\}, \quad 0 \leq m \leq N-1 \quad (2-1)$$

X_n is the transmitted complex data symbol on the n -th sub-carrier. Equation (2-1) is equivalent to the N -point inverse discrete Fourier transform (IDFT) operation on the data sequence with the omission of a scaling factor. The IDFT can be implemented efficiently using the IFFT when N is power of 2 [14]. Therefore, in practice, the IFFT is performed on the data sequence at an OFDM transmitter to generate the baseband time domain waveform and the FFT is performed at the receiver to generate the frequency domain signal. Finally, a baseband OFDM symbol is modulated by a radio frequency carrier to become a bandpass signal for transmission. In the frequency domain, this corresponds to translating all the sub-carriers from baseband to the carrier frequency simultaneously [15]. Figure 2-1 shows a

schematic of OFDM transmitter. In Figure 2-1, the P/S refers to converting the signal from parallel to serial and D/A refers to digital to analogue conversion.

By transmitting information on N sub-carriers, the symbol duration of an OFDM signal is N times longer than the symbol duration of an equivalent single-carrier signal. This property reduces the intersymbol interference (ISI) effects introduced by a linear time dispersive channel on individual subchannels. In order to eliminate ISI between OFDM symbols completely, a guard interval (GI) of time is inserted of a duration longer than that of the impulse response of the multipath channel [11, 15].

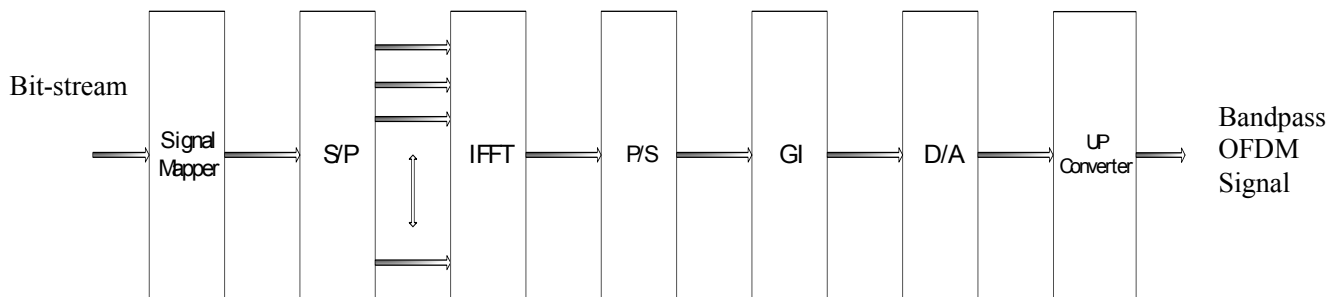


Figure 2-1 A schematic of the OFDM transmitter

2.2.2 IEEE 802.11n Overview

In January 2004 IEEE announced that it had formed a new 802.11 Task Group N (TGn) to develop a new amendment to the 802.11 standard for wireless local-area networks [16]. TGn's goal was to achieve 100 Mbit/s net throughput, after subtracting all the overhead for protocol management features like preambles, interframe spacing, and acknowledgments. The IEEE 802.11n standard [7] specifies a Multiple-Input/Multiple-Output (MIMO) based physical layer. MIMO is a signal processing technique for transmitting multiple data streams

through multiple antennas for better spectral efficiency, higher data rate, and range extension. Independent streams are sent at each antenna. Therefore, the diversity order (number of different paths available) increases by a factor equal to the number of streams. The IEEE 802.11n standard uses spatial multiplexing in conjunction with Orthogonal Frequency Division Multiplexing (OFDM) to achieve this.

2.2.2.1 MIMO SYSTEMS

The New 802.11n standard builds upon previous 802.11 standards especially 802.11a, by adding MIMO operation. Space-time block coding (STBC) is a technique used in wireless communications to transmit multiple copies of a data channel stream across a number of antennas and to exploit the received versions of the data to improve the reliability of data-transfer. The fact that transmitted data must traverse potentially difficult environments with scattering, reflection, refraction and so on as well as be corrupted by thermal noise in the receiver means that some of the received copies of data will be 'better' than others. The STBC mode 2X2 is also known as the Alamouti algorithm [17] which is used in 802.11n and is described below.

At a given time symbol period, two signals are simultaneously transmitted from two antennas. Figure 2-2 shows the Alamouti algorithm for two transmitting and two receiving antennas. Table 2-2 defines the channels between the transmitting and receiving antennas, and Table 2-3 defines the received signal at the two receive antennas

Table 2-2: Channels between transmitting and receiving antennas

	r_x antenna 0	r_x antenna 1
t_x antenna 0	h_0	h_2
t_x antenna 1	h_1	h_3

Table 2-3: The received signals at the two receive antennas

	r_x antenna 0	r_x antenna 1
Time t	r_0	r_2
Time $t+T$	r_1	r_3

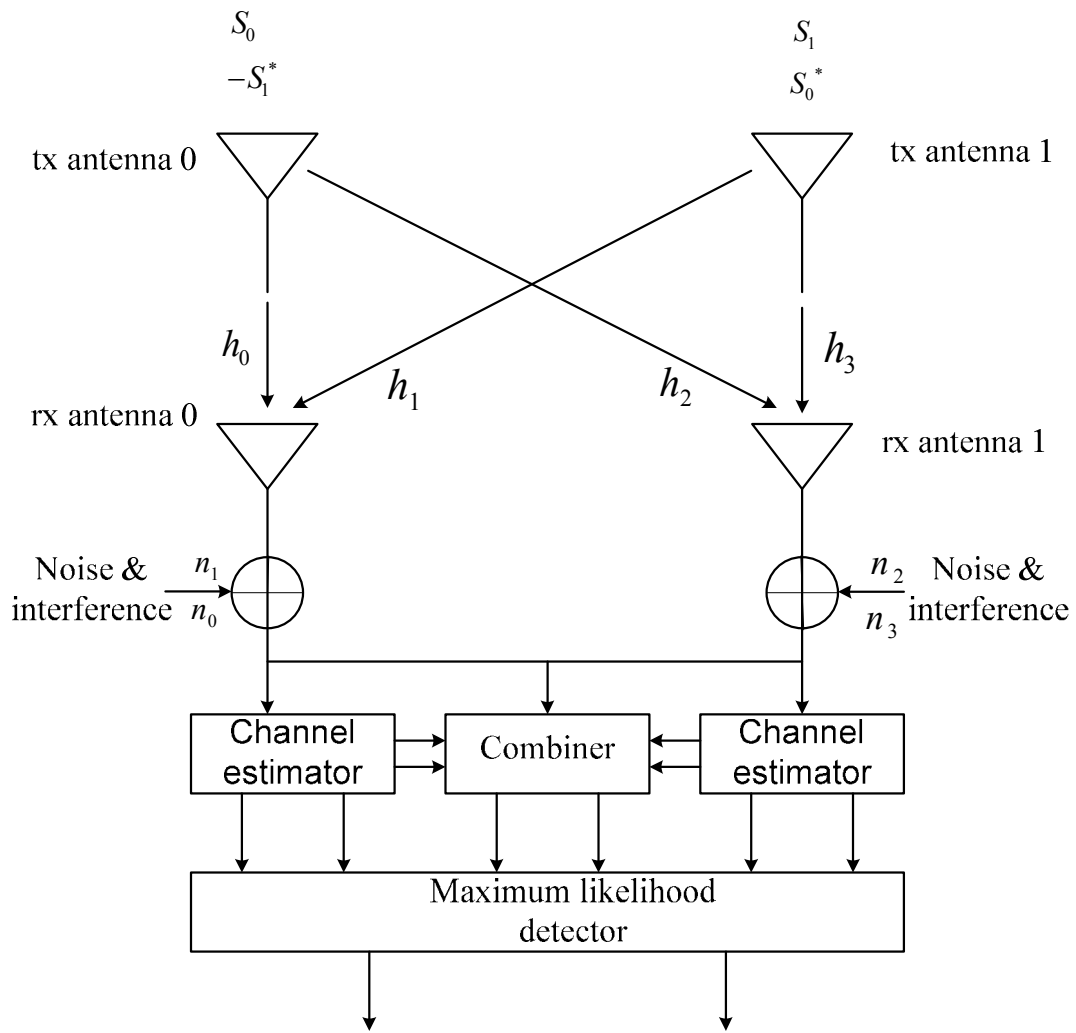


Figure 2-2: Two-branch transmit diversity scheme with two receivers

The notation of the received signals is defined in the Table 2-4 and are expressed below where.

$$r_0 = h_0 s_0 + h_1 s_1 + n_0 \quad 2-2$$

$$r_1 = -h_0 s_1^* + h_1 s_0^* + n_1 \quad 2-3$$

$$r_2 = h_2 s_0 + h_3 s_1 + n_2 \quad 2-4$$

$$r_3 = -h_2 s_1^* + h_3 s_0^* + n_3$$

Where n_0, n_1, n_2 and n_3 are representing the additive white Gaussian noise (AWGN) at the receiver. The combiner in Figure 2-2 builds the following two signals that are sent to the maximum likelihood detector:

$$\tilde{s}_0 = h_0^* r_0 + h_1 r_1^* + h_2^* r_2 + h_3 r_3^* \quad (2-6)$$

$$\tilde{s}_1 = h_1^* r_0 - h_0 r_1^* + h_3^* r_2 - h_2 r_3^* \quad (2-7)$$

2.2.2.2 MIMO-OFDM

Figure 2-3 illustrates the general block diagram of a STBC MIMO-OFDM transmitter. Baseband modulated symbols are passed through serial-to-parallel (S/P) converter which generates complex vector X of size N . The complex vector, X is then passed through the STBC encoder (2×2) which generates two sequences S_0 and S_1 . Both these sequences are then passed through each IFFT block for antenna 0 and antenna 1 respectively. These sequences converted back to serial and the guard interval is inserted to be ready for transmission through antenna 0 and antenna 1. The STBC achieves a full diversity gain by implementing the maximum-likelihood (ML) decoding algorithm. According to [17], the 2×2 orthogonal STBC can be defined as in (2-8). The baseband STBC MIMO-OFDM signal for antenna i with N subcarriers is shown in (2-9) [18].

$$X = \begin{bmatrix} S_0 & -S_1^* \\ S_1 & S_0^* \end{bmatrix} \quad (2-8)$$

$$\hat{x}_{n,i} = \frac{1}{\sqrt{N}} \sum_{k=0}^{N-1} S_{k,i} e^{j \frac{2\pi n k}{N}} \quad n = 0, 1, 2, \dots, N-1 \quad (2-9)$$

Where ($i = 0, 1$) denote the antenna number.

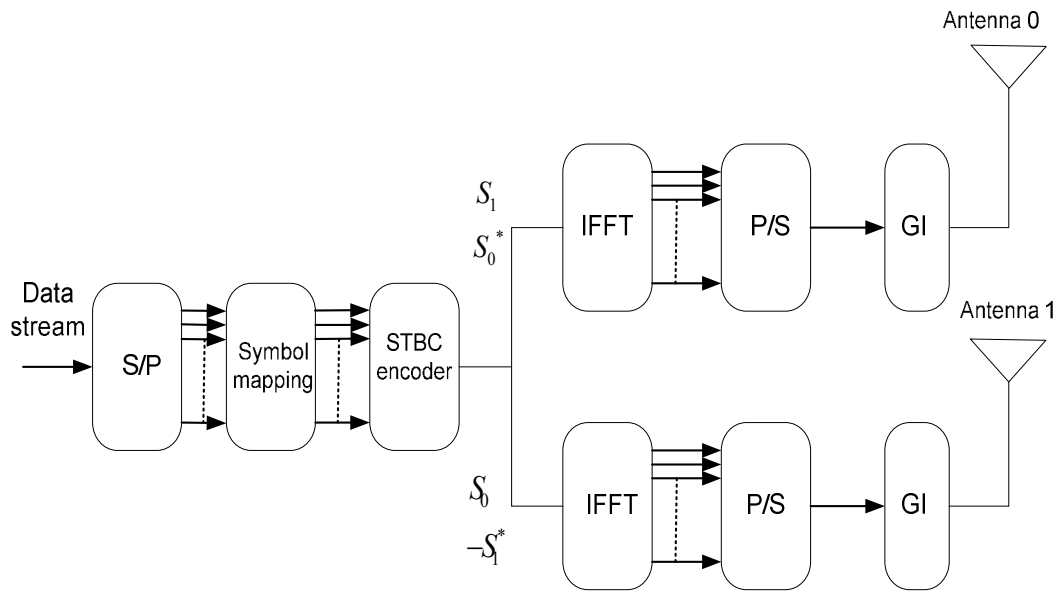


Figure 2-3: STBC MIMO-OFDM (2×2) transmitter

2.3 IEEE 802.11 MAC and IEEE 802.11e Overview

The IEEE 802.11 standard covers the MAC (Medium Access Control) sub-layer and the physical layer, in this section a general description of the MAC part will be given.

2.3.1 IEEE 802.11 MAC

The IEEE 802.11 standard supports two services: Distributed coordination function (DCF) and point coordination function (PCF). In the first mode, wireless stations have to contend for use of the channel at each data packet transmission. In the second (optional) mode, the medium usage is controlled by the Access Point (AP), polling the stations to access the medium, thus eliminating the need for contentions.

The DCF is the basic medium access mechanism of IEEE 802.11, and uses a carrier sense multiple access collision avoidance (CSMA/CA) algorithm to mediate the access to the shared medium. It includes a basic access method and optional channel access methods with

request-to-send (RTS) and clear-to-send (CTS). In this section we explain the basic access method only.

If the channel is busy for the source station, a backoff time (measured in slot times) is chosen randomly in the interval $[0, CW)$, where CW stands for the contention window. This timer is decremented by one as long as the channel is sensed idle for a DIFS, i.e. Distributed Inter Frame Space time. A DIFS period is equal to $SIFS + 2 \times SlotTime$ where SIFS is Short Inter Frame Space. It stops when the channel is busy and resumes when the channel is idle again for at least a DIFS period. CW is an integer whose range is determined by the PHY layer characteristics: CW_{min} and CW_{max} . CW is doubled after each unsuccessful transmission, up to the maximum value which is determined by $CW_{max} + 1$. When the backoff timer reaches zero, the source transmits the data packet. The acknowledgment (ACK) is transmitted by the receiver immediately after SIFS interval which is less than a DIFS. When a data packet is transmitted, all other stations hearing this transmission adjust their network allocation vector (NAV), which is used for virtual carrier sense (CS) at the MAC layer. The NAV maintains a prediction of future traffic on the medium based on the duration information that is announced in data frames prior to the actual exchange of data. In addition, whenever a node detects an erroneous frame, the node defers its transmission by a fixed duration indicated by EIFS, i.e. Extended Inter Frame Space time. This time is equal to the $SIFS + ACK\ time + DIFS$ time [6].

2.3.2 IEEE 802.11e

To provide quality of service (QoS) support, the IEEE developed the IEEE 802.11e standard which is an improved version of the 802.11 MAC. A priority mechanism has been introduced in the enhanced version to support the QoS requirements. It deals with each type of data traffic according to their QoS requirements. Applications are categorized into four Access

Categories (AC) on the basis of their QoS requirements. Every frame with a specific priority of data traffic is then assigned to one of these access categories. For each AC, service differentiation is performed by assigning a different set of contention parameters to gain medium access [19].

The Hybrid Coordination Function (HCF) is the most recent centralized coordination function introduced by the IEEE 802.11e standard. It combines the features of a distributed medium access like DCF and centrally controlled medium access like PCF with improved QoS techniques. HCF defines two types of access mechanisms. The distributed contention-based channel access mechanism is called EDCA (Enhanced Distributed Channel Access) and the centrally controlled contention free access mechanism is called HCCA (HCF Controlled Channel Access). In next section, the focus is on the EDCA.

2.3.3 EDCA protocol

The EDCA mechanism is an enhanced version of the DCF mechanism, which provides distributed medium access with the use of access categories (ACs). The EDCA describes four ACs to deal with several different types of data traffic. The four access categories AC VO, AC VI, AC BE and AC BK are introduced for Voice, Video, Best Effort and Background respectively. Frames are then mapped according to their QoS requirements on their particular AC's where AC VO and AC BK have the highest and the lowest priority respectively. When a frame arrives at the MAC layer, it has a specific priority value which is known as the User Priority (UP). User Priority of the frame is mapped to its related AC [19].

Every station has four transmit queues, one for each AC, and four independent EDCA's one for each queue, as illustrated in Figure 2-4. EDCA is an enhanced version of DCF, and contends for the medium on the same principles of CSMA/CA and backoff, but based on the

parameters specific to the AC it is contending for. An EDCA contends for the medium based on the following parameters associated with an AC:

- AIFS - The time period the medium is sensed idle before the transmission or backoff is started.
- CW_{\min} , CW_{\max} - Size of Contention Window used for backoff.
- TXOP (Transmit opportunity) Limit - The maximum duration of the transmission after the medium is acquired.

The values of the EDCA parameters are different for different ACs. The higher priority ACs wait a small AIFS time period while the lower priority ACs have to wait a longer AIFS time before they can access the medium. The size of CW varies such that the higher priority ACs choose backoff values from a smaller CW compared to the lower priority ACs. TXOP Limit is also set in a way that the higher priority ACs can access the medium for longer durations. Basically, the higher the priority of an AC, the smaller the AIFS, CW_{\min} and CW_{\max} , and the larger the TXOP Limit.

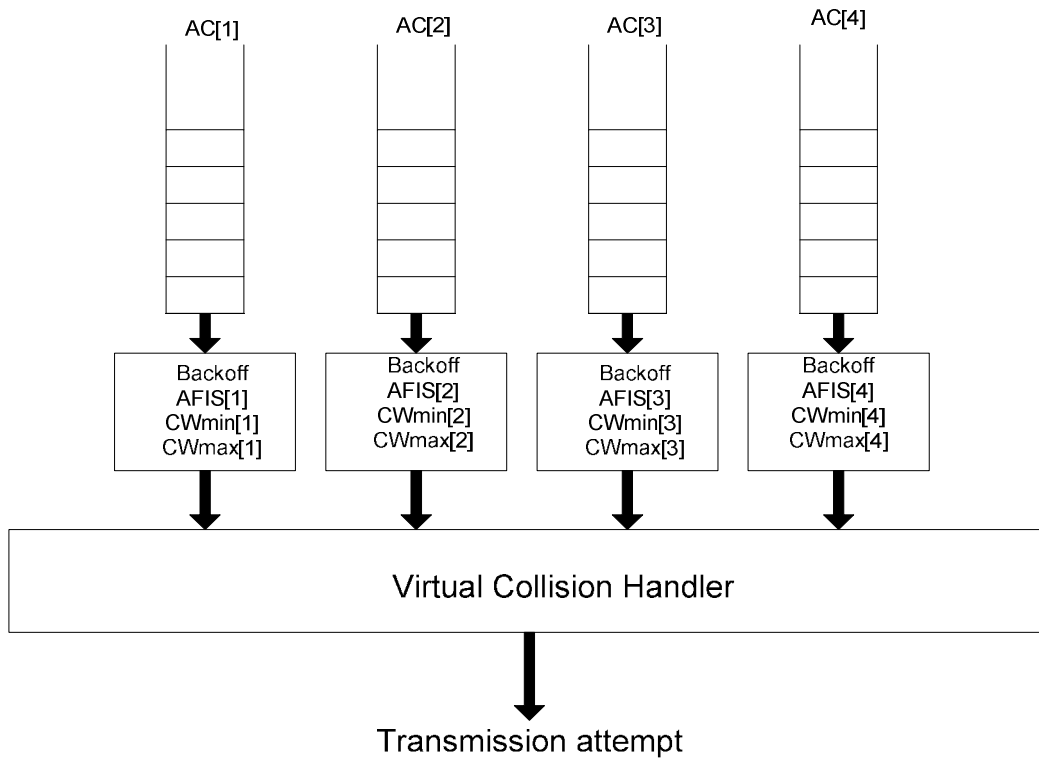


Figure 2-4 Transmission queues of EDCA

2.4 Persistent CSMA protocol

In this section three different persistent CSMA protocols are discussed, namely non-persistent, 1-persistent and p -persistent.

A non-persistent CSMA protocol

The basic purpose of this protocol is to minimise the interference among packets by always rescheduling a packet which finds the channel busy upon arrival. In this protocol, a station with a packet ready to send senses the channel and implement the following steps: (1) If the channel is idle, it sends the packet; (2) If the channel is sensed busy, then the packet is scheduled to be retransmitted some time later according to the retransmission policy [20,21] as shown in Figure 2-5.

At this new point in time the station senses the channel and repeats steps 1 and 2 above. A slotted version of the non-persistent CSMA can be considered in which the time axis is slotted and the slot size is a seconds. All terminals are synchronized and are forced to start transmission only at the beginning of a slot. When a packet arrival occurs during a slot, the terminal senses the channel at the beginning of the next slot and operates according to the protocol described above.

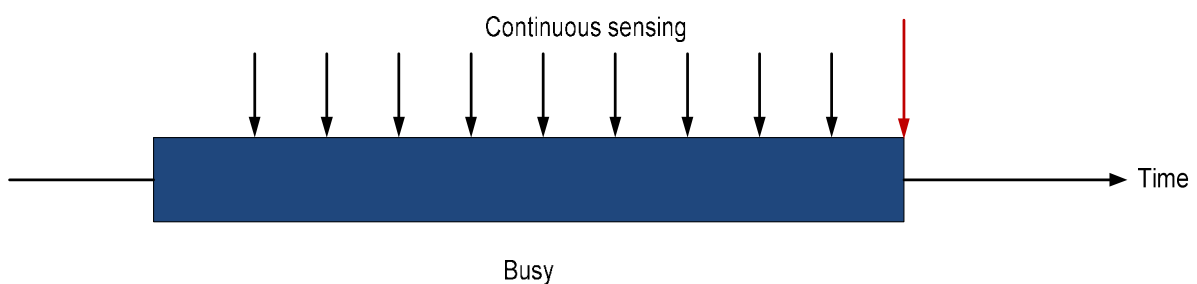


Figure 2-5: Non-persistent CSMA protocol

B 1-persistent CSMA protocol

This protocol aims to achieve an acceptable throughput performance by never letting the channel become idle if some ready packets are available. This protocol works as follows: (1) If the channel is idle, the station transmits the packet with probability one; (2) If the channel is sensed busy, the station defers until the channel becomes idle (i.e. persisting on transmitting) and only then transmits the packet with probability one; hence, the name of 1-persistent [20, 21] as shown in Figure 2-6.

A slotted version of this 1-persistent CSMA protocol can also be implemented by dividing the time axis into timeslots of duration, a , and synchronizing the transmission of packets at the beginning of each timeslot in the same manner as non-persistent CSMA.

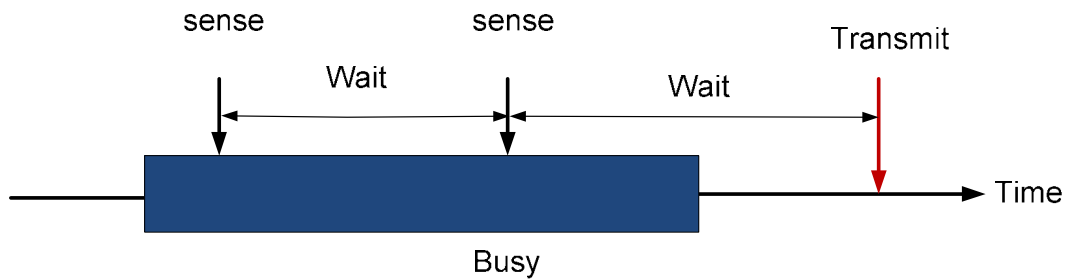


Figure 2-6: 1-persistent CSMA protocol

C p -persistent CSMA

In 1-persistent CSMA protocol, when two or more stations become ready during a transmission period, they wait for the channel to become idle and then they all transmit with probability one. A collision will also occur with probability one. The idea of randomising the starting time of transmission of packets accumulated during the transmission period is suggested for a collision reduction and therefore the throughput is improved. The protocol consists of including an additional parameter p , the probability that a ready packet persists ($q=1 - p$ being the probability of delaying transmission). The parameter p is chosen to reduce the number of collisions while keeping the idle periods between any two consecutive non-overlapped transmissions as small as possible. This protocol is known as p -persistent CSMA which is considered to be a generalization case of 1-persistent CSMA [20, 21].

More precisely, the protocol executes the following procedures: If the channel is sensed idle then, with probability p , the station transmits the packet, or with probability q , the station defers the transmission of the packet by one slot. If this slot is also idle, it either transmits again with the probabilities p or defers with the probabilities q . The process is repeated until either the packet has been transmitted or another station has commenced transmission. If another station has begun transmission, the station acts as if there had been a collision and

waits a random time and starts again. If the station initially senses the channel is busy, it waits until the next slot and implements the whole process again as shown in Figure 2-7 .

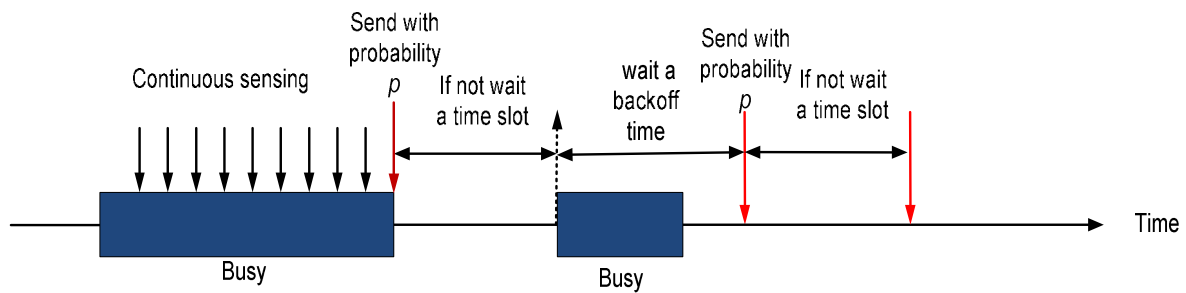


Figure 2-7: p -persistent CSMA protocol

2.5 Literature review

IEEE 802.11 WLANs have been increasingly popular recently due to their flexibility and low cost. Extensive research is being carried out to increase the data rates and provide a higher quality of service. Extensive research is also being carried out on techniques to improve the QOS of 802.11e. The performance evaluation of 802.11e EDCA has been investigated across a broad range of different aspects including the coexistence of data, voice and video applications [22]. In [22] it has been shown that the service differentiation provided by 802.11e EDCA can improve the throughput and delay for higher priority traffic. However, in the case of heavy traffic loads, low priority traffic can be easily starved by high priority traffic. Therefore, there is a need for some kind of admission control and scheduling scheme to guaranteed service to real time traffic and some fairness of channel access to the other types of traffic. Performance analysis for 802.11e was carried out by Ni [23] and his results showed that the contention-based EDCA mechanism can provide effective service differentiation between different types of traffic, but for a large number of users the default

CW values provided in 802.11e are too small and there is a need for adaptation of the backoff parameters when the channel conditions vary. A detailed investigation of the performance of the priority mechanisms defined in the 802.11e EDCA specifications was carried out by G. Bianchi in [24]. Bianchi's work was focused on the two basic priority mechanisms for accessing the channel: Different per-class setting of the contention window (CW) backoff parameters (CW_{\min} and CW_{\max}), and different per-class setting of idle time after which a transmission may occur (arbitration interframe space, AIFS). The results of this study showed that AIFS differentiation is superior to CW differentiation, whilst analysis of the coexistence between EDCA and DCF stations illustrated that the different backoff counter decrement mechanism used in EDCA provide one extra slot to be used for AIFS differentiation. Further, by setting the EDCA AIFS period equal to DCF DIFS period, EDCA traffic has higher access priority.

Some studies have considered the effect of the physical layer on the MAC by taking into account when two packets arrive in the same station at the same time, the packet with larger received power can be successfully received. This phenomenon is called the capture effect. The capture effect in a WLAN in the presence of multipath, shadowing and the near far effect was investigated in [25, 26]. In [25] the performance of various wireless MAC protocols with Rayleigh fading, shadowing and capture effect was analyzed. The study considered the performance of throughput and delay in the basic p -persistent CSMA and stop-and-wait CSMA. The numerical results showed that the performance of the throughput and delay of p -persistent CSMA is enhanced as the transmission probability p increases and is sensitive to the capture effect threshold. The capture effect was also investigated in [26]. CSMA/CA protocol where fading, shadowing and near-far effect were considered using a similar capture model in [27]. The paper showed that the capture effect predicts substantially increased

throughputs in CSMA/CA. For the basic CSMA/CA protocol, the throughput increase is significant compared to the model without the capture effect.

Another aspect of considering the effect of the physical layer on the performance of the MAC layer is taking into account the PHY packet error rate. In [28], Qiang Ni *et al* investigated the MAC layer saturated throughput performance of 802.11 DCF in the presence of packet error rates. The analysis considered the packet error rates of the data packets and error rate of ACK packets. The model assumes a fixed number of stations with saturated traffic sources, no hidden terminals, no capture effect and no link adaptation mechanisms. The results demonstrate that packet error rates significantly degrade the MAC layer throughput. Jun Yin [29] also presented an analytical model for the throughput and the delay of the 802.11 DCF in an error-prone channel. The model includes the situation when different stations have different packet error rates.

In systems such as WLANs with a very low mobility, the channel condition is often dominated by the distance between the AP and the associated station. In this case, the farther the distance between the AP and the station, the lower the transmission rate adopted. IEEE 802.11WLAN employs a link adaptation mechanism to select one out of multiple available data rates. Link adaptation mechanisms for IEEE802.11 WLAN have been studied in [30-34]. In our work we consider the impact of the link adaption on the WLAN performance rather than the link adaption mechanism itself. The throughput performance of stations transmitting with high data rate are significantly affected by stations transmitting with low data rate and the throughput of such stations is heavily degraded even though they are close to the AP [35]. This is primarily due to the fact that the 802.11 MAC provides the same channel access opportunities for all contending stations. If the same amount of data is to be sent over the wireless channel, the stations transmitting at low data rates (i.e. stations far from the AP) will occupy the wireless channel longer than those transmitting at high data rates (i.e. stations

close to the AP). This phenomenon is often known to as the “*performance anomaly*” of IEEE 802.11 which explains the unexpected performance degradation of stations transmitting with high data rate. Therefore, the overall system performance is dominated by the stations with the lowest data rates. This, of course, causes a serious issue in calculating network capacity and the network should be planned carefully to provide the required QoS. This means the anomaly issue should be avoided or mitigated. As high density WLANs containing many stations are being deployed at an ever increasing pace, this problem becomes even more important. The following sections are focusing more closely on the PHY/MAC cross-layer approach and multirate modelling.

2.5.1 PHY/MAC Modelling

The demand for WLAN services has grown substantially and it has become a crucial issue to further improve the throughput and delay performance for CSMA/CA-based WLANs. In the literature there are two main research directions for this issue. The first direction is from the basic MAC protocol perspective. In [36] and [37] a dynamic tuning algorithm is proposed to adjust the backoff window size according to the traffic loads. A fast backoff procedure was proposed in [38] while packet scheduling was investigated to reduce the packet collisions. Authors in [39] introduced a frame concatenation mechanism to reduce the protocol overhead.

The second direction is from PHY/MAC perspective, where the PHY layer effects are incorporated for more accurate evaluation of WLAN performance. This direction is one of our main topics in this thesis. Bianchi in [5] provided an analysis for the saturated throughput of the basic 802.11 protocol based on a two dimensional Markov model of the MAC layer. In fact a large number of works have investigated almost every aspect of the behaviour of DCF under different traffic loads and channel transmission conditions [40-43]. The research in

[43] has been extended by many studies to model IEEE 802.11e performance using Markov chain techniques. To solve these types of models, the transition probability matrix of the Markov chain must be created which contain a very large number of transition probabilities. Iterative methods are then used to solve a set of non-linear equations, or in some cases an analytical solution can be found instead. More complicated systems such as 802.11 EDCA create models with multiple transition matrices and non-linear equations, which have to be solved simultaneously. Xiao in [44] evaluated the differentiation between priority classes using both the contention window and the arbitrated interface spacing schemes, while the authors in [45-47] improve Xiao's analysis to give a more accurate analysis. All of these models remain inaccurate due to a large degree of complexity, which makes it difficult to apply them to a wide range of 802.11e. In order to simplify the analytical analysis several fundamental assumption are made: 1) stations always have a packet to send, 2) there are no hidden terminals, 3) there is no capture effect, 4) packets collide with constant and independent probability, 5) the transmission channel is ideal and the only cause of packet failure is the collision. In these models each access category has to be modelled using the Markov chain transition probabilities. As the number of access categories increase the model becomes significantly more mathematically challenging and too numerically complex to solve. In [48] an analytical model for a priority scheme providing a differentiated service in 802.11 is investigated. In their work saturation throughput and delay of different priority classes are derived analytically using a Markov model. Three control parameters were defined; initial contention window size, window increasing factor and maximum backoff stage and by proper selection of these parameters, a service differentiation can be achieved. These complexity issues were broadly discussed in [49] and the authors tried to simplify the model by decomposing the problem into two easily solved Markov chains that can be jointly solved by numerical methods.

The p -persistent CSMA scheme was first proposed in [20] for infinite population networks. An analytical model of the saturated and non-saturated throughput of the slotted p -persistent CSMA protocol were provided for a finite population in [21] and average packet delay analysis for this model was investigated in [50]. The p -persistent CSMA protocol can be used to accurately model the DCF and EDCA protocols of the 802.11 standard even though p -persistent CSMA and 802.11 employ different backoff mechanisms. This equivalence is achieved when the p value in p -persistent CSMA is chosen such that the average backoff intervals of the two protocols are the same [37]. The p -persistent CSMA model is less complex than the Markovian model, and therefore simpler to solve. Thus the p -persistent CSMA model highly suited to modelling IEEE 802.11e.

Most of the research in the literature assumes ideal channel conditions and those collisions always result in destroying the packets. This is especially true of the studies that have considered the differentiated services in WLANs. Channel conditions are far from ideal due to Rayleigh and shadow fading mechanisms and usually the packet is retransmitted several times until the data are correctly received. However, a packet can be received successfully in the presence of interference from other packets if its power is greater than the interfering power by a certain threshold. The effect of channel errors on the saturated throughput was studied in [28, 51, 52], while the research papers [25, 53] investigated the effect of capture on the saturated throughput of 802.11. In [25] the effect of the capture on the p -persistent CSMA protocol was investigated in the case of a single traffic type. In this study, the throughput and delay analysis for both a basic and stop-and-wait p -persistent CSMA protocol were considered. The numerical results showed that the performance of p -persistent CSMA is enhanced when the capture effect is included. Authors in [54] investigated the saturated throughput performance of IEEE 802.11DCF. The assumptions are similar to those stated above with the exception that channel errors and capture effects due to the transmission over

Rayleigh fading channels are included in the model. This research extends the Bianchi work [5] to a more realistic model. The results showed that for decreasing values of the capture threshold, the throughput increases while decreasing the SNR values the throughput decreases and at SNR <20 dB the packet error rate dominates the throughput behaviour. When the number of stations in the network is 28 and $z = 6$ dB the throughput reaches the optimum throughput predicted by Bianchi in [5], where an optimum contention window size is employed. The authors in [55] provided throughput analysis of the Transmit Opportunity (TXOP) feature in IEEE 802.11e with bursty error channels. The authors in [56] have extended the model in [21] to achieve a service differentiation using p -persistent CSMA and clearly proved that differentiated p -persistent CSMA can be applied to IEEE 802.11e EDCA through the conversion between p and the contention window. Their results show very good agreement between the analytical model and the simulated version of IEEE 802.11e EDCA in NS-2 and OPNET. In [57], it has been shown how EDCA systems can be accurately modelled using p -persistent CSMA analysis. In the study, the basic p -persistent CSMA analysis was modified to include most of the EDCA features such as TXOP, internal collision resolution, AIFS differentiation and retry limit. In WLAN deployment, the QoS requirement of an application is a key parameter that needs to be taken into account when designing and planning the network. The work addressed in the literature analysed the effect of the capture and channel errors on the performance of IEEE 802.11 DCF WLAN systems.

The research addressed in the literature clearly shows that after Bianchi's work all the models subsequently evolved toward more accurate and realistic versions that make the characterization of WLAN as close as possible to real environments. However, in WLANs with QoS differentiation, the capture effect has not been investigated by any study which motivated our research to develop a more accurate and practical model. This lack of analysis is partly due to the complexity of using the Markov chain technique to model the

802.11e as discussed above. However, excluding the capture effect from the analysis results in substantially underestimating the throughput performance of the network, which leads to inaccurate calculations of the network capacity. In this thesis an important gap is filled to improve the QoS differentiated p -persistent CSMA protocol model by developing the model in [56, 57] into a more accurate model by including the PHY layer effects. A cross-layer MAC/PHY approach is developed to accurately estimate the throughput and delay for QoS differentiated p -persistent CSMA, which is a critical element for an accurate network design and planning.

The previous research discussed in the literature considered the saturated case which models the situation of high density networks. However, the non-saturated case is more realistic scenario in the low density networks where some stations have no packets in the buffer to send. This means including the post-backoff feature of 802.11 along with the probability of an empty queue. Modelling the non-saturated case is more complicated and difficult to solve than the saturated case. The behaviour of IEEE 802.11 DCF WLANs under non-saturated traffic loads was investigated in [58-62]. These models extended the Bianchi model in [5]. In [58] and [59] use M/G/1 queuing analysis while [60] and [61] allow for heterogeneous loads where different stations can have different arrival rates. In [61], the authors developed an extension of the Bianchi model to a non-saturated environment and show that a station can approach the saturation throughput depending on many factors such as the number of stations in the system and their relative loads. The non-saturated throughput of IEEE 802.11 in the presence of packet error rates and capture effects is investigated in [63]. In this study also the Bianchi model in [5] was extended to develop an expression for the non-saturation throughput as a function of the number of stations, packet sizes, packet error rates and capture effect. A non-saturated model of IEEE 802.11e EDCA is presented in [64] and [65]. This model includes the retry limits, backoff freezing, AIFS differentiation and virtual

collision handling. In this model also the arrival rate can be different for each traffic type. The throughput performance of IEEE 802.11e EDCA was investigated in error-prone channels in [66-68]. Abu-Sharkh and Tewfic in [67] extended Xiao's work by including more parameters such as arbitration inter-frame space (AIFS), virtual collision handler and the packet error rates. In this model, the performance of IEEE 802.11e EDCA under a finite load was evaluated. Further study in [69] considered the performance of IEEE 802.11e to support QoS with packet error rates. These models are very complicated and are difficult to solve, making them inaccurate around the channel capacity which is the main area of interest. In [70] a p -persistent CSMA system was presented that considered non-saturated stations with both heterogeneous loads and heterogeneous priorities. In this research a more accurate model was provided to calculate the non-saturated throughput and delay around the channel capacity. This model allows for non-saturated stations to have their own unique offered load and priority values with less complexity compared to the studies that used the Markovian model. The model in [70] was developed on the basis of the packet is unsuccessful only due to collisions, i.e. the channel is ideal. It is clear from the literature that there is a need to calculate the non-saturated throughput and delay as accurately as possible, which is the main factor in network planning and design. This thesis fills this gap by developing the model in [70] into a more accurate model in realistic and practical environments. This was done by incorporating the packet error rates and the capture effect into the model provided [70]. Our objective was to develop a cross-layer (PHY/MAC) analytical model to accurately evaluate the non-saturated throughput and delay of p -persistent CSMA with both heterogeneous loads and heterogeneous priorities.

2.5.2 Multirate Modelling

IEEE 802.11 wireless LANs (WLANs) stations support multiple rates, and use them adaptively depending on the channel condition via the link adaptation mechanisms. The *performance anomaly* issue arises due to the same access probability of all the stations regardless of their different transmission data rates. This means that lower transmission rates occupy the channel for a longer time. Hence stations that transmit at low data rates significantly reduce the overall system throughput. The throughput of a station that transmits at a high data rate may be degraded to the throughput value of a station that transmits at the lowest data rate. Multirate modelling of DCF has received more attention after the anomaly issue was discovered experimentally and studied via a simple analysis in [35]. This study motivated many researchers to deeply investigate the issue and propose solutions that mitigate the *anomaly performance* of WLANs. Authors in [71] investigated the anomaly problem using Markov chains and derived an analytical solution to calculate the saturated throughput. Several mechanisms to mitigate the performance degradation due to anomaly issue are also proposed such as adjusting initial backoff window and/or packet size depending on the employed data rate of low-rate stations. The results in [71] showed that the anomaly problem can be alleviated by appropriate adjustment of the MAC layer parameters. Adjusting the packet size based on an ideal channel is not accurate as the larger packets usually required high SNR (signal-to-noise ratio) values which may result in dropping the data rate. Authors in [72] also provided a saturated throughput analysis with multirate capability. An adaptive mechanism to adjust the packet size according to data rates proposed to improve the packet size mechanism was presented in [71] as the packet size has upper and lower limits; the larger packets are more susceptible to errors; whereas the smaller packets can result in an underutilized channel. In [73], a more generalized mathematical model for the throughput and channel utilization for successful transmission with packet error rates for multirate WLANs

was investigated. A contention window and payload adjustment scheme was proposed to mitigate the performance anomaly by achieving temporal fairness. The fairness issue has been studied by many authors [74-77] and most of the work has focused on the time-based fairness criteria. This criteria guarantees equal channel occupancy irrespective of the station data rate. The authors in [78] introduced two fairness indices, channel occupancy time and throughput, among the contending stations. The approach maximised the total throughput while maintaining time fairness between competing stations by adjusting the minimum contention window size and MAC frame size. The non-saturated throughput performance of multirate IEEE 802.11 WLANs with packet error rates was analysed in [79]. Further study in [80] provided a general model of the non saturated throughput for 802.11 DCF where packet errors at physical layer and variable loaded multirate stations (i.e. stations have different arrival rates) are considered. Also, this study proposed a novel resource allocation criterion that improves the fairness among contending stations by modifying the proportional fair (PF) algorithm to take into account the traffic load and channel conditions. The results showed that the proposed throughput allocation improved the total throughput of the DCF and ensuring fairness levels between the stations. Authors in [81] provided an analytical approach to resolve the performance anomaly of IEEE 802.11 through configuring the initial contention window size inversely proportional to the bit rate based on the same principle of throughput differentiation among equal bit rate terminals. QoS support over IEEE 802.11e in multirate networks was studied by simulation only in [82] using NS-2. In their work they proposed a hybrid method based on the Transmit Opportunity (TXOP) feature and contention window to maintain the quality of highest priority applications and improve the overall system throughput simultaneously. The results showed the hybrid method outperforms the other proposed mechanisms especially in the voice flows. There is no doubt that modelling the multirate is a very important factor in network planning especially in high density networks.

This was very clear from the literature review where there is a great interest in modelling the multirate and many solutions were proposed to mitigate the *anomaly performance*. This thesis takes the state-of-the art research a step forward by developing the model in [56] into a model that evaluate the performance of saturated throughput and delay of a QoS differentiated p -persistent CSMA-based WLANs with multirate capability. The p -persistent CSMA is proposed to mitigate the anomaly issue in the QoS differentiated systems such as 802.11e EDCA. This model is further improved to a more accurate and realistic model by incorporating the PHY layer effects in terms of packet error rates and capture effect.

2.6 Summary

In this chapter, an overview has been provided for IEEE 802.11a/g/n, IEEE 802.11e and persistent CSMA protocols. The principles of OFDM, the Alamoutie algorithm for 2x2 MIMO and MIMO-OFDM are also presented.

This chapter also provided a literature review for the area of work relevant to this thesis. First, the most recent work is discussed in 802.11 MAC protocol and the state-of-the art in providing QoS in EDCA is also discussed. The literature highlights that the anomaly issue significantly degrades the throughput of the WLANs. Some key studies showed that p -persistent CSMA can closely model 802.11 and the most recent study [57] has shown that QoS over 802.1e can be modelled using a QoS differentiation p -persistent CSMA.

The literature review then took a close look at the field of cross-layer approaches in 802.11/802.11e system modelling in terms of packet error rates and capture effect. The gaps in this literature are highlighted as: (1) While the p -persistent CSMA analysis has been used successfully for modelling 802.11e, there is no accurate model of a QoS differentiated p -persistent CSMA that takes into account the PHY layer effects, ie. PHY/MAC analysis. (2) Although some PHY/MAC cross-layer approaches investigated the non-saturated case of 802.11 MAC protocol, there is no cross-layer approach that investigates the QoS

differentiation based WLANs systems. (3) Since the anomaly issue in WLANs was discovered experimentally in 2003, it has received attention from many researchers and several mechanisms were proposed to solve this issue. However, there is no analysis that models the anomaly issue in QoS differentiated services WLAN. Additionally, there is no model of a cross-layer approach of a QoS differentiated p -persistent CSMA with multirate capability. This thesis fills these gaps by developing more accurate models of a QoS differentiated p -persistent CSMA protocol, which accurately calculate the throughput and delay leading to a more efficient network planning and design. These models can be applied to evaluate the 802.11e networks.

Chapter 3

Saturated Throughput and Delay

Analysis of p -persistent CSMA protocol

In practical WLAN deployment, the capture effect has been shown to enhance the throughput performance of the network. Analysing the effect of fading, shadowing and near–far effect on the performance of 802.11 is a fundamental consideration in practical situations since the wireless channels are error-prone. Developing an accurate closed form solution of the throughput and delay is crucial for network planning and design. This chapter develops a physical/medium-access-control- (PHY/MAC) -cross-layer model to characterise the throughput/delay performance of WLANs in a realistic environments. The developed model incorporates the capture effect and the packet error rates effects from the PHY layer perspective, while from the MAC perspective the approach considers the QoS differentiated p -persistent CSMA protocol. This chapter is organized as follows: In the next section, the system model of p -persistent CSMA is presented. In section 3.2, the capture model is discussed. Simulation setup is provided in section 3.3. In section 3.4 and 3.5, throughput analysis and delay analysis are provided, respectively. In section 3.6, our new model is validated and we show how the various parameters of the model can affect the system

performance. The application of our model in WLAN planning is presented in section 3.7. Finally, our conclusion is drawn in section 3.8.

3.1 System Model of p -persistent CSMA

This p -persistent CSMA model is a modified form of the model in [56]. The model consists of an AP surrounded by M wireless stations. The main modifications to the model in [56] are the incorporation of the PHY layer effects in terms of the packet error rate and the capture effect. The transmission failures are caused by either collisions with other packets on the channel or by channel errors. All transmitted packets have a fixed packet size. The system contains M stations, where $M=M_1+M_2+\dots+M_{d_{max}}$, and M_d represents the number of stations with type d traffic and d_{max} is the total number of traffic types in the system. Each station has only one traffic type and all stations are saturated which means each station always has a packet to transmit. Within a busy transmission period there are regenerative cycles of busy subperiods (B), that consists of a deferral time (R) and a transmission time (T) as shown in figure 1. Each timeslot during R has a duration of a . Each traffic type is given the p -persistent CSMA parameter p_d and each station will start its transmission with probability p_d and defer with probability $(1 - p_d)$. A transmission will be successful if one station commences a transmission at the start of the timeslot during R or the received power of the concerned packet that experiences a collision is higher than a threshold z .

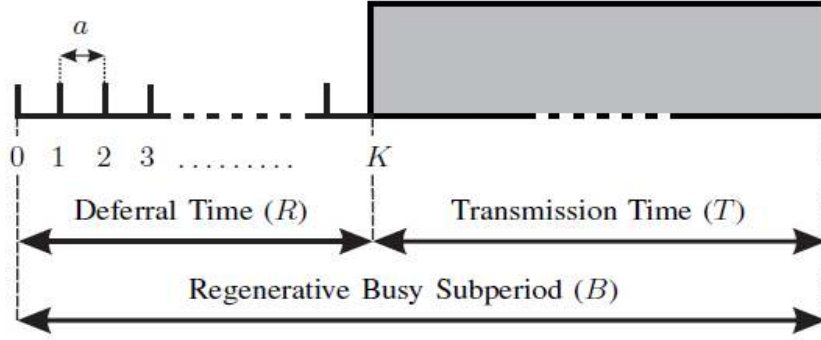


Figure 3-1: Channel state cycle for saturated case

3.2 Capture Model

The capture model used in this study assumes that the wanted packet is received successfully by the AP if its instantaneous power is larger than the joint instantaneous power of other interfering packets (i.e. the signal to interference ratio, SIR) by at least a certain minimum threshold factor, z , as shown in (3-1).

$$z \geq \frac{p_0}{\sum_{i=1}^{\beta-1} p_i} \quad (3-1)$$

In this formula p_0 is the power of the wanted packet and p_i is the power of interfering packet i . When the power levels of different packets are compared, as in [25, 53], we assume the packet powers do not change during a packet interval as the indoor channel such as Rayleigh fading channel does not change rapidly.

Path loss, lognormal shadowing and multipath fading are the three main independent and multiplicative propagation mechanisms of the wireless channel. For distance r between the AP and station, path loss is proportional to r^γ with γ the path loss exponent, which depends on the environment (typically $3 \leq \gamma \leq 4$). The area-mean power, p_a , is an average received

signal power without shadowing and fundamentally is determined by the path loss. A conventional lognormal model is used to describe the shadowing effect based on the superposition of a zero mean local power, p_l , on the area-mean power of normal distribution in dB and logarithmic standard deviation σ_s . The unconditional probability density function (pdf) of the instantaneous power p_s , of a received signal packet at the AP is given by (3-2) as shown in [27] and takes into account the near-far effect, shadowing and multipath Rayleigh fading effects.

$$f_{p_s}(p_s) = \int_0^{\infty} \int_0^{\infty} \frac{1}{p_l} \exp\left(-\frac{p_s}{p_l}\right) \frac{f(r)}{\sqrt{2\pi} \sigma_s p_l} \cdot \exp\left(-\frac{(\ln p_l + \gamma \ln r)^2}{2\sigma_s^2}\right) dr dp_l \quad (3-2)$$

Where $f(r)$ is the pdf of the distance describing the spatial distribution of the offered packets around the AP. A uniform spatial distribution in which stations are uniformly distributed in a circle of unit radius is considered. In this case, the pdf is given by $f(r) = 2r$ and $r \in (0,1)$.

The total received interference power is due to the incoherent summation of β independently fading signals, the pdf of the summed signal is the convolution of the pdf of each component. After Laplace transformation, convolution becomes multiplication, and the joint pdf of the received power is β -fold convolution of the pdf of the individual signals. Hence, the probability of capture, conditional on $\beta - 1$ interferers can be expressed as in (3-3) as presented in [27].

$$q((\beta - 1)|z) = \int_0^{\infty} \int_0^{\infty} \frac{f(r)}{\sqrt{2\pi} \sigma_s p_l} \exp\left(\frac{(\ln p_l + \gamma \ln r_t)^2}{2\sigma_s^2}\right) \left[\Phi\left(\frac{z}{p_l}\right)\right]^{\beta-1} \cdot dr dp_l \quad (3-3)$$

Here, r_t is the distance between the AP and the station transmitting the wanted packet and $p_{l,t}$ is its local mean power. The term in $\Phi(\cdot)$ is the Laplace image of the pdf of one single interferer and $\Phi(\cdot)$ can be expressed as in (3-4).

$$\Phi\left(\frac{z}{p_l}\right) = \int_0^{\infty} \int_0^{\infty} \frac{1}{1 + sp_l} \frac{f(r)}{\sqrt{2\pi} \sigma_s p_l} \cdot \exp\left(-\frac{(\ln p_l + \gamma \ln r)^2}{2\sigma_s^2}\right) dr dp_l \quad (3-4)$$

The probability q_β that one out of β packets is captured by the AP is then given by (3-5).

$$q_\beta = \beta \times q((\beta - 1)|z) \quad (3-5)$$

Equation (3-5) can only be applied for a single traffic type (i.e. homogenous condition) but for the case where the QoS differentiation among the traffic types is considered (i.e. heterogeneous condition) equation (3-5) should be modified as shown in (3-6).

$$q_{\beta_d} = \beta_d \times q((\beta - 1)|z_d) \quad (3-6)$$

Here β_d and z_d is the number of stations and the threshold value of traffic type d respectively. β is the number of stations of all traffic types as shown in (3-7).

$$\beta = \sum_{d=1}^{d_{max}} \beta_d \quad (3-7)$$

In order to calculate the capture probability the path loss exponent (γ) is set equal to 4 and numerical integration methods are used to solve equation (3-3) [83]. Figure 3-2 shows the

capture probability as a function of contending stations at different threshold (z) values. In order to be consistent with the wireless channel used for generating the PER curves of IEEE 802.11g/n, the shadowing effect is not considered for generating the capture probabilities. The curves show that the capture probability is sensitive to the number of contending stations when less than 10 stations are transmitting and after that the capture probability converges to a constant finite value. The results also illustrate that the higher the values of the threshold the lower the probability of the packet to capture the channel.

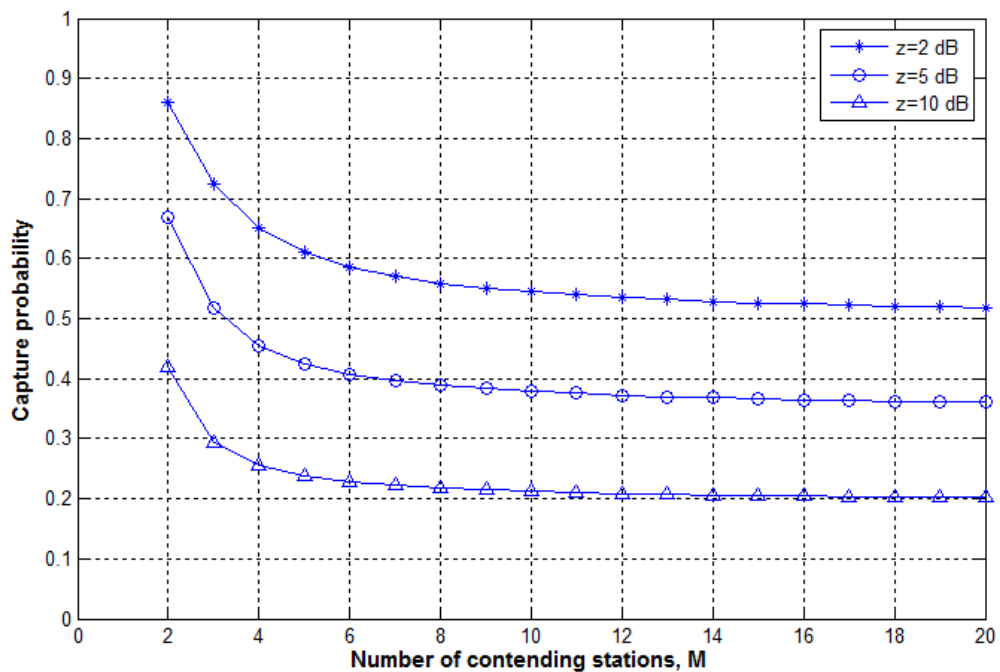


Figure 3-2: Capture probability as a function of colliding stations at different threshold (z) values

3.3 Simulation Modelling of p -persistent CSMA protocol with PHY layer effects

In this section, the main functionalities of the developed simulator that models the system presented in section 3-1 are described. The WLAN configuration consists of an infrastructure mode BSS (Basic Service Set) with an AP surrounded by a pre-specified number of stations per traffic type (M_d), where the number of traffic types are also pre-specified. The QoS differentiation among the traffic types was achieved according to Hui's ratio [84]. All the parameters used in the simulations and the analysis are shown in Table 3-1. The simulator has been developed using MATLAB to model the system described in section 3.1. The simulator consists of two main functions: Contend and Transmit. Each station always has a packet to send. This means all stations are in a saturated condition and continuously contend for the channel with accumulating delay until the contending packet is successfully received. For the case of MAC layer only, when only one station wins the channel the transmission will be considered successful and the packet transmitted using the Transmit function; but if more than one station win the channel, the transmission is considered to be unsuccessful also transmitted using Transmit function, which causes the degradation in throughput/delay performance, and the delay is updated for both cases.

Table 3-1: p -persistent CSMA parameters

parameter	value		parameter	Value	
	802.11a/g	802.11n		802.11a/g	802.11n
Data rate	24 Mbit/s	26 Mbit/s	a	9/606	9/567
Payload size	1500 bytes	1500 bytes	b	500/606	461/567
Payload duration	500 μ s	461 μ s	T	606 μ s	567 μ s

In order to model packet errors at the PHY layer, a MATLAB simulator was developed based on the IEEE 802.11n standard. The IEEE 802.11 scheme specifies a physical layer and a medium access control (MAC) protocol for channel access [6]. The 802.11n standard builds on the successful 802.11a/g standards by adding MIMO capabilities. Space-Time Block Coding (STBC), as used in 802.11n, involves transmitting multiple copies of a symbol stream across two or more antennas. Various modulation modes and coding rates are defined by the standard and are represented by a Modulation and Coding Scheme (MCS) index value. The simulator was implemented for 6 transmission modes with different coded modulation configurations, giving data rates ranging from 6.5 Mbit/s to 58.5 Mbit/s as shown in Table 3-2. Also shown in Table 3-2 are the MCS data rates for SISO 802.11a/g. The operational channel is 20 MHz and the guard interval is 0.8 μ s. The simulator was used to evaluate the system performance of both 802.11n and 802.11g in an AWGN and multipath Rayleigh fading channel, with τ_{rms} set to 100 ns to model an office environment. Packet error rate (PER) curves for salient data rate modes for 2x2 Alamouti 802.11n and SISO 802.11a/g are shown in Figure 3-3a and Figure 3-3 respectively. A uniformly distributed binary random variable X is generated in order to decide if a transmitted packet is received successfully or not. The statistics associated with this random variable are $P(X = 1) \geq 1 - P_e^d$ and $P(X = 0) < 1 - P_e^d$. If the packet is involved in a collision, the number of stations that transmitted at the same time is counted and the capture probability is obtained based on the capture threshold. The decision on whether or not the packet is captured uses the same statistical procedure applied for generating a packet error.

Table 3-2: MCS indexes for 2x2 IEEE 802.11g/n WLANs

MCS	Coding rate	Modulation type	802.11n 2x2 MIMO Data rate (Mbit/s)	802.11a/g SISO Data rate (Mbit/s)
0	$\frac{1}{2}$	BPSK	6.5	6
1	$\frac{1}{2}$	QPSK	13	12
3	$\frac{1}{2}$	16QAM	26	24
4	$\frac{3}{4}$	16QAM	39	36
5	$\frac{2}{3}$	64QAM	52	48
6	$\frac{3}{4}$	64QAM	58.5	54

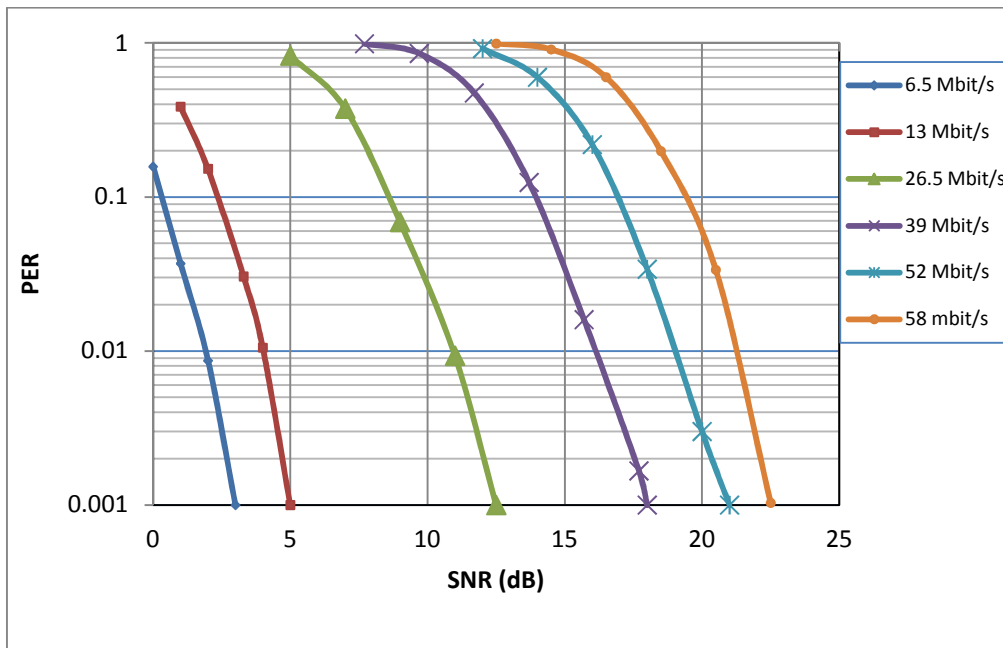


Figure 3-3a: PER versus SNR for IEEE 802.11g in multipath channel in time domain

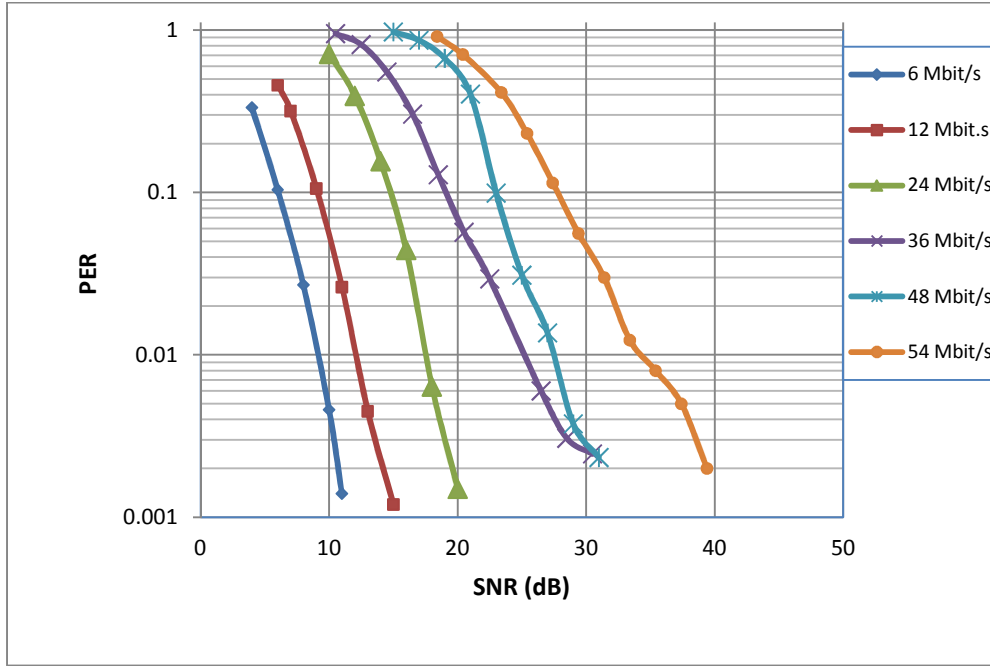


Figure 3-3b. PER versus SNR for IEEE 802.11n in multipath channel

3.4 p -Persistent CSMA protocol Throughput

An analytical model for evaluating throughput of the p -persistent CSMA with service differentiation under error free channel conditions has been reported in [56]. In this section, we will propose a PHY/MAC cross-layer analytical model for the QoS differentiated p -CSMA MAC protocol that extends from [56] to include the effects of packet error rates and capture effect. The work in [56] is summarized first, then the modified throughput analysis including the packet error rates and capture is developed.

3.4.1 Basic analysis of differentiated p -persistent CSMA protocol

The overall system throughput, S , can be calculated using equation (3-8).

$$S = \frac{E[U]}{E[B]} \quad (3-8)$$

B denotes the duration of a busy subperiod with expected value $E[B]$ while U denotes the duration of successful transmissions during a busy subperiod with expected value $E[U]$. In [56] the system throughput for traffic type d stations only, S_d , was calculated using (3-9).

$$S_d = \frac{E[U_d]}{E[B]} \quad (3-9)$$

Where $E[U_d]$ is the expected time spent on useful type d transmissions per busy subperiod. With reference to fig.1, $E[B]$ is calculated as in (3-10).

$$E[B] = E[R] + E[T] \quad (3-10)$$

Where $E[R]$ and $E[T]$ are expected values for R and T in a busy subperiod. This analysis considers a single data rate (i.e, all stations in the system transmit with the same data rate) so $E[T]$ can be normalised to have unity value, i.e. $E[T] = 1$. In order to calculate $E[R]$ each station that is likely to transmit during R must be considered. The timeslot boundaries are numbered as $k = 0, 1, 2, \dots, K$ where K is a random variable ranging from 0 to ∞ . The expected length of the deferral period can be calculated as shown in (3-11).

$$E[R] = a \sum_{k=1}^{\infty} \left(\prod_{d=1}^{d_{max}} (1 - p_d)^{M_d k} \right) \quad (3-11)$$

The probability that only a type 1 transmission commences at timeslot boundary k and that no transmissions have started before this for $k = 0, 1, 2, \dots, \infty$ is given by (3-12).

$$P(1tx_1) = M_1 p_1 (1 - p_1)^k [(1 - p_1)^{k+1}]^{M_1 - 1}$$

The probability that no transmission, defined by $P(0tx_d)$, has occurred before time slot boundary $k+1$ for each other traffic type d is calculated from (3-13).

$$P(0tx_d) = [(1 - p_d)^{k+1}]^{M_d} \quad (3-13)$$

Using equations (3-12) and (3-13) the probability of a successful type 1 packet commencing transmission at time slot boundary k for $k = 0, 1, 2, \dots, \infty$ can be calculated by (3-14).

$$P(S_1) = P(1tx_1) \prod_{d \neq 1} P(0tx_d) \quad (3-14)$$

Now the expected time per busy subperiod spent on successful transmissions can be calculated by (3-15).

$$E[U_1] = b \sum_{k=0}^{\infty} \left(P(1tx_1) \prod_{d \neq 1} P(0tx_d) \right) \quad (3-15)$$

Where b is the fraction of time spent on useful transmission. The throughput of traffic type 1 (S_1) can be calculated by substituting (3-11) and (3-15) into (3-2) as shown in (3-16) and the total throughput can be calculated by (3-17).

$$S_1 = \frac{b \sum_{k=0}^{\infty} (P(1tx_1) \prod_{d \neq 1} P(0tx_d))}{a \sum_{k=1}^{\infty} (\prod_{d=1}^{d_{max}} (1 - p_d)^{M_d k}) + 1} \quad (3-16)$$

$$s = \sum_{d=1}^{d_{max}} s_d \quad (3-17)$$

3.4.2 Throughput analysis of p -persistent CSMA with PHY layer effects

In a wireless channel, a packet may not be received correctly for two main reasons. Firstly, when the channel signal-to-noise ratio (SNR) is too low there is a high chance that a single packet will experience a bit error due to multipath fading channel. Secondly, when two or more packets from different stations collide, the signal-to-interference ratio (SIR) typically degrades significantly and packets are lost. To establish the interaction between the PHY and MAC layers, the probability of success for a packet of traffic type d , $P(S_d)$, in the MAC only analysis is modified to account for the PHY layer effects, denoted by $P(S_{dphy})$. This probability is the sum of the probability of success for a single packet of traffic type d , $P(S_{dpe})$, when received successfully in multipath fading channel (i.e. no collisions occurred) and the probability of success for a packet of traffic type d , $P(S_{dcap})$, when captured during a collision. Then, for M stations with traffic type d , the probability of packet success is given by (3-18).

$$P(S_{dphy}) = P(S_{dpe}) + P(S_{dcap}) \quad (3-18)$$

Considering traffic type 1, a packet received successfully in an error-prone channel without any interference from other stations is calculated by modifying equation (3-12) as shown in (3-19).

$$P(S_{1pe}) = P(1tx_1) \prod_{d \neq 1} P(0tx_d) \times (1 - P_e^1) \quad (3-19)$$

Here, P_e^1 is the packet error rate (PER) of a type 1 station.

The probability that a packet is captured is calculated as follows: the probability that more than one station transmits at the same time is obtained by modifying (3-12) to give (3-20).

$$P(\beta_d tx_d) = \binom{M_d}{\beta_d} (p_d(1-p_d)^k)^{\beta_d} [(1-p_d)^{k+1}]^{M_d-\beta_d} \quad (3-20)$$

Where β_d is the number of stations of type d transmitting at the same time. The probability of success for a packet of traffic type 1, ($P(S_1 cap)$) when more than one station (i.e. $\beta > 1$) transmits at the same time can be calculated from (3-21).

$$P(S_1 cap) = \sum_{\beta_1=2}^{M_1} \sum_{\beta_2=0}^{M_2} \dots \sum_{\beta_{d_{max}}=0}^{M_{d_{max}}} \left(\prod_{d=1}^{d_{max}} P(\beta_d tx_d) \right) (\beta_1) q((\beta-1)|z_1) \quad (3-21)$$

Where β_1 is the number of stations of type 1 transmitting at the same time. Substitution of (3-19) and (3-21) into (18) calculates the probability that a type 1 packet is successfully received in the presence of PHY layer effects. If equation (3-18) is evaluated over the full range of k then $E[U_1 phy]$ can be obtained as shown in (3-22).

$$E[U_1 phy] = b \sum_{k=0}^{\infty} \left(P(1tx_1) \prod_{d \neq 1} P(0tx_d) \times (1 - P_e^1) + \sum_{\beta_1=2}^{M_1} \sum_{\beta_2=0}^{M_2} \dots \sum_{\beta_{d_{max}}=0}^{M_{d_{max}}} \left(\prod_{d=1}^{d_{max}} P(\beta_d tx_d) \right) (\beta_1) q((\beta-1)|z_1) \right) \quad (3-22)$$

The throughput of traffic type 1 with PHY layer effects ($S_1 phy$) is calculated by substituting (3-11) and (3-22) into (3-2) and the total throughput is calculated as shown in (3-23).

$$S_{phy} = \sum_{d=1}^{d_{max}} S_{d_phy} \quad (3-23)$$

Equations (3-17) and (3-23) give the normalized throughput. The absolute throughput S_1abs is given by $S_1abs = S_1phy \times r$, where r is the PHY layer transmission bit rate.

3.5 Delay analysis of p -persistent CSMA protocol

The delay in this analysis is defined as the time from when a packet becomes head of the line at a station until it is successfully received. When analysing the p -persistent CSMA protocol, the delay begins at the start of R following the station's previous successful transmission and ends once the station's next successful transmission has completed. An analytical model for calculating the delay of p -persistent CSMA protocol with PHY layer effects will be provided. We first summarize the work of [85] and then provide the analysis of incorporating the PHY layer effects in terms of packet error rates and capture effect.

3.5.1 Delay analysis of basic p -persistent CSMA protocol

The probability that a type 1 station is successful (P_1) in the pure MAC layer can be as in (3-24).

$$P_1 = \frac{P(S_1)}{M_1} \quad (3-24)$$

Where $P(S_1)$ is given by (3-14). The number of busy subperiods, N_1 , before a particular type 1 station successfully transmits forms a geometric distribution, $(N_1 = X) = P_1(1 - P_1)^{X-1}$, whose mean, \bar{N}_1 , can be calculated by (3-25).

$$(3-25)$$

$$\bar{N}_1 = \frac{1}{P_1} = \frac{M_1}{P(S_1)}$$

The average delay for a type 1 packet can be calculated as shown in (3-26).

$$\bar{D}_1 = \bar{N}_1 \times E[B] \quad (3-26)$$

By substituting equations (3-10) and (3-25) in equation (3-26) the average delay can be calculated as in (3-27).

$$\bar{D}_1 = \frac{M_1(E[R] + E[T])}{P(S_1)} \quad (3-27)$$

3.5.2 Delay analysis of p -persistent CSMA with PHY layer effects

The probability that a type 1 station is successful, P_{1_phy} , in the presence of channel errors (i.e. packet error rates) and capture effect is shown in (3-28).

$$P_{1_phy} = \frac{P(S_{1_phy})}{M_1} \quad (3-28)$$

The average delay for a type 1 packet can then be calculated as shown in (3-29)

$$\bar{D}_{1_phy} = \frac{E[R] + 1}{P_{1_phy}} \quad (3-29)$$

3.6 Numerical Results and Discussion

This section is divided into two subsections. The first subsection presents saturated throughput results, while the second subsection provides the results for the system delay. The results include the packet error rates effect, the capture effect, demonstrate the PHY layer effect in terms of both the packet error rates, and capture effect. In the delay results, we focused on the effect of the capture only and the effect of both together packet error rates and capture effect.

3.6.1 Throughput Results

The first experiment investigates the packet error rates on the throughput performance of a QoS differentiated p -persistent CSMA protocol. Four traffic types are investigated with p_1 set to 0.05, the values of p_2, p_3, p_4 are modified in order to achieve throughput ratios $S_1:S_2:S_3:S_4=8:4:2:1$ according to Hui's ratio [84]. In [84] the ratio between throughput of stations of different traffic types when the contention window (CW) settings provide the service differentiation is identified as $S_1:S_2:\dots:S_{d_{max}} = (p_1)/(1 - p_1):(p_2)/(1 - p_2): \dots:(p_{d_{max}})/(1 - p_{d_{max}})$, where the relationship between p and CW is $p = 2/(CW + 2)$ as calculated in [86]. Figure 3-4 shows throughput versus number of stations with SNR as parameter. In Figure 3-4, "Basic" denotes results without including the packer error rates effect. The results show that as the number of stations increases the throughput decreases due to more collisions occurred. The results also show the throughput is further decreased due to the packet error rates, for example when SNR =9 dB the throughput decreased by 6% compared to the basic case while at SNR=8 dB the throughput decreased but 10 %. These results demonstrate that the throughput performance degrades due to congestion in the network and the channel conditions.

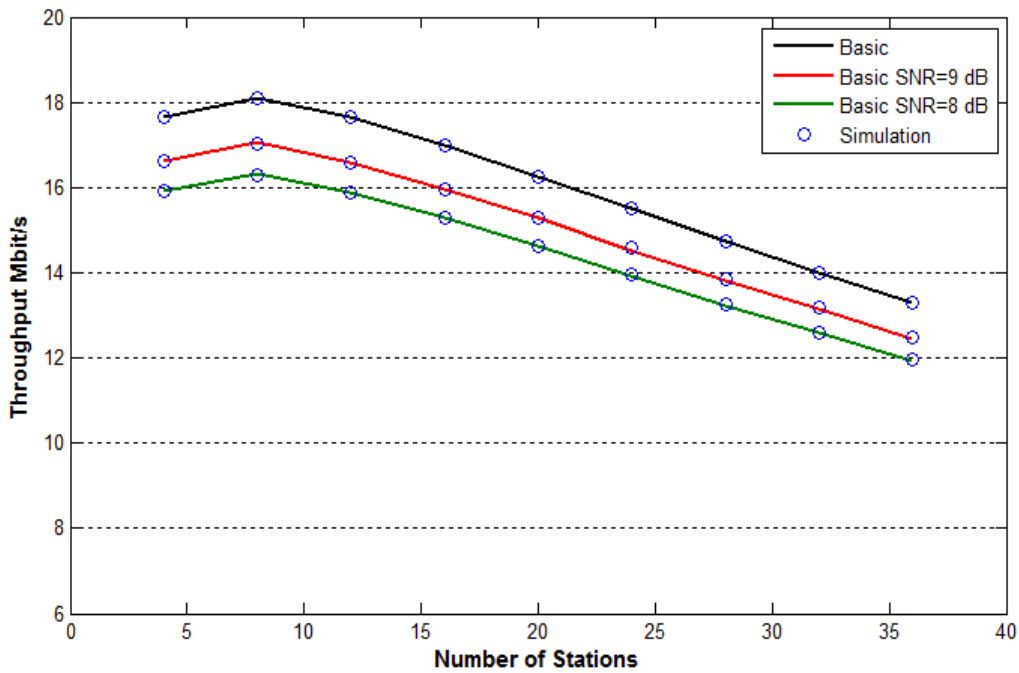


Figure 3-4: Total throughput vs. number of stations with SNR as a parameter with $p_1=0.05$

In the following test the effect of capture only is investigated, there are four traffic types (AC1, AC2, AC3 and AC4) and their throughputs are S_1 , S_2 , S_3 and S_4 respectively, with $M_1=M_2=M_3=M_4=5$ stations. Here again, when the value of p_1 varies, the values of p_2 , p_3 , p_4 are modified in order to achieve throughput ratios $S_1:S_2:S_3:S_4=8:4:2:1$ according to Hui's ratio [84]. Figure 3-5 shows the normalized throughput for 4 access categories and threshold, z , value of 5 dB. When the capture effect is taken into account, the system performance trend is similar to the basic p -persistent CSMA; as p_1 increases the throughput increases up to a point where the maximum throughput is reached.

The results show that when p_1 is less than 0.02 there is no significant difference between the case with capture and the case without. This is due to the small values of p_1 which results in fewer collisions in the system though the system efficiency and system capacity are very low. In Figure 3-5, $z = 5$ dB denotes results with capture, "Basic" denotes results without capture, and "Stot" refers to the total system throughput. At $p_1=0.05$ the total system throughput with

capture is improved by 18.3% while at higher p values, for example $p_1=0.09$, the throughput is improved by 40% when compared to the basic case. The improvement in system throughput is derived from the increase in the packet success rate due to capture, which reduces the amount of time spent in failed collision attempts.

This result demonstrates that in real systems the efficiency is higher than it appears in the basic systems, when the capture is not included. This increase in the efficiency means that the rate of decrease of the system throughput as p_1 moves away from the optimum value (i.e. the p value at maximum throughput) is less than for the basic case. This also means that in real systems a higher p values can be used which leads to more efficient system throughput performance.

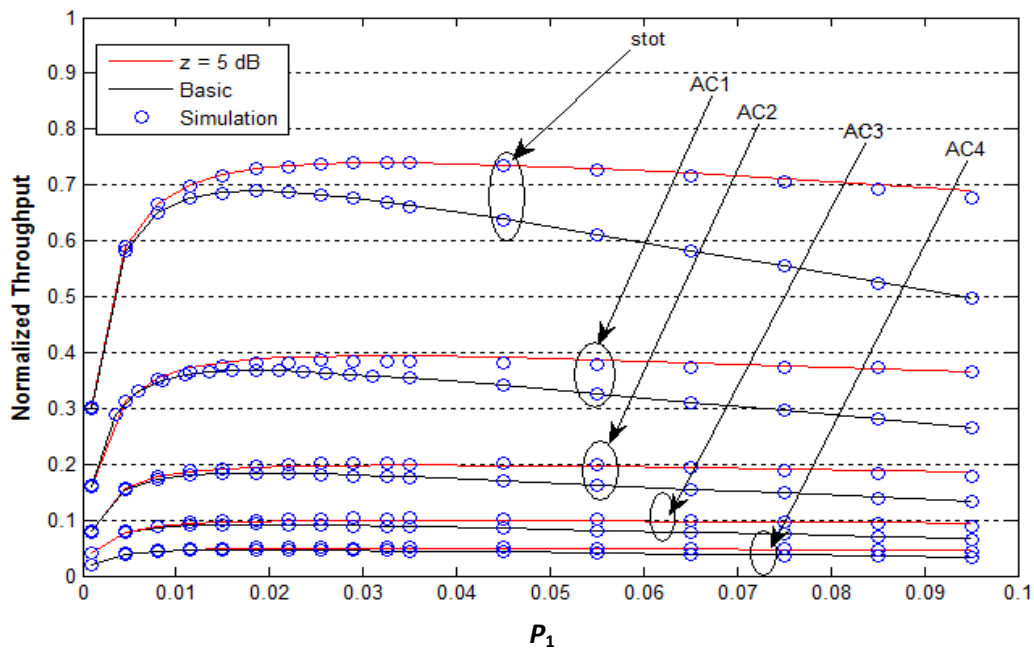


Figure 3-5: Normalised throughput vs p_1 for 5 stations per traffic type comparing capture with basic mode

In the following experiment, the effect of packet error rates and the capture effects are investigated. Figure 3-6a and b graph throughput versus number of stations with the capture

threshold and SNR as parameters. Four traffic types are again investigated with p_1 set to 0.05, which yields the maximum throughput for the same target throughput ratios used in Figure 3-5. The threshold, z , was set to 5 dB and the SNR values were 8 and 9 dB. Figure 3-6a compares the throughput of the differentiated p -persistent CSMA MAC protocol based on different approaches for four traffic types, while Figure 3-6b compares the total throughputs for the same scenario. The results show that at a low number of stations (less than 10) the packet error rate impact is visible on the system throughput at SNR equal to 8 dB where the throughput decreased by from 18 Mbit/s to 16.5 Mbit/s. The basic MAC achieves a maximum throughput of 18 Mbit/s with 8 stations whereas with capture only, the maximum throughput achieved is 19 Mbit/s.

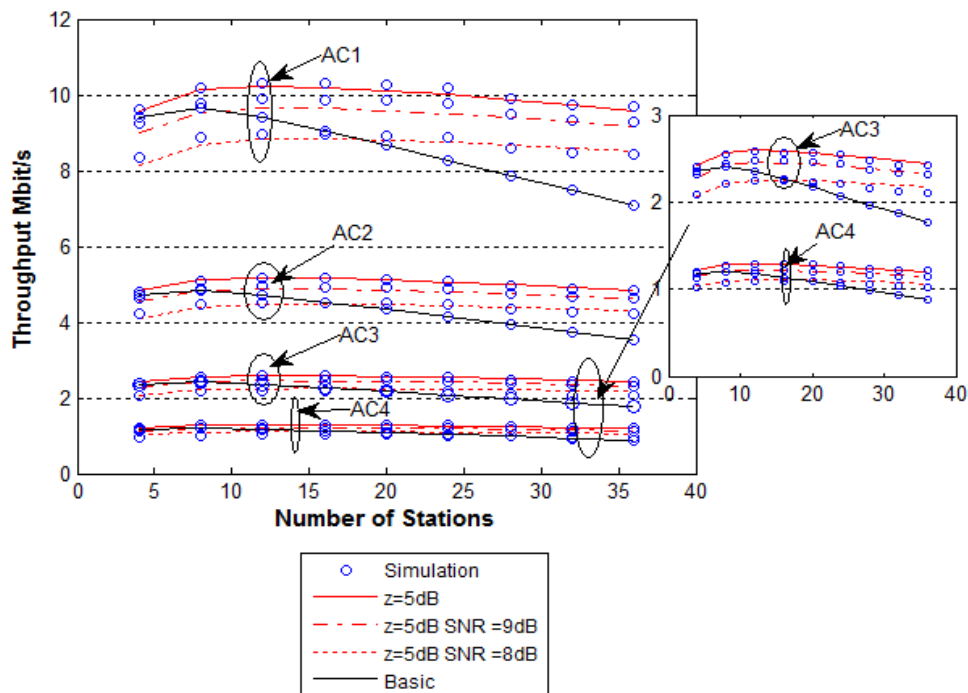


Figure 3-6a: Throughput per access categories vs. number of stations with SNR as a parameter for capture threshold $z=5$ dB and $p_1=0.05$

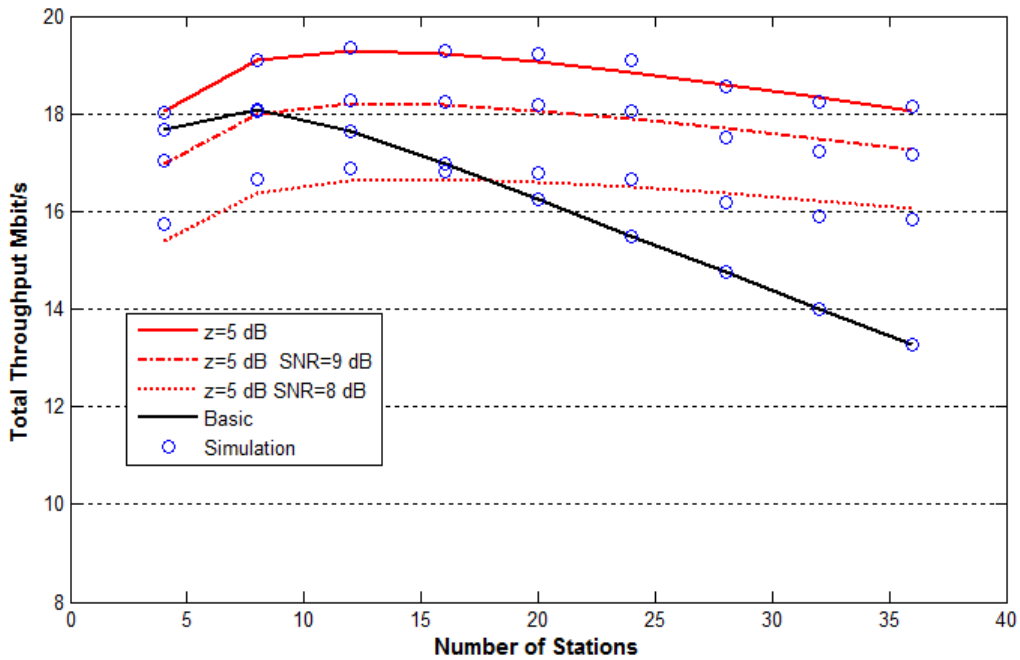


Figure 3-6b: Total throughput vs. number of stations with SNR as a parameter with $p_1=0.05$ and $z=5$ dB

Figure 3-7 compares the total throughput of four traffic types for capture threshold $z=2, 5$ and 10 dB with $SNR = 8$ dB. The results show that as the threshold increases from 2 dB to 10 dB, the absolute throughput is reduced. However, comparing to the basic mode throughput, for large numbers of contending users when the collision probability is high, the throughput with capture degrades more slowly even at low SNR values. For 36 contending stations and $z = 2$ dB, the system throughput is improved by 47% when compared to the basic throughput performance. At $z = 10$ dB, the system throughput is still improved by 20.7% . In contrast, when the number of contending stations is below 16 the throughput performance is dominated by the channel errors rather than collisions, such that the absolute throughput falls below the basic mode throughput at low SNR values.

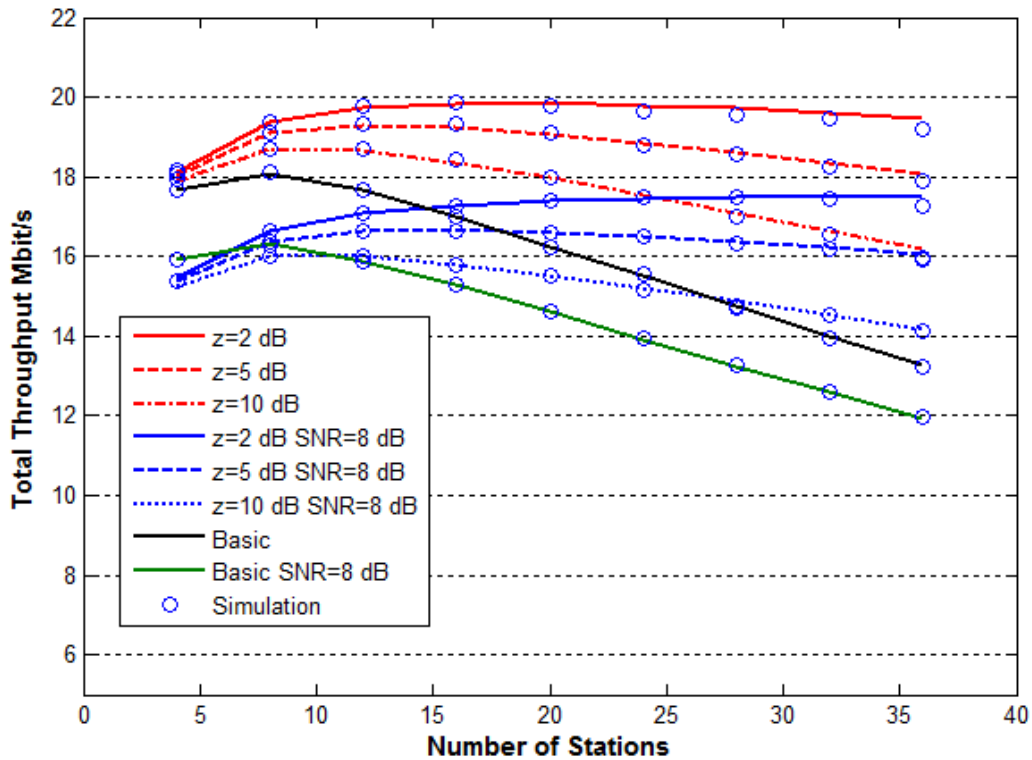


Figure 3-7: Total saturated throughput vs. number of contending stations with capture threshold z as a parameter for SNR=8 dB and $p_1=0.05$

The behaviour of the saturated throughput as a function of the channel SNR is depicted in Figure 3-8 for two access categories with z as a parameter. Curves are plotted for the 802.11n and 802.11a/g systems at data rates 26 and 24 Mbit/s, respectively, for $M_1=M_2=10$ contending stations and a payload size of 1500 bytes. With two ACs, the value of p_1 (i.e., high priority channel) was fixed at 0.05, while p_2 is varied in order to maintain $S_1:S_2 = 2:1$. By repeating the process, similar curves can be generated for other data rates, by using the PER versus SNR curves in Figures 3-3a and b.

From Figure 3-8, the results for the basic p -persistent CSMA protocol illustrate that the throughput reaches a maximum value of 14 Mbit/s in 802.11n for SNR > ~12 dB and just above 13 Mbit/s in 802.11a/g for SNR > 19 dB. When capture and packet errors are modelled, the maximum throughput attained increases to almost 20 Mbit/s in 802.11n and just above 18

Mbit/s in 802.11a/g for a capture threshold of $z=2$ dB. Importantly, 802.11n with capture and packet errors achieves a throughput of 14 Mbit/s at just below 7 dB SNR, which represents an operational SNR gain of just over 5 dB. 802.11a/g with capture and packet errors achieves a throughput of 13 Mbit/s at 12 dB SNR, representing an operational SNR gain of 7 dB. Though the maximum throughput decreases when the capture threshold is increased from 2 to 10 dB, corresponding to a reduction in capture probability, the operational SNR gains reduce from 5 to 4.25 dB in .11n and 7 to 5.5 dB in .11a/g. These results demonstrate that over the potential operating ranges of z , the model with capture and packet errors predicts significant performance improvement over the basic p -persistent CSMA model with moderate sensitivity to variations in z . Again, excellent agreement between simulated and theoretical results is obtained showing the validity of the mathematical model developed

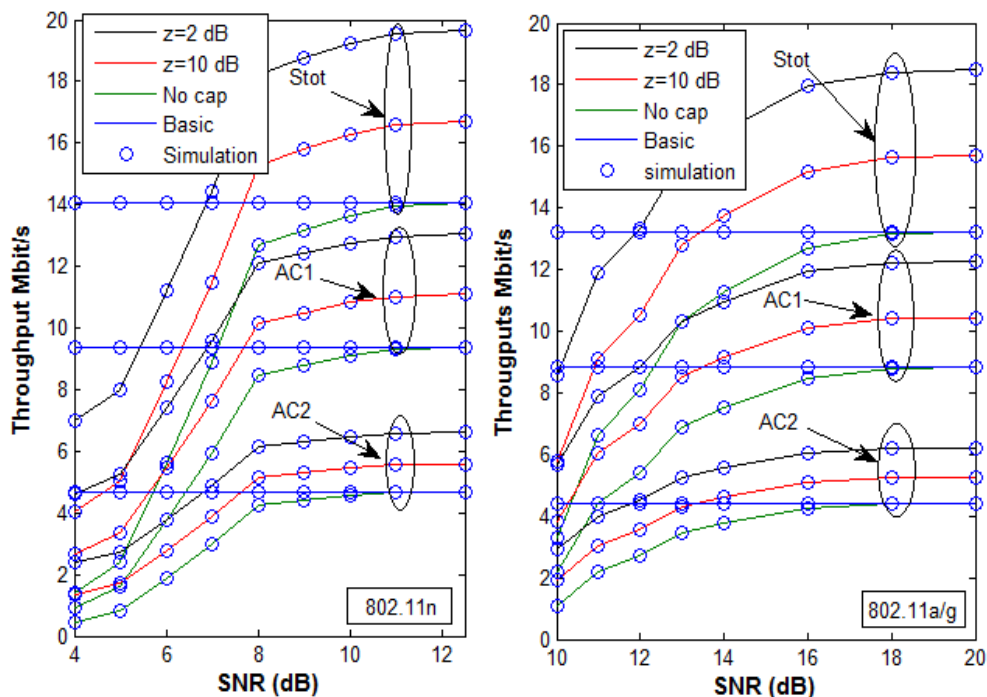


Figure 3-8: Saturated throughput vs. SNR for 802.11n and 802.11a/g with z as a parameter: 2 AC categories with $M_1=M_2=10$

3.6.2 Delay Results

The average delay is another important parameters in network optimisation for providing the required QoS. This experiment investigates the average delay of the QoS differentiated p -persistent CSMA protocol. A similar scenario to that in Figure 3-5 investigates the throughput performance. When the value of p_1 varies, the values of p_2 , p_3 , and p_4 are modified in order to achieve throughput ratios $S_1:S_2:S_3:S_4 = 8:4:2:1$ according to Hue's ratio. A similar trend to that in Figure 3-5 is obtained in Figure 3-9. When the capture effect is taken into account, the system delay performance decreases as p_1 increases until the minimum average delay is reached. For example, at $p_1=0.05$ the average delay of AC1 for the basic case decreased from 55 ms to 47 ms when the capture is included. This result demonstrates that capture extends the operating range of p_1 . Without capture a value of p_1 between 0.01 and 0.02 minimises delay across all ACs and from Figure 3-5 maximises throughput. However, this gives a restrictive range on p_1 when managing the overall network loads in differential mode. By modelling capture, we see that the operating range of p_1 can be increased from 0.01 to 0.05 in order to keep delays across ACs low and throughput high. This is important for the lower priority ACs which are more sensitive to the capture effect. The results shown in Figure 3-11 are obtained from the same throughput experiment in Figure 3-6. The results demonstrate the channel impacts on the required capture threshold as the number of stations varies. This result also demonstrates that at low load the packet error rates dominate the behaviour of the network and the delay is increased. When the network becomes heavily loaded the capture effect dominates the behaviour of the network due to a high collision rate in the network. From a network control perspective it is therefore important to model capture in differential mode in order to correctly optimise the delay throughput behaviour.

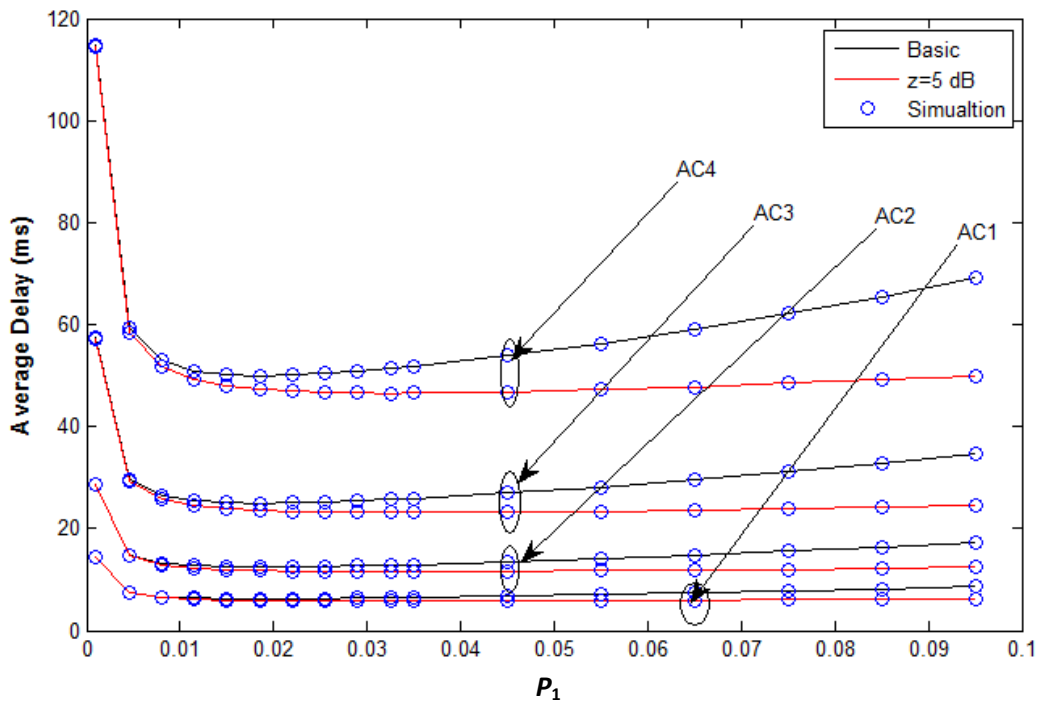


Figure 3-9: Average Delay vs p_1 for 5 stations per traffic type with $z=5$ dB

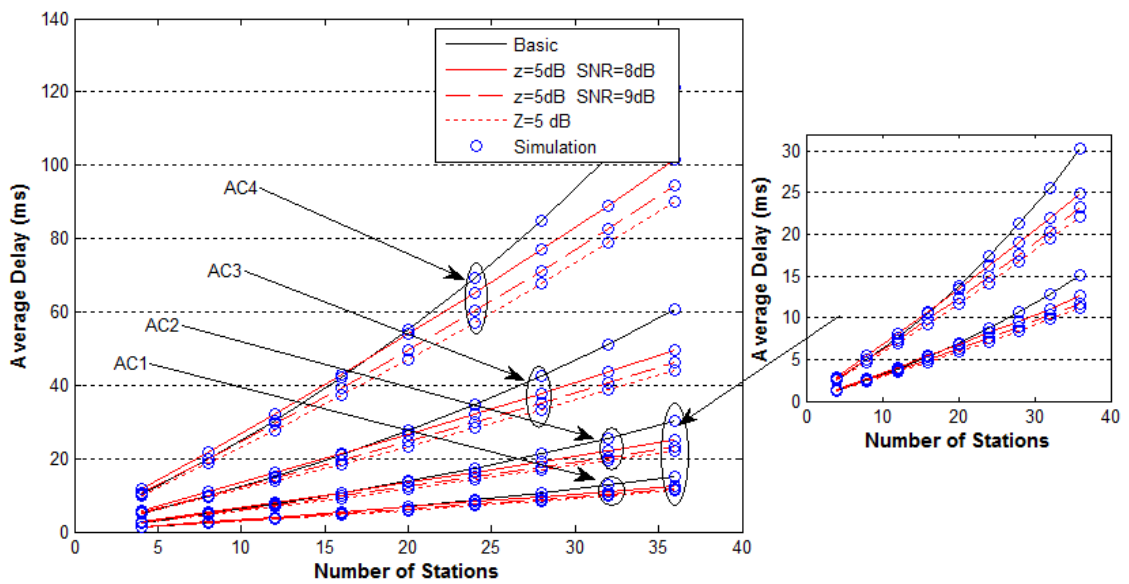


Figure 3-10: Average delay vs number of stations with SNR as a parameter and $p_1=0.05$ and capture threshold $z=5$ dB

3.7 WLAN Planning

Wireless LAN deployment is more complicated than wired network deployment due to the dynamic nature of the wireless channel that makes providing uninterrupted connectivity a challenging task. In general, deploying a WLAN requires consideration of five key issues: coverage, capacity, security, mobility and QoS required [87] [8]. To simplify deployment planning in WLANs, the capacity is evaluated for each cell independently, as a non-overlapping criterion between the cells is used during the planning phase which omits accounting for the interference between the adjacent APs. Calculating the optimum number of APs required in the network is a fundamental task in the network planning, based on the number of users and their QoS required in the network.

The mean throughput per user and per traffic type of service is obtained by dividing the average throughput of an AP by the number of users it covers at a given data rate. In [88], in order to estimate an optimal number of APs and their placement in the planning process, the Markovian analysis is used to evaluate the throughput for each AP with a differentiated QoS. This means that the throughput should be calculated accurately in order to achieve efficient network deployment. Accurate modelling of the key mechanisms that affects the throughput performance results in more valid network configurations. In this case study, two traffic types were considered with p_1 set to 0.05, and p_2 set to provide throughput ratio $S_1:S_2=2:1$. The throughput per user per traffic type, S_{du} , is calculated by $S_{du} = \frac{S_d}{M_d}$. Figure 3-11 compares throughput per user per traffic type with threshold, $z = 2$ dB and SNR= 9 dB, with the basic case at a data rate of 26 Mbit/s. The results show that when the capture effect and channel error rates are included, the AP can serve 12 users of traffic type 1 with QoS requirements of 1 Mbit/s, and 12 users of traffic type 2 with QoS requirements of 500kbit/s. For the basic case, the AP can only serve 9 users of traffic type 1 with QoS requirements of 1

Mbit/s, and 9 users of traffic type 2 with QoS requirements of 500Kbit/s. In total, when the capture effect is taken into account, the AP can serve 26 users while in the basic case it can only serve 18 users. This is equivalent to a 33% improvement in the capacity of the system meaning fewer APs should be deployed. Thus saving infrastructure costs and energy consumption. This result demonstrates that efficient network planning can be achieved with the use of our realistic model to calculate the throughput.

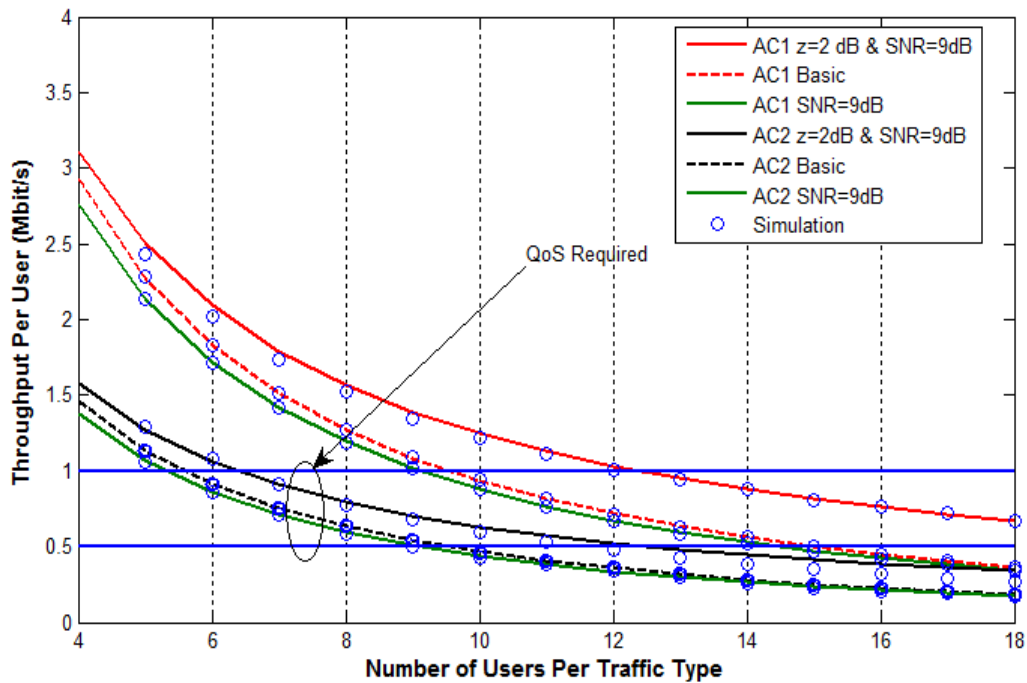


Figure 3-11: Saturated throughput per user as a function of number of users per traffic type with capture effect

3.8 Conclusions

In this chapter, we have developed a PHY/MAC cross-layer analytical model to consider the PHY layers effects, which include packet error rates and capture effect. Through MATLAB simulations, the interaction of the PHY/MAC layers throughput and delay was modelled more accurately than in the existing models. We have derived an analytical expression for the

throughput and delay of the QoS differentiated p -persistent CSMA protocol in the presence of multipath Rayleigh fading channel. This accuracy of the analytical model was validated by the PHY/MAC cross-layer simulation model. This approach offers an accurate characterisation of the performance of EDCA systems in a more realistic environment, with less complexity compared to the Markovian analytical models. The results showed that modelling the capture effect leads to more realistic network characterisation. In heavily loaded networks (36 stations), when the system includes 4 traffic types, the throughput is higher by 47% with threshold $\alpha=2$ dB compared to the basic case. The results clearly demonstrated the need to model the throughput and delay in the presence of the capture effect and channel error rates for heterogeneous networks, which is crucial for network design and deployment. An analytical approach for the performance of a QoS differentiated p -persistent CSMA in the case of non-saturated systems in the presence of channel errors and capture effect is developed in chapter 4.

Chapter 4

Non-Saturated Throughput and Delay Analysis of p -Persistent CSMA protocol

This chapter develops the QoS differentiated p -persistent CSMA protocol for the non-saturated case into an accurate and practical model that takes into account the impact of channel errors and the capture effect in a Rayleigh multipath fading environment. This builds up on the p -persistent CSMA model in chapter 3 by allowing the stations to be non-saturated. This is done by allowing each station to have a variable offered load, which accounts for heterogeneous loads and priorities. The developed model expresses the throughput/delay performance as a function of the number of stations, packet sizes, raw channel error rates and capture threshold. This advances on the analysis of the saturation case in chapter 3 by considering the case where the stations are non-saturated.

This chapter is organized as follows: The non-saturated system model of p -persistent CSMA with multiple traffic types is described in section 4-1. The throughput analysis of the p -persistent CSMA protocol follows in section 4-2. The corresponding delay analysis is provided in section 4-3. The numerical results for the system throughput are presented in section 4-4. The delay results are presented in section 4-5. An adaptive p -persistent CSMA

protocol is proposed in section 4-6. WLAN planning is presented in section 4-7. Finally, section 4-8 concludes the chapter.

4.1 System Model of p -CSMA protocol

The model in this analysis is based on the non-saturated model for slotted p -persistent CSMA in [70], which is modified to include the channel errors and capture effect. The model contains an Access Point (AP) giving coverage to M stations, where $M=M_1+M_2+\dots+M_{d_{max}}$, M_d represents the number of stations with type d traffic and d_{max} is the total number of traffic types in the system. All packets have a constant size and are transmitted within a unit of time. When any station commences a transmission it is from the beginning of a timeslot (a). An empty station of traffic type d will have an arrival with a probability of g_d at any timeslot or no arrival with a probability of $(1-g_d)$. The range of possible values of g_d are $(0 \leq g_d \leq 1)$. Non-empty stations will transmit at the beginning of the next time slot with a probability of p_d and defer with a probability of $(1-p_d)$. The p_d values for each traffic type are defined in a vector as $p = [p_1, p_2, \dots, p_{d_{max}}]$. The total normalised offered load in the system per unit of time is represented by G . This load, G , is shared between all traffic types in the system where the offered load of each traffic type, for example type d , is $Gr_d \times G$ where Gr_d is the offered load ratio among the traffic types and the possible range of its value are $(0 \leq Gr_d \leq 1)$ and $\sum_{d=1}^{d_{max}} Gr_d = 1$. The offered load per timeslot for traffic type d is calculated as $g_d = \min[(a \times Gr_d \times G/M_d), 1]$. The complete set of Gr_d values are defined in a vector as $Gr = [Gr_1, Gr_2, \dots, Gr_{d_{max}}]$. Figure 4-1 shows the basic model for two traffic types for simplicity. The dotted arrows represent an arrival of one traffic type while the full arrows represent an arrival from another traffic type. The channel alternates between idle period I (all stations are empty) and busy period B , which forms a regenerative cycle. When the packet arrives at any station, a busy period begins at the next time slot and ends if no packet has arrived during the

transmission. The transmission will be considered successful in if only one station commences a transmission at the start of the timeslot or the received power of the concerned packet that experiences a collision is higher than a threshold z , as explained in section 3-4.

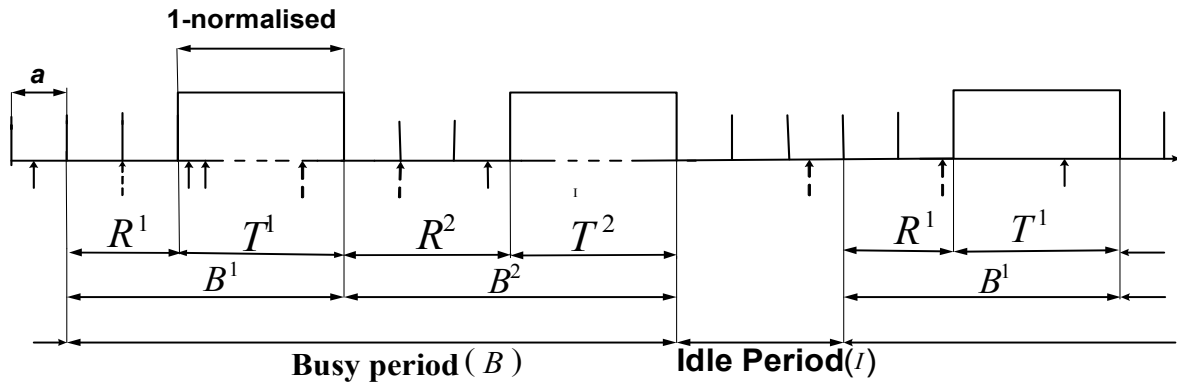


Figure 4-1: p -persistent CSMA Channel state cycle for saturated case

4.2 Throughput analysis

In this section, we present the mathematical analysis of the proposed model in section 4-1 for evaluating the throughput of a QoS differentiated p -persistent CSMA protocol under non-saturated conditions. The following assumptions are made: the number of stations is finite, the channel is prone to errors, and capture in a Rayleigh fading transmission scenario can occur. We start our analysis by summarising the basic throughput analysis in [70]. This is followed by a PHY/MAC cross-layer analytical model for QoS differentiated p -persistent CSMA with the capture effect.

4.2.1 Basic p -persistent CSMA

In this section the non-saturated throughput analysis in [70] is summarised. In [70] the throughput S_d of p -persistent CSMA for traffic type d was calculated using (4-1).

$$S_d = \frac{b \cdot \bar{U}_d}{\bar{B} + \bar{I}} \quad (4-1)$$

Here, \bar{U}_d is the average time of useful transmission of traffic type d , and b represents the fraction of each successful transmission period which contains useful data. The overall channel throughput can be calculated by (4-2).

$$S = \sum_{d=1}^{d_{max}} S_d \quad (4-2)$$

The j th busy subperiod B^j consists of deferral time R^j and unity transmission time T^j ; hence, B^j can be calculated as $B^j = R^j + 1$ for $j=1,2,\dots, \infty$, and the expected value of B^j can be calculated by (4-3).

$$E[B^j] = E[R^j] + 1 \quad (4-3)$$

J represents the number of busy subperiods in each busy period, so B can be defined as $B = \sum_{j=1}^J B^j$ and $U_d = \sum_{j=1}^J U_d^j$. The probability that the busy period is a particular length forms a geometric distribution, which can be calculated by (4-4).

$$\bar{J} = \frac{1}{\prod_{d=1}^{d_{max}} (1 - g_d)^{(1/a)M_d}} \quad (4-4)$$

\bar{B} and \bar{U}_d can be calculated as in [1,2] by (4-5) and (4-6) respectively.

$$\bar{B} = E[B^1] + (\bar{J} - 1)E[B^2] \quad (4-5)$$

$$\bar{U}_d = E[U_d^1] + (\bar{J} - 1)E[U_d^2] \quad (4-6)$$

$E[B^j]$ and $E[U^j]$ are independent for $j=1$ and are independent and identically distributed for

$j=2, 3, \dots, J$; thus $E[B^1]$ and $E[U^1]$ are used to represent $E[B^j]$ and $E[U^j]$ respectively for $j=1$. Also, $E[B^2]$ and $E[U^2]$ are used to represent $E[B^j]$ and $E[U^j]$ respectively for $j=2, 3, \dots, J$. This concept holds for any variable superscripted with j throughout the analysis in this chapter (i.e. any variable with superscript 1 means $j=1$ and superscript 2 means $j=2, 3, \dots, J$, which determine the value of X_j in (4-8)).

The probability that an idle period is a particular length, k timeslots, also forms a geometric distribution which can be calculated by (4-7).

$$\bar{I} = \frac{a}{1 - \prod_{d=1}^{d_{max}} (1 - g_d)^{M_d}} \quad (4-7)$$

In order to calculate $E[R^j]$ or $E[U^j]$, the probability distributions for the number of packets of each traffic type that are waiting for transmission at the beginning of the j th busy subperiod must be calculated. The number of timeslots that these packets can accumulate over before the j th busy subperiod commences is X_j , where X_j is as shown in (4-8).

$$X_j = \begin{cases} 1 & \text{if } j=1 \\ 1/a & \text{if } j=2,3,\dots \end{cases} \quad (4-8)$$

The number of type d stations that have a packet to transmit over X_j is represented by $N_{0,d}^j$ the index 0 refers to X_j period and d refers to the traffic type. The probability that $N_{0,d}^j = n$ is given by (4-9), as in [70].

$$P(N_{0,d}^j = n) = \binom{M_d}{n} [1 - (1 - g_d)^{X_j}]^n (1 - g_d)^{X_j(M_d - n)} \quad (4-9)$$

The number of non-empty type d stations when $R_d^j \geq ka$ is $N_{k,d}^j$. The probability that $R_d^j \geq ka$ when $N_{k,d}^j = n + m$ is calculated given that $N_{0,d}^j = n$, as shown in (4-10).

$$\begin{aligned}
P(R_d^j \geq ka, N_{k,d}^j = n + m | N_{0,d}^j = n) \\
= (1 - p_d)^{kn} (1 - g_d)^{k(M_d - n)} \binom{M_d - n}{m} \left(\frac{g_d}{p_d - g_d} \right)^m \left[1 - \left(\frac{1 - p_d}{1 - g_d} \right)^k \right]^m \quad (4-10)
\end{aligned}$$

In order to calculate the distribution R^j , the distributions for R_d^j which represent the deferral time for traffic type d is given by (4-11).

$$\begin{aligned}
P(R^j \geq ka) = \frac{[(\prod_{d=1}^{d_{max}} P(R_d^j > ka)) - (\prod_{d=1}^{d_{max}} P(R_{0,d}^j > ka))]}{1 - \prod_{d=1}^{d_{max}} (1 - g_d)^{M_d X_j}} \\
k = 0, 1, 2, \dots, \infty \quad (4-11)
\end{aligned}$$

Where $P(R_d^j > ka)$ and $P(R_{0,d}^j > ka)$ are calculated as shown in (4-12) and (4-13), respectively.

$$\begin{aligned}
P(R_d^j \geq ka) = \left[(1 - p_d)^k - (1 - g_d)^{X_j} p_d \left(\frac{(1 - p_d)^k - (1 - g_d)^k}{p_d - g_d} \right) \right]^{M_d} \\
k = 0, 1, 2, \dots, \infty \quad (4-12)
\end{aligned}$$

$$\begin{aligned}
P(R_{0,d}^j \geq ka) = \left[(1 - g_d)^{X_j} \left(\frac{p_d(1 - g_d)^k - g_d(1 - p_d)^k}{p_d - g_d} \right) \right]^{M_d} \\
k = 0, 1, 2, \dots, \infty \quad (4-13)
\end{aligned}$$

$E[R^j]$ can be calculated by evaluating (4-13) over the range $k = 1, 2, \dots, \infty$ as shown in (4-14).

$$E[R^j] = a \sum_{k=1}^{\infty} P(R^j \geq ka) \quad (4-14)$$

$\bar{B} + \bar{I}$ represents the average time of the regenerative cycle that contains an average time of the busy period B and the idle period I , and can be calculated by (4-15).

$$\bar{B} + \bar{I} = \frac{(1 + a \sum_{k=1}^{\infty} (\prod_{d=1}^{d_{max}} P(R_d^2 \geq ka)))}{\prod_{d=1}^{d_{max}} (1 - g_d)^{M_d(1/a)}} \quad (4-15)$$

From this point we calculate the throughput for traffic type $d = 1$. However, this analysis can be applied to any of the traffic types in the system by simple substitution.

In order to calculate the throughput of traffic type 1, the probability of successful transmission of traffic type 1 $P(s_1^j)$ should be calculated as shown in (4-16).

$$P(s_1^j) = \frac{[(P(1tx_1^j) \prod_{d \neq 1} P(0tx_d^j)) - (P(1tx_{0,1}^j) \prod_{d \neq 1} P(0tx_{0,d}^j))]}{1 - \prod_{d=1}^{d_{max}} (1 - g_d)^{M_d X_j}} \quad (4-16)$$

$k = 0, 1, 2, \dots, \infty$

$P(1tx_{0,1}^j)$ denotes to the probability that only one type 1 station transmits in a particular timeslot and is calculated by (4-17).

$$\begin{aligned}
P(1tx_1^j) &= M_1 p_1 \left[(1 - p_1)^k \right. \\
&\quad \left. - (1 - g_1)^{x_j} \left(\frac{p_1(1 - g_1)^k - g_1(1 - p_1)^k}{p_1 - g_1} \right) \right] \left[(1 - p_1)^{k+1} \right. \\
&\quad \left. - (1 - g_1)^{x_j} p_1 \left(\frac{p_1(1 - g_1)^{k+1} - g_1(1 - p_1)^{k+1}}{p_1 - g_1} \right) \right]^{M_1 - 1} \\
k &= 0, 1, 2, \dots, \infty
\end{aligned} \tag{4-17}$$

$P(1tx_{0,1}^j)$ is the probability of transmission of only one type 1 station transmitting when $N_{0,1}^j = 0$ and is calculated by (4-18).

$$\begin{aligned}
P(1tx_{0,1}^j) &= M_1 p_1 g_1 (1 - g_1)^{M_1 x_j} \left(\frac{(1 - g_1)^k - (1 - p_1)^k}{p_1 - g_1} \right) \cdot \left(\frac{p_1(1 - g_1)^{k+1} - g_1(1 - p_1)^{k+1}}{p_1 - g_1} \right)^{M_1 - 1} \\
k &= 0, 1, 2, \dots, \infty
\end{aligned} \tag{4-18}$$

$P(0tx_d^j)$ represents the probability of no transmission occurring in a particular timeslot for each traffic type d station where $d \neq 1$, and is given by (4-19).

$$\begin{aligned}
P(0tx_d^j) &= \left[(1 - p_d)^{k+1} - (1 - g_d)^{x_j} p_d \left(\frac{(1 - p_d)^{k+1} - (1 - g_d)^{k+1}}{p_d - g_d} \right) \right]^{M_d} \\
k &= 0, 1, 2, \dots, \infty
\end{aligned} \tag{4-19}$$

$P(1tx_{0,d}^j)$ is the probability of transmission of type 1 when $N_{0,d}^j = 0$ and is calculated by (4-20).

$$P(1tx_{0,d}^j) = \left[(1 - g_d)^{x_j} \left(\frac{p_d(1 - g_d)^{k+1} - g_d(1 - p_d)^{k+1}}{p_d - g_d} \right) \right]^{M_d} \quad (4-20)$$

$$k = 0, 1, 2, \dots, \infty$$

By evaluating (4-16) over range $k = 0, 1, 2, \dots, \infty$, the expected time spent on successful transmission of traffic type 1, $E[U_1^j]$, can be calculated as in (4-21).

$$E[U_1^j] = \sum_{k=0}^{\infty} P(s_1^j) \quad (4-21)$$

\bar{U}_1 can be calculated using (4-4), (4-6) and (4-21) as shown in (4-22).

$$\bar{U}_1 = \frac{\sum_{k=0}^{\infty} (P(1tx_1^2) \prod_{d \neq 1} P(0tx_d^2))}{\prod_{d=1}^{d_{max}} (1 - g_d)^{M_d(1/a)}} \quad (4-22)$$

Finally, using (4-1), (4-15) and (4-22) the throughput of traffic type 1 can be calculated as shown in (4-23).

$$S_1 = \frac{b \sum_{k=0}^{\infty} (P(1tx_1^2) \prod_{d \neq 1} P(0tx_d^2))}{1 + a \sum_{k=1}^{\infty} (\prod_{d=1}^{d_{max}} P(R_d^2 \geq ka))} \quad (4-23)$$

4.2.2 p -persistent CSMA with PHY layer effects

This section presents the interaction between PHY and MAC layers in the same way as in chapter 3. To establish this interaction between the two layers, the probability of successful traffic type d , $P(s_d^j)$, in the basic MAC layer analysis must be replaced by the probability of successful traffic type d , $P(s_d^j phy)$, with PHY layer effects in terms of packet error rate and

capture effect. This probability is the sum of the probability of a successful traffic type d transmission, $P(s_d^j pe)$, when only one packet is received in the presence of channel errors and the probability of a successful traffic type d transmission, $P(s_d^j cap)$, when the packet is collided with one or more packets in the system but still can be received successfully by the receiver. For M stations in the system with traffic type d , we can write:

$$P(s_d^j phy) = P(s_d^j pe) + P(s_d^j cap) \quad (4-24)$$

In order to include the packet error rates into the analysis, the probability that a packet of traffic type 1 ($d = 1$) is received successfully in an error-prone channel without any collisions from other packets in the system is calculated by modifying equation (4-16) as shown in (4-25).

$$P(s_1^j pe) = P(s_1^j) \times (1 - P_e^1) \quad (4-25)$$

Here, P_e^1 is the PER of a MAC data packet for stations with traffic type 1.

The major difference between this analysis and the model in [70], is calculating the probability of successful transmissions in the event that more than one station transmits a packet at the same time. Based on that probability, the probability that one of these packets captures the channel is calculated. In order to include the capture effect in the analysis, the probability that more than one station of traffic type 1 transmit at the same time in a particular timeslot of the j th busy subperiod, $P(\beta_1 tx_1^j)$, can be calculated given that $R_1^j \geq ka$, $N_{k,1}^j = n + m$, and $N_{0,1}^j = n$ as shown in (4-26).

$$P(\beta_1 tx_1^j | R_1^j \geq ka, N_{k,1}^j = n + m, N_{0,1}^j = n) = \binom{n + m}{\beta_1} (p_1)^{\beta_1} (1 - p_1)^{n+m-\beta_1} \quad (4-26)$$

Equation (4-26) can be unconditioned of $(\beta_d tx_d^j | R_d^j \geq ka, N_{k,d}^j = n + m)$ using (4-10), which produces $P(\beta_1 tx_1^j | N_{0,1}^j = n)$ as shown in (4-27). This means that $P(\beta_1 tx_1^j)$ is now only conditioned on $N_{0,1}^j = n$.

$$\begin{aligned}
P(\beta_1 tx_1^j | N_{0,1}^j = n) &= \sum_{m=0}^{M_1-n} \binom{n+m}{\beta_1} (p_1)^{\beta_1} (1-p_1)^{n+m-\beta_1} (1-p_1)^{kn} (1 \\
&\quad - g_1)^{k(M_1-n)} \binom{M_1-1}{m} \left(\frac{g_1}{p_1-g_1} \right)^m \left[1 - \left(\frac{1-p_1}{1-g_1} \right)^k \right]^m \quad (4-27)
\end{aligned}$$

Using (4-9), (4-27) can be unconditioned of $N_{0,1}^j = n$ using by evaluating over the range of possible values for $N_{0,1}^j$ which is from 0 to M_1 . This produces $P(\beta_d tx_d^j)$ as shown in (4-28).

$$\begin{aligned}
P(\beta_1 tx_1^j) &= \sum_{n=0}^{M_1} \sum_{m=0}^{M_1-n} \binom{n+m}{\beta_1} (p_1)^{\beta_1} (1-p_1)^{n+m-\beta_1} (1-p_1)^{kn} (1 \\
&\quad - g_1)^{k(M_1-n)} \binom{M_1-1}{m} \left(\frac{g_1}{p_1-g_1} \right)^m \left[1 - \left(\frac{1-p_1}{1-g_1} \right)^k \right]^m \binom{M_1}{n} [1 \\
&\quad - (1-g_1)^{X_j}]^n (1-g_1)^{X_j(M_1-n)} \quad (4-28)
\end{aligned}$$

In order to remove the condition that $N_{0,1}^j = 0$ equation (4-26) should be unconditioned by (4-9) and evaluating both equations over range $N_{0,1}^j = 0$. This produces $P(\beta_d tx_{0,d}^j)$ as shown in (4-29). The reason for this is that the condition $N_{0,1}^j = 0$ means that the j th busy subperiod will not occur.

$$\begin{aligned}
P(\beta_1 tx_{0,1}^j) = \\
\sum_{m=0}^{M_1-n} \binom{m}{\beta_1} (p_1)^{\beta_1} (1-p_1)^{m-\beta_1} (1-g_1)^{k(M_1)} \binom{M_1-1}{m} \left(\frac{g_1}{p_1-g_1}\right)^m (1-g_1)^{X_j(M_1)}
\end{aligned} \tag{4-29}$$

Using equations (4-28) and (4-29), the probability of success for traffic type 1 can be calculated as shown in (4-30).

$$\begin{aligned}
P(s_1^j cap) = \frac{1}{1 - \prod_{d=1}^{d_{max}} (1-g_d)^{M_d X_j}} \\
\times \sum_{\beta_1=2}^{M_1} \sum_{\beta_2=0}^{M_2} \dots \sum_{\beta_{d_{max}}=0}^{M_{d_{max}}} \left[\left(\prod_{d=1}^{d_{max}} P(\beta_d tx_d^j) - \prod_{d=1}^{d_{max}} P(\beta_d tx_{0,d}^j) \right) \beta_1 q((\beta \right. \\
\left. - 1) | z_1) \right]
\end{aligned} \tag{4-30}$$

The $\prod_{d=1}^{d_{max}} P(\beta_d tx_d^j)$ term represents the probability of a transmission for all combinations of values of $N_{k,d}^j$ and $N_{0,d}^j = n$ that each traffic type may have. The $\prod_{d=1}^{d_{max}} P(\beta_d tx_{0,d}^j)$ term excludes the scenario where $N_{0,d}^j = 0$ in the case of the j th subperiod will not have occurred.

The $\frac{1}{1 - \prod_{d=1}^{d_{max}} (1-g_d)^{M_d X_j}}$ term includes the condition that j th busy subperiod will occur.

$E[U_{1_phy}^j]$ represents the expected time spent on successful type1 transmissions with PHY layer effects. $E[U_{1_phy}^j]$ can be now calculated by adding (4-25) and (4-30) and evaluate them over the range $k = 0, 1, 2, \dots, \infty$ as shown in (4-31).

$$E[U_{1_phy}^j] = \sum_{k=0}^{\infty} (P(s_d^j pe) + P(s_1^j cap)) \tag{4-31}$$

The throughput of traffic type 1 can be calculated by substituting (4-31) into (4-6) and then

substituting in (4-1) and also substituting (4-15) in (4-1).

$$S_{1_phy} = \frac{b_1 \sum_{k=0}^{\infty} [P(s_d^j pe) + P(s_1^j cap)]}{1 + a \sum_{k=1}^{\infty} (\prod_{d=1}^{d_{max}} P(R_d^2 \geq ka))} \quad (4-32)$$

4.3 Delay Analysis of p -persistent CSMA with PHY Effects

In this analysis, the delay is defined as the time from when a new packet arrives at a specific station until this packet has been received successfully. The delay is calculated for a particular station of traffic type 1 and this station is called the current station. $P_{s,1}^j$ denotes the probability of the current station transmitting successfully in the j th busy subperiod in the presence of PHY layer effects, as given by (4-33).

$$P_{s,1}^j = \frac{\sum_{k=0}^{\infty} P(s_d^j phy)}{M_1} \quad (4-33)$$

In this analysis, all packets that are not successfully received are assumed to be rescheduled until all have been successfully received and the rescheduled packets are assumed to be virtually buffered.

$P_{PreX,1}^j$ represents the probability that the current station has a packet during the X_j period, as shown in (4-34). The current station is the station whose delay is being calculated.

$$P_{PreX,1}^j = \frac{\sum_{v=0}^{X_j-1} g_1 (1 - g_1)^v}{1 - \prod_{d=1}^{d_{max}} (1 - g_d)^{M_d X_j}} \quad (4-34)$$

$P_{PostX,1}^j$ represents the probability that the current station did not have a packet during the X_j period and is shown in (4-35).

$$P_{PostX,1}^j = \frac{(1 - P_{startPreX,1}^j) \sum_{k=0}^{\infty} g_1 (1 - g_1)^k P(R^{j*} \geq (k + 1)a)}{(1 - [(1 - g_1)^{(M_1-1)X_j} \prod_{d \neq 1} (1 - g_d)^{M_d X_j}]})} \quad (4-35)$$

R^{j*} refers to the situation when the current stations have no involvement in the j th busy subperiod. For more details about how R^{j*} is calculated refer to [70]. The probability that the current station is involved in the j th busy subperiod, $P_{i,1}^j$, can be calculated by (4-36).

$$P_{i,1}^j = P_{PreX,1}^j + P_{PostX,1}^j \quad (4-36)$$

The probability that the current station fails to transmit a packet successfully given that it is involved in the j th busy subperiod is given by (4-37).

$$P_{fail,1}^j = 1 - \frac{P(s_d^j phy)}{P_{i,1}^j} \quad (4-37)$$

$E[D_{new,1}^j]$ is the expected time from when the packet first arrives for the j th busy subperiod until the start of T^j and is calculated as in (4-38).

$$E[D_{new,1}^j] = \frac{E[D_{preX,1}^j] P_{PreX,1}^j}{P_{i,1}^j} + \frac{E[D_{postX,1}^j] P_{PostX,1}^j}{P_{i,1}^j} \quad (4-38)$$

Where $E[D_{preX,1}^j]$ and $E[D_{postX,1}^j]$ are the expected delays in the j th busy subperiod from the arrival of the packet until the beginning of T^j , given that the packet arrives during X_j and R^{j*} respectively and can be calculated as shown in (4-39) and (4-40).

$$E[D_{preX,1}^j] = \frac{a}{(1 - \prod_{d=1}^{d_{max}} (1 - g_d)^{M_d X_j}) P_{PreX,1}^j} \left\{ \sum_{v=0}^{X_j-1} g_1 (-g_1)^v \right. \\ \left. \left[(X_j - v) + \sum_{k=1}^{\infty} (1 - p_1)^k \prod_{d=1}^{d_{max}} P(R_d^{j*} \geq ka) \right] \right\} \quad (4-39)$$

$$E[D_{postX,1}^j] = \frac{a(1 - P_{PreX,1}^j)}{(1 - [(1 - g_1)^{(M_1-1)X_j} \prod_{d \neq 1} (1 - g_d)^{M_d X_j}]) P_{startPreX,1}^j} \cdot \sum_{k=0}^{\infty} [g_1 (1 - g_1)^k P(R^{j*} \geq ka) \cdot \left(1 + \sum_{y=k+2}^{\infty} \frac{(1 - p_1)^{y-(k+1)} P(R^{j*} \geq ka)}{P(R^{j*} \geq ka)} \right)] \quad (4-40)$$

Now the expected delay experienced by a packet from when it arrives at the current station for first time until the start of the next transmission can be calculated as shown in (4-41).

$$E[D_{new,1}] = \frac{(E[D_{new,1}^1] P_{i,1}^1)}{(P_{i,1}^1 + (\bar{J} - 1) P_{i,1}^2)} + \frac{(E[D_{new,1}^2] (\bar{J} - 1) P_{i,1}^2)}{(P_{i,1}^1 + (\bar{J} - 1) P_{i,1}^2)} \quad (4-41)$$

The probability that the current station has a successful transmission at any busy subperiod, $P(s_{d^j}^{phy})$, is given by (4-42).

$$P(s_d^j phy) = \frac{P(s_d^1 phy) + (\bar{J} - 1)P(s_d^2 phy)}{\bar{J}} \quad (4-42)$$

The probability of the required number of further busy subperiods until the current station has a successful transmission, N_R , is f and forms a geometric distribution. \bar{N}_R can be calculated as shown in (4-43).

$$P(N_R = f) = \left(1 - P_{sphy,1}\right)^{f-1} P_{sphy,1}, \quad f = 0, 1, 2, \dots, \infty$$

$$\bar{N}_R = \frac{1}{P_{s,1}} \quad (4-43)$$

The retransmission delay, $\bar{D}_{r,1}$, is the time from the end of the busy subperiod of the first attempt of the current station to send a packet, until the end of the busy subperiod when the packet is successfully transmitted and can be calculated by (4-44).

$$\bar{D}_{r,1} = \frac{P_{fail,1}}{\bar{J} P_{sphy,1}} (\bar{J} + E[R^1] + 1) + \frac{P_{fail,1}(\bar{J} - 1)}{\bar{J} P_{s,1}} (E[R^1] + 1) \quad (4-44)$$

Using (4-38) and (4-44), the total end to end delay with PHY layer effects for a packet at the current station can be calculated as shown in (4-45).

$$\bar{D}_1(phy) = E[D_{new,1}] + \bar{D}_{r,1} \quad (4-45)$$

4.4 Numerical results and discussion

The MATLAB simulator that was developed to simulate the saturation case in chapter 3 was modified to model the system described in section 4-1, where a new function called IDLE is added to simulate the idle period. This section is divided into two subsections. The first subsection presents non-saturated throughput results, while the second subsection provides the results for delay. The results include the effects of packet error rate, the capture effect and demonstrate the PHY layer effect in terms of the packet error rates and capture effect.

4.4.1 Throughput Results

In this section, we provide three different sets of results. In the first set the effect of packet error rate is presented, followed by the results for the capture effect and finally the PHY/MAC interaction is demonstrated.

A. Packet Error Rate Effect

The throughput performance of QoS differentiated p -persistent CSMA with variable traffic loads in an error-prone channel for 4 traffic types [AC1, AC2, AC3, AC4] is investigated. For all the tests $M_1=M_2=M_3=M_4=5$. All the parameters used in the analysis and simulations are shown in Table 4-1. In all figures, the term "Basic" in the legend refers to p -persistent CSMA in an error-free channel and "S" refers to throughput with an index to access category number. In this set of results, the effect of channel error on the non-saturated throughput performance with heterogeneous priorities is investigated. In this test $p = [0.1, 0.05, 0.025, 0.0125]$ and $G_r = [0.25, 0.25, 0.25, 0.25]$. The results in Figure 4-2 shows that for SNR = 7dB, as the traffic loads increase the throughput degradation increases from 15 % at $G = 0.1$ up to 23% at G higher than 10. This result demonstrates that the system behaviour can be characterized by three main parameters: the p values, the G_r values and the channel errors.

Table 4-1 p -persistent CSMA parameters

Parameter	Value	Parameter	Value
Data rate	26 Mbit/s	a	9/567
Payload size	1500 byte	b	0.81
Payload duration	461 μ s	T	567 μ s

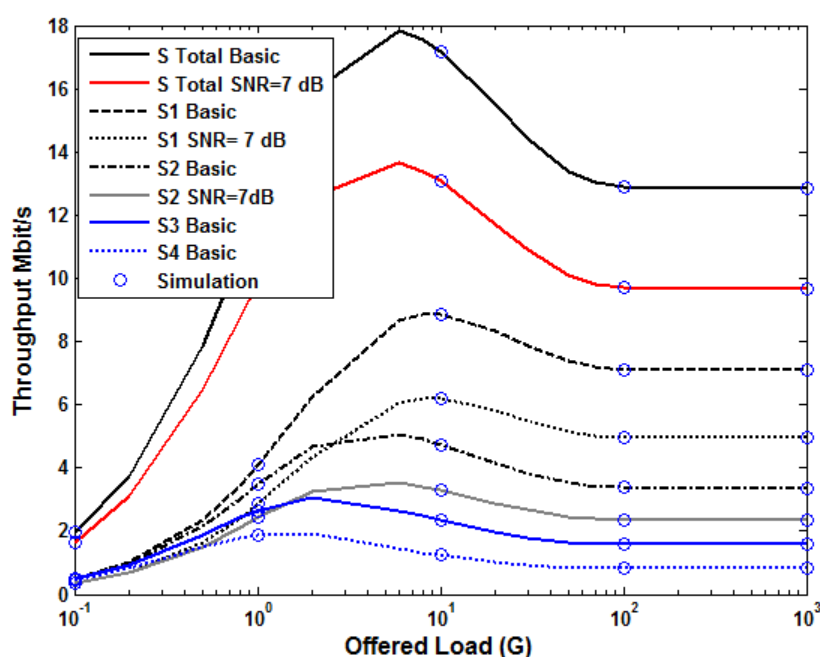


Figure 4-2: Throughput with heterogeneous priorities at data rate 26 Mbit/s and SNR= 7 dB

In order to show the system behaviour more clearly, the next set of results show the throughput performance versus p value and the offered load G for 5 stations per traffic type. $G_r = [8/15, 4/15, 2/15, 1/15]$ respectively. In this experiment, the channel condition of each traffic type is at SNR = 7 dB. The results in Figure 4-3 demonstrate that in order to improve the throughput performance in an error-prone channel, small p values should be used. In the case of an error-free channel, at low offered loads high p values should be used while at high offered loads small p values should be adopted.

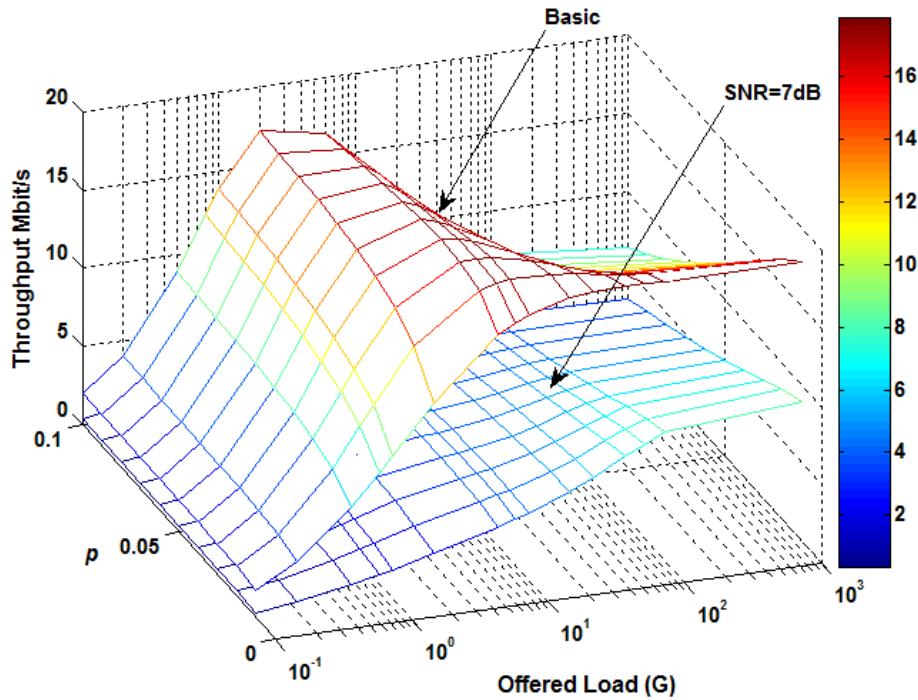


Figure 4-3: Total throughput with heterogenous traffic loads versus p values

B. Capture Effect

In the first experiment, two traffic types are considered. In the experiment $M_1 = M_2$ and the transmit rate is at 26Mbit/s. The parameters used in this section are shown in Table 4-1. The first set of results show the throughputs for traffic types 1 and 2 (S_1 and S_2 respectively) for a network with 5 stations per traffic type where the traffic types have heterogeneous priorities. In this system $p_1 = 0.1$, $p_2 = 0.05$ and $Gr_1 = Gr_2 = 0.5$. Figure 4-4 shows that when the offered load, G , is less than 1 there is no noticeable difference between the two cases (i.e. with and without the capture effect). This is due to the low chance of collisions as there is little traffic in the network. However, as G increases the difference between the two cases increases and reaches the maximum when the network is saturated. Comparing the performance of this new model with the capture effect to the model in [70] we can see, for example, that at $G = 10$ the throughput of traffic type 1 is increased by 12% while the throughput of traffic type 2 is

increased by 19%. As saturation is approached, the throughput of both traffic types is increased by around 22% when capture effect is considered, compared to the case when the capture is ignored.

The second set of results illustrate this new model in the case of heterogeneous loads. Figure 4-5 shows the results for a network of 5 stations per traffic type with heterogeneous loads. Here $p_1 = p_2 = 0.1$, $Gr_1 = 0.75$ and $Gr_2 = 0.25$. The same trends are shown as with the heterogeneous priorities example; as G increases the capture effect shows increasing throughput gains compared to the model with a perfect channel. Again, when comparing the performance of this new model to that in [70] we see that the throughput of traffic type 1 and 2 are increased by 19% and 21% respectively at $G=10$ and when the system is saturated both throughputs are increased by 41% .

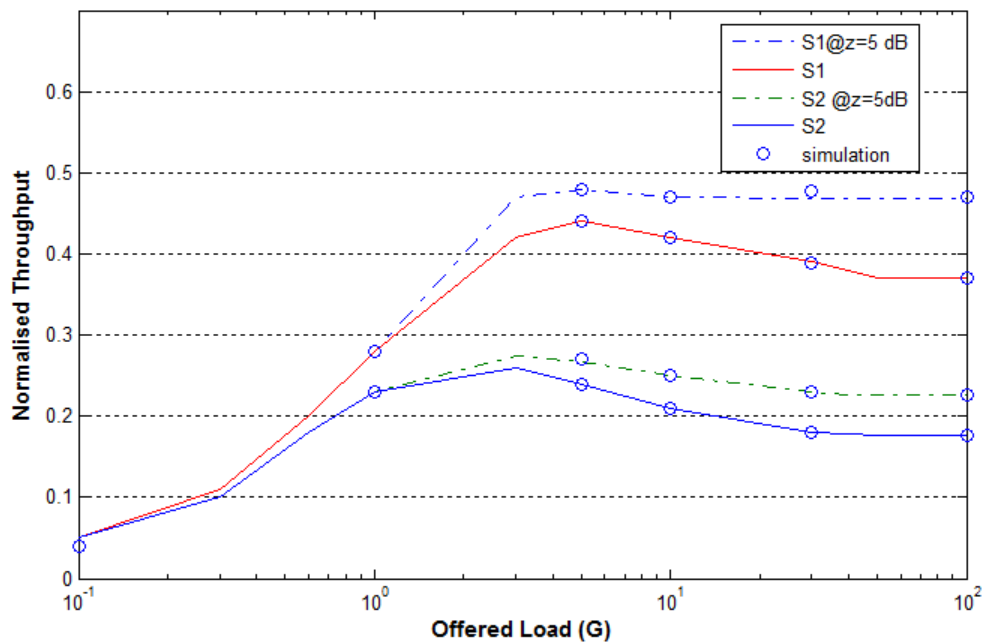


Figure 4-4: Throughput versus offered load for 2 traffic types with heterogeneous priorities. $z=5$ dB, $p_1=0.1$, $p_2=0.05$ and $Gr_1=Gr_2=0.5$

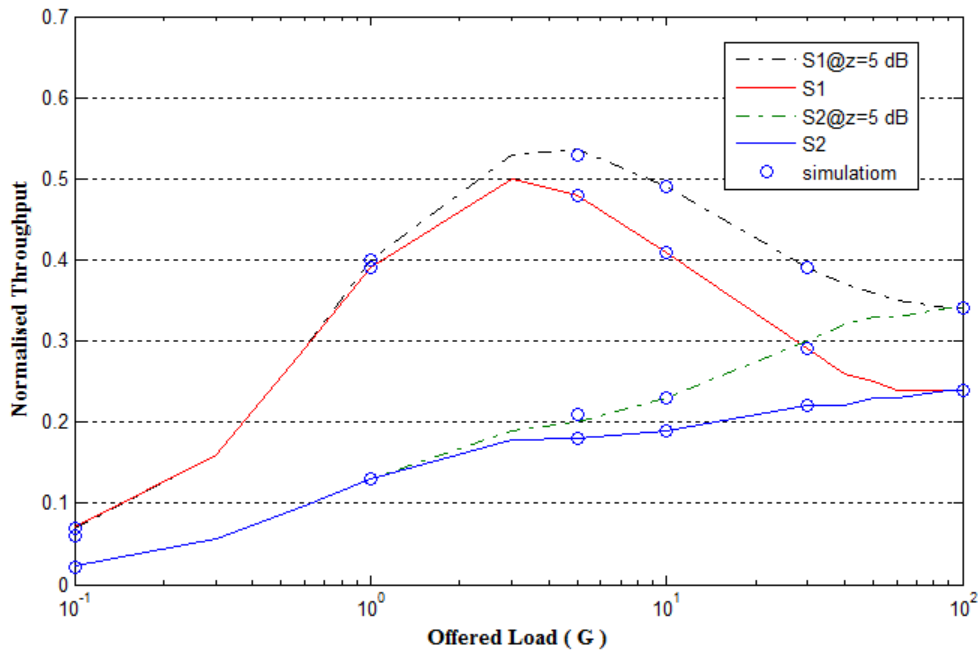


Figure 4-5: Throughput versus offered load for 2 traffic types with heterogeneous offered loads. $z=5$ dB, $p_1=p_2=0.1$, $Gr_1=0.75$ and $Gr_2=0.25$

Figure 4-6a shows the throughput versus the number of stations, with the capture threshold as a parameter. Here $p_1=p_2=0.1$, $Gr_1=0.75$ and $Gr_2=0.25$. Based on the results in Figure 4-6a, the percentage throughput gain was calculated. Figure 4-6b shows the percentage throughput gain versus the number of stations with heterogeneous loads. The percentage gain in the throughput due to the number of stations is calculated relative to a network with 4 stations (i.e., 2 stations per traffic type). We can see that at low offered loads there is little gain in the throughput when the number of stations is increased. However, at high offered loads the percentage throughput gain increase as the network becomes larger. When there are 20 stations the percentage throughput gain is 5% at $G=10$, while at $G=30$ the gain in throughput is 17.5%. The same experiment was repeated for 4 traffic types. Here, $p = [0.1, 0.1, 0.1, 0.1]$ and $Gr = [8/15, 4/15, 2/15, 1/15]$. Based on the results on Figure 4-7a the percentage throughput gain was calculated as in the previous experiment. Figure 4-7b shows a similar

trend as to that in Figure 4-6b. When there are 20 stations the percentage throughput gain is 27% at $G=10$, while at $G=30$ the gain is 66%. Comparing the results for 2 traffic types and 4 traffic types we see that the capture effect is sensitive to the number of traffic types and their heterogeneous loads and priorities. Also, the results show that in the non-saturation region the gain in the throughput converges to a finite value as the number of stations increases.

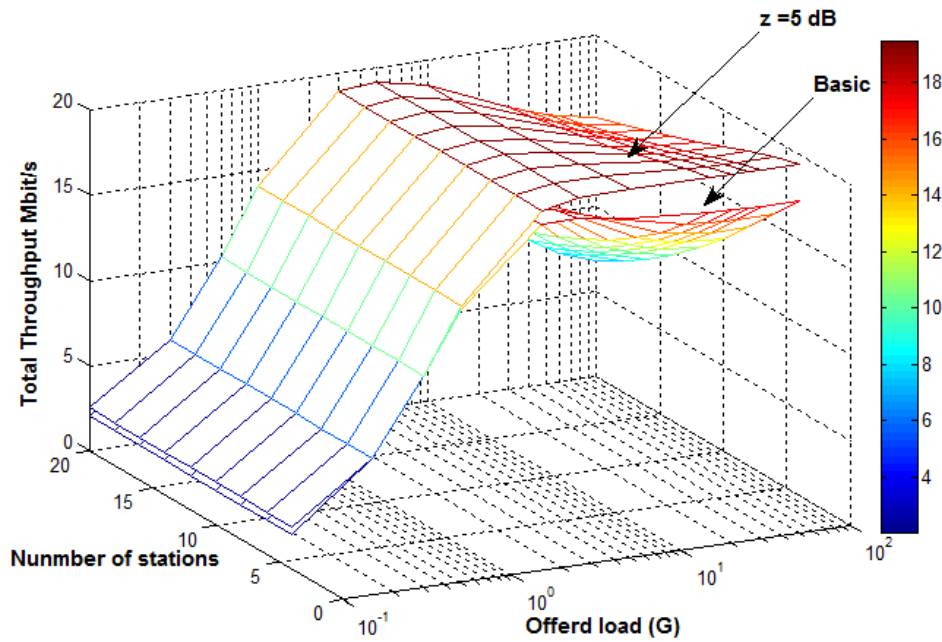


Figure 4-6a: Total throughput of 2 traffic types versus number of stations for varying of the offered load with $z=5\text{dB}$, $p_1=p_2=0.1$, $Gr_1=0.75$ and $Gr_2=0.25$

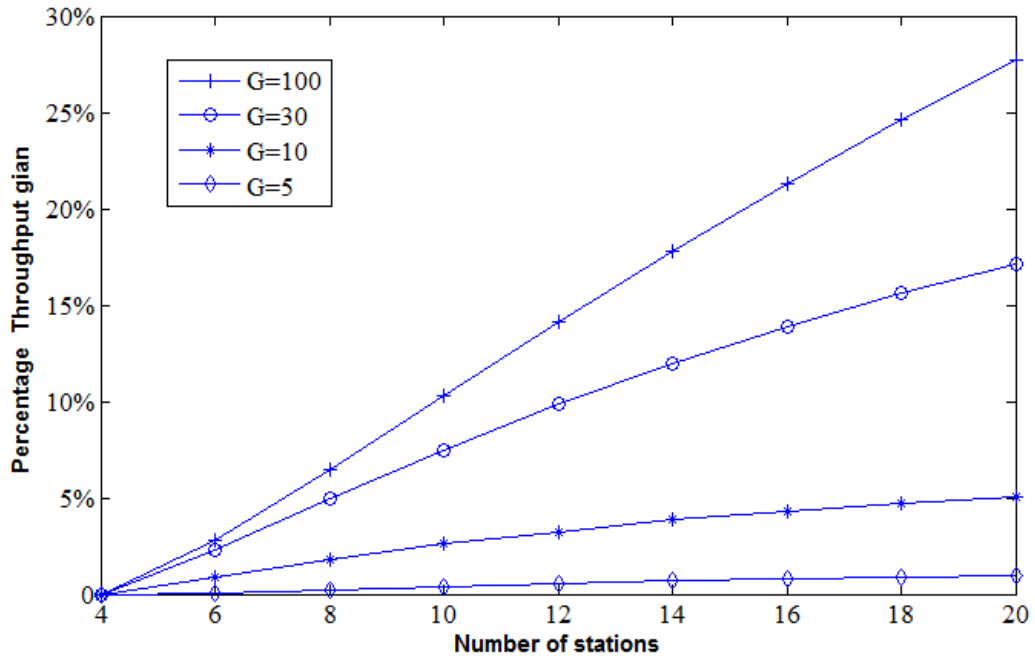


Figure 4-6b: total throughput of 2 traffic types gain versus number of stations the with $z=5$ dB, $p_1=p_2=0.1$, $Gr_1=0.75$ and $Gr_2=0.25$

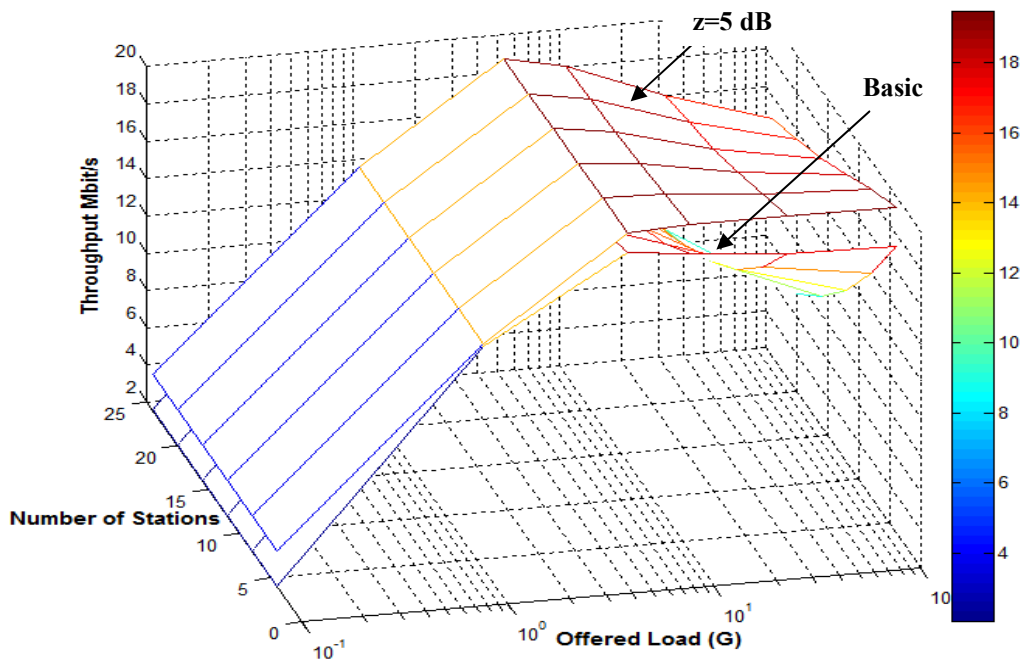


Figure 4-7: Total throughput of 4 traffic types versus number of stations for varying of the offered load with $z=5$ dB, $p=[0.1, .1, .1 .1]$ and $Gr = [8/15, 4/15, 2/15, 1/15]$

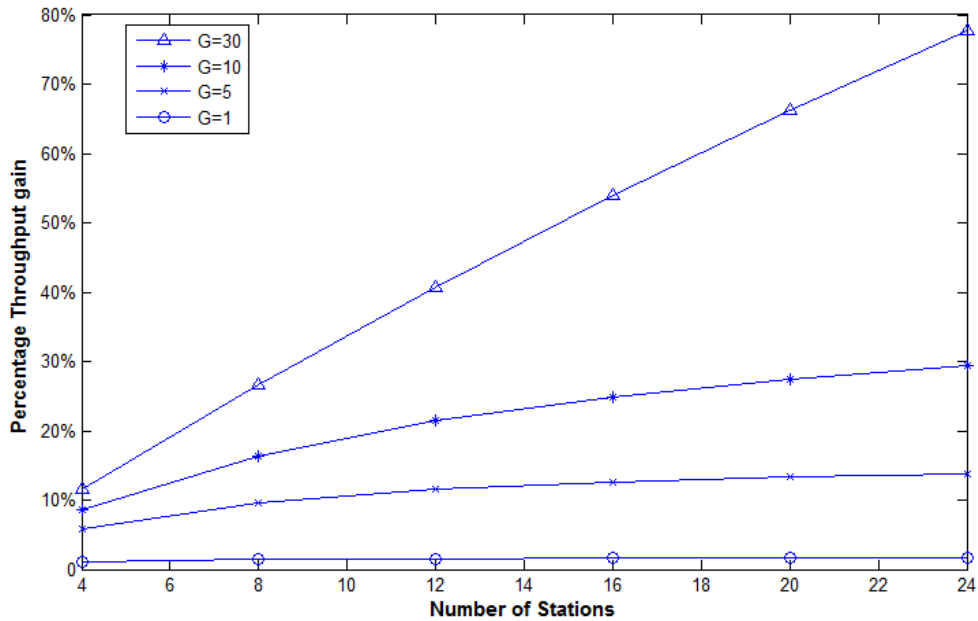


Figure 4-7b: Total throughput gain of 4 traffic versus number of stations the percentage types with $z=5$ dB, $p=[0.1, 0.1, 0.1, 0.1]$ and $Gr = [8/15, 4/15, 2/15, 1/15]$

C- Packet error rate and capture effect

In this part of the results, we demonstrate the interaction between the PHY and MAC layers in terms of packet error rates and capture effects. The first set of the results show the throughputs for traffic types 1 to 4 for a network with 5 stations per traffic type. In this system $p = [0.1, 0.05, 0.025, 0.0125]$ and $Gr = [0.25, 0.25, 0.25, 0.25]$. Traffic type 1 and 2 have channel conditions of SNR = 7 dB and 8 dB, while traffic type 3 and 4 have ideal channel conditions (i.e. SNR >12.5 dB). Figure 4-8 shows that when the offered load, G , is less than 1 there is no noticeable difference between the two cases (i.e. with and without the capture effect) and channel conditions have very little effect on the throughput performance. This is due to the low chance of collisions as there is little traffic in the network. As the offered load increases, the benefit from the capture effect becomes more obvious and the packet error rate has a clear effect on the throughput performance. For example, at $G=10$ and SNR= 7, the throughput is degraded by 9.7% compared with the basic model due to the

channel errors. When the channel condition improves to SNR = 8 dB the throughput is similar to the basic model, while at SNR > 12.5 dB the total system throughput is improved by 12.3 % compared to the basic model.

The second set of results shows this new model in the case of heterogeneous loads. Figure 4-9 shows the results for a network of 5 stations per traffic type with heterogeneous loads. Here $p = [0.1, 0.1, 0.1, 0.1]$ and $Gr = [8/15, 4/15, 2/15, 1/15]$. The same trends are shown as with the heterogeneous priorities. The results demonstrate that as G increases the capture effect shows increasing throughput gains compared to the basic model. Again, when comparing the performance of this new model with PHY layer effects to that shown in [70], the total throughput is increased by 28 % at $G=10$ and SNR > 12.5 dB while at SNR = 7 dB, the total throughput is only improved by 7% compared to the basic model.

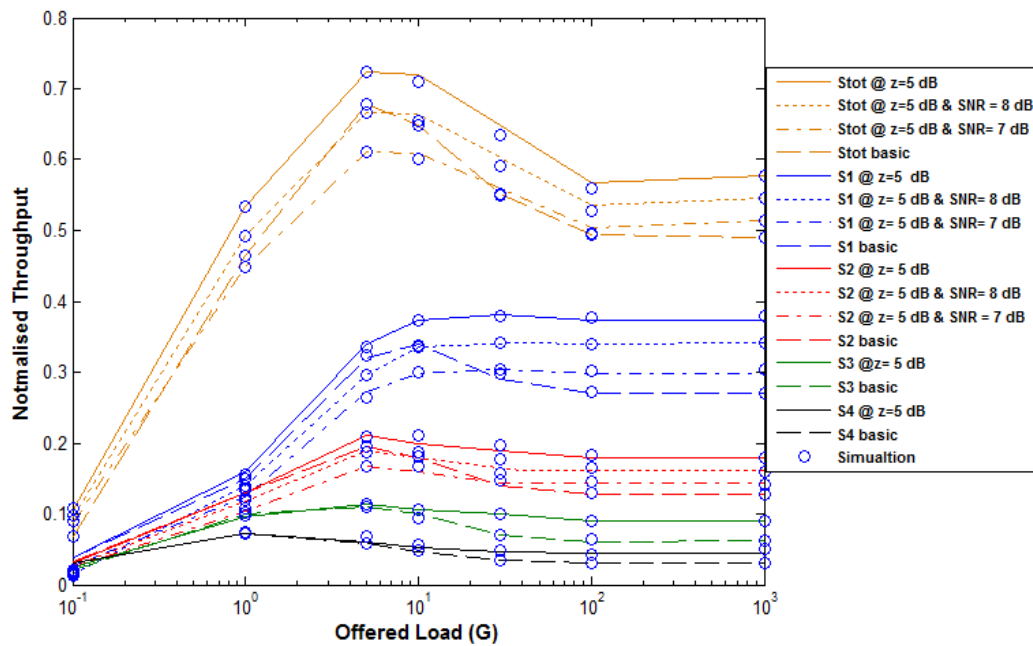


Figure 4-8: Throughput versus offered load for 4 traffic types with heterogeneous priorities. $z=5$ dB, $p=[0.1, 0.05, 0.025, .0125]$, and $Gr=[0.25, 0.25, 0.25, 0.25]$

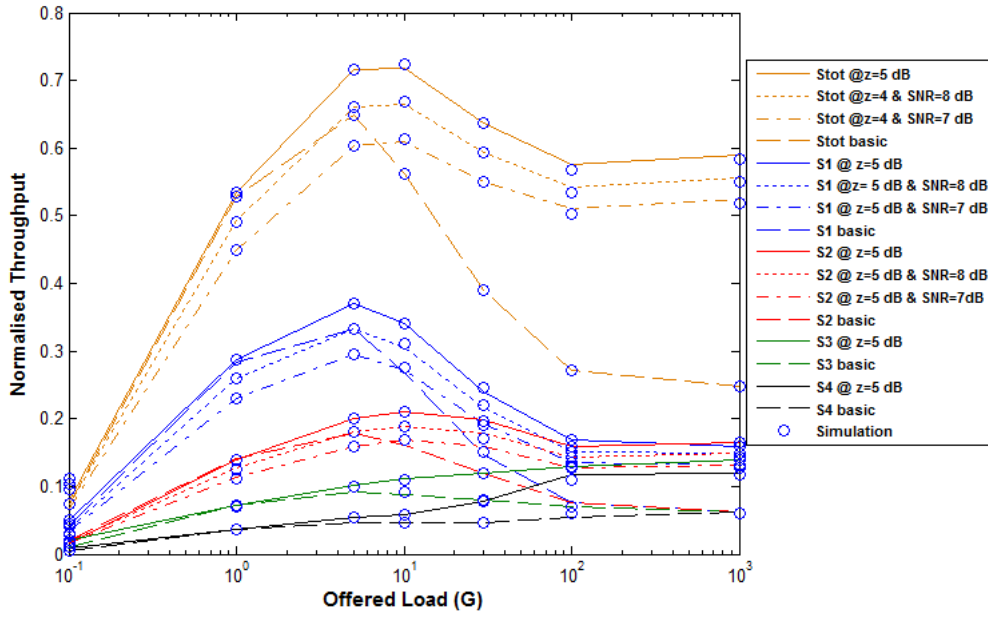


Figure 4-9: Throughput versus offered load for 4 traffic types with heterogeneous offered loads. $z=5$ dB, $p = [0.1, 0.1, 0.1, 0.1]$ and $Gr = [8/15, 4/15, 2/15, 1/15]$

In the following test, the behaviour of the non-saturated throughput as a function of the channel SNR is depicted in Figure 4-10 and Figure 4-11. The results are for $M_1=M_2=M_3=M_4=5$ contending stations and the payload size is equal to 1500 bytes for 802.11a/g and 802.11n with data rates of 24 and 26 Mbit/s, respectively. The graphs have been parameterised with respect to the capture threshold z ; with $p = [0.1, 0.1, 0.1, 0.1]$ and $Gr = [8/15, 4/15, 2/15, 1/15]$. By repeating the process, similar graphs can be generated for all other data rates by using the PER as a function of SNR graph in Figure 3-3a and b.

The results show that when the quality of the wireless channel is improved, as exemplified by the SNR values, the throughput increases up to the maximum level, around 12.5dB for 802.11n and at 20 dB for 802.11a/g. Above these values, the channel quality can be considered to be ideal channel. Furthermore, comparative analysis of Figure 4-10a with b and Figure 4-11a with b reveals that the throughput increases when the capture effect is included. When the $PER \rightarrow 0$ and $z \rightarrow \infty$, i.e. $q_{\beta_d} = 0$ the throughput model is exactly as defined in

[70]. In this respect, our new model is more general and also embraces the model in [70]. The results also demonstrate the benefit of using MIMO-OFDM techniques in 802.11n, as there is a gain of up to 7.5 dB over 802.11a/g

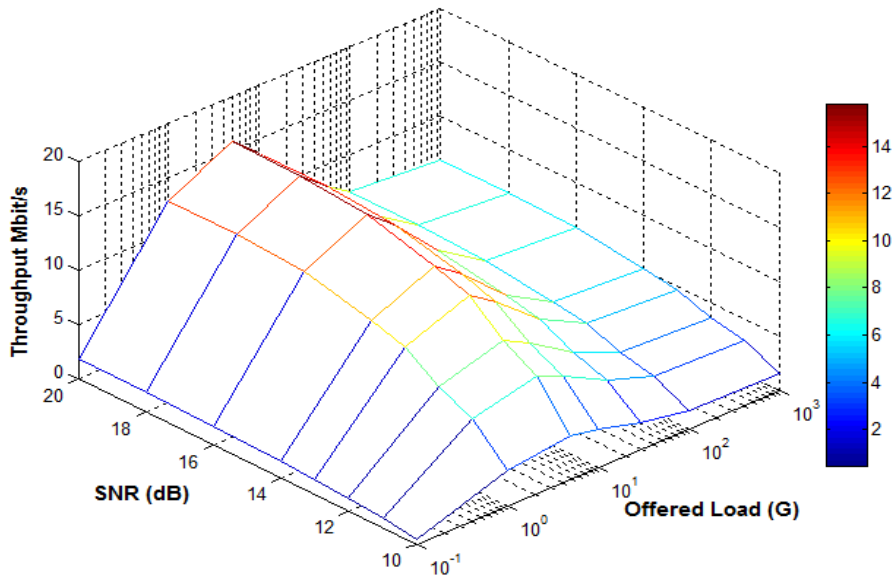


Figure 4-10a : Non-saturated throughput of 4ACs vs.SNR for 802.11a/g with with $p = [0.1, 0.1, 0.1, 0.1]$ and $G_r = [8/15, 4/15, 2/15, 1/15]$

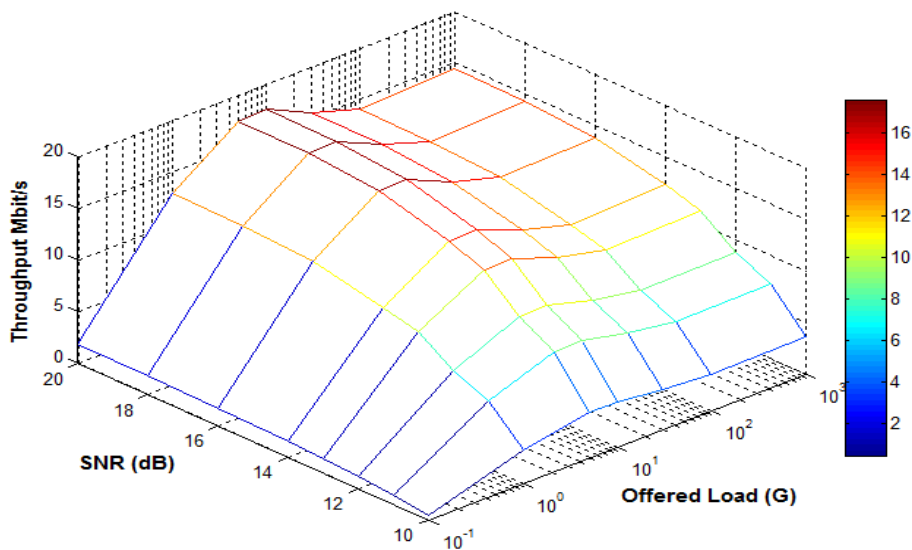


Figure 4-10b: Non-saturated throughput of 4ACs vs.SNR for 802.11a/g with with $p = [0.1, 0.1, 0.1, 0.1]$, $G_r = [8/15, 4/15, 2/15, 1/15]$ and $z=5\text{dB}$

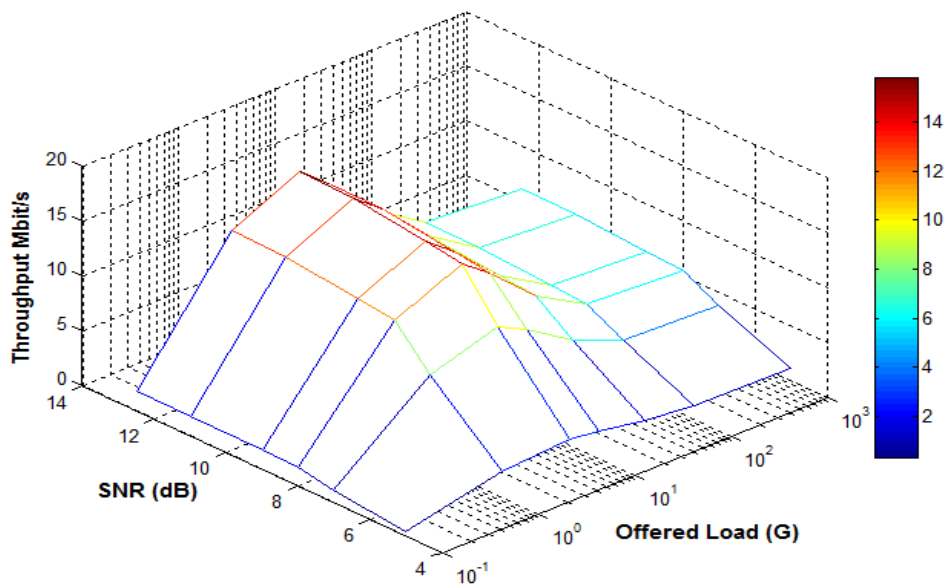


Figure 4-11a: Non-saturated throughput of 4ACs vs.SNR for 802.11n with with $p = [0.1, 0.1, 0.1, 0.1]$ and $G_r = [8/15, 4/15, 2/15, 1/15]$

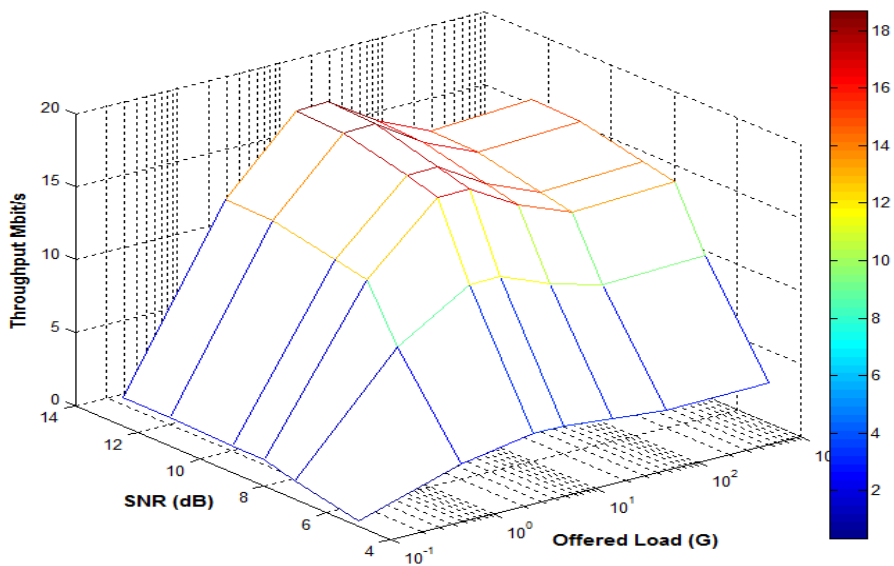


Figure 4-11 b: Non-saturated throughput of 4ACs vs.SNR for 802.11a/g with with $p = [0.1, 0.1, 0.1, 0.1]$, $G_r = [8/15, 4/15, 2/15, 1/15]$ and $z=5$ dB

4.5 Delay Results

Figure 4-12 shows the normalised delay performance versus the offered load G for 4 traffic types [AC1, AC2, AC3, AC4] with 5 stations per traffic type. $G_r = [8/15, 4/15, 2/15, 1/15]$ and $p = [0.1, 0.1, 0.1, 0.1]$. Stations of traffic type 1 and 2 have channel errors with SNR =7 dB, while stations of traffic type 3 and 4 have ideal channel conditions (i.e, SNR > 12.5 dB). The results show an interesting behaviour of the system. At a very low offered load, the delay of traffic type 1 and 2 is increased significantly because of a very long idle period and channel errors. As the offered load is increased, the idle period becomes a shorter and the channel errors have less effect on the delay. At $G=0.1$ the delay of traffic type 1 is increased from 3 to 43 while at $G=1$ the delay is increased from 5 to 12. When the offered load reaches the saturation condition the delay for both traffic type 1 and 2 is increased by 42% compared to the basic case. Figure 4-13 shows the PHY/MAC normalised delay versus the offered load with heterogeneous priorities. Here, 4 traffic types [AC1, AC2, AC3, AC4], $M_1=M_2=M_3=M_4=5$, $p = [.1, .05, .025, .0125]$ and $G_r = [0.25, 0.25, 0.25, 0.25]$ respectively. The results show that the capture effect reduces the delay while the channel errors increase the delay. The channel errors have a significant effect at low offered loads and as the offered load increase, the benefit from the capture effect becomes more apparent. For example, at $G=10$ and $z=5$ dB, the average delay is reduced by 19 % compared to the basic model.

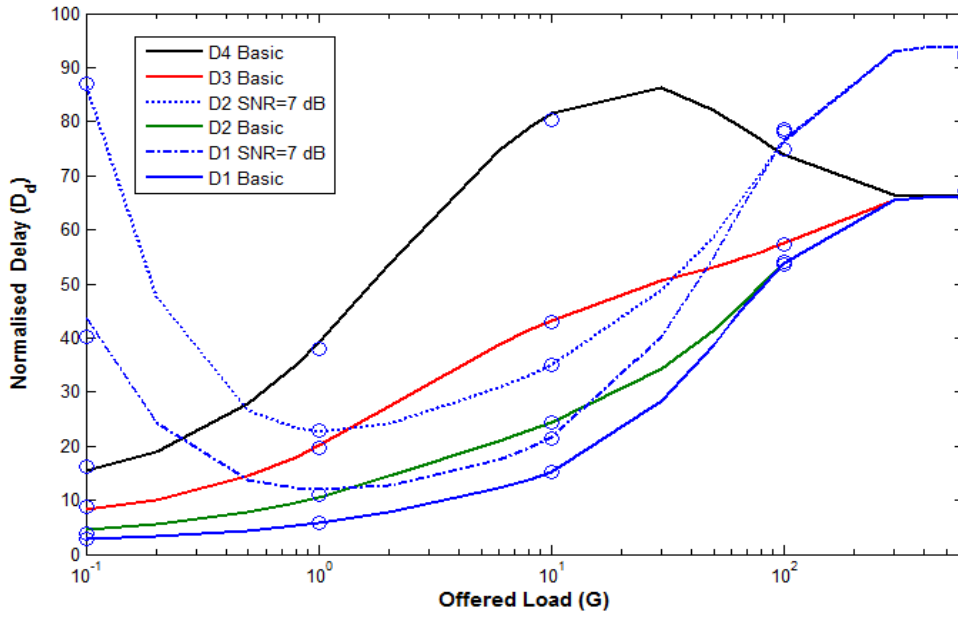


Figure 4-12 : Normalised delay for 4 traffic types with heterogeneous traffic loads $G_r = [8/15, 4/15, 2/15, 1/15]$ and $p = [0.1, 0.1, 0.1, 0.1]$ with AC1 & AC2 have SNR=7 dB

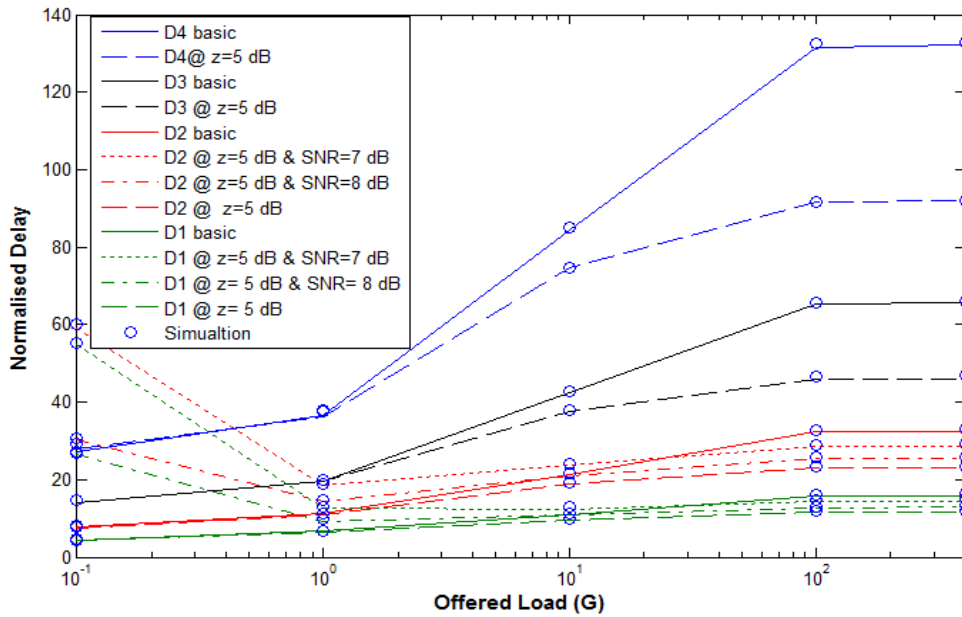


Figure 4-13: Normalised delay with heterogeneous traffic loads= $[8/15, 4/15, 2/15, 1/15]$ and $p = [0.1, 0.1, 0.1, 0.1]$ at SNR=7 and 8 dB and $z = 5$ dB

4.6 Adaptive p -persistent CSMA protocol

The main requirement of the p -persistent CSMA protocol is calculating the optimum value of p that maximizes throughput. In [70], p -persistent CSMA with service differentiation used the p value to assign different priorities to different access categories according to QoS requirements. The authors in [70] considered the case of perfect channel conditions. Therefore, if the physical link of any access category degrades, its p value does not change. This constant p value results in wasting the system capacity as degradation in the throughput is mainly due to channel errors, not collisions in the network. Hui's ratio defines the saturated throughput, or s-ratio between stations of different traffic types when the contention window (CW) setting provides service differentiation as given by (4-46) when p is used to model the CW [84].

$$S_1:S_2:\dots:S_{d_{max}} = (p_1)/(1-p_1):(p_2)/(1-p_2):\dots:(p_{d_{max}})/(1-p_{d_{max}}) \quad (4-46)$$

In order to modify this expression to consider the non-saturated case in ideal channel conditions, equation (4-46) should be modified as shown in (4-47). The following formula is not an exact calculation but an approximation.

$$\begin{aligned} S_1:S_2:\dots:S_{d_{max}} \\ = (g_1)(p_1)/(1-p_1):(g_2)(p_2)/(1-p_2):\dots:(g_{d_{max}})(p_{d_{max}})/(1-p_{d_{max}}) \end{aligned} \quad (4-47)$$

For simplicity only two traffic types are considered and an expression for S_1 in terms of S_2 is given by (4-48).

$$S_2 = \left(\frac{g_1}{g_2}\right) S_1 (p_2(1-p_1))/(p_1(1-p_2)) \quad (4-48)$$

If the s-ratio is 2:1 then p_2 can be calculated from equation (4-48) as shown in (4-49).

$$p_2 = \left(\frac{g_1}{g_2}\right) 0.5p_1 / (1 - 0.5p_1) \quad (4-49)$$

In this new adaptive p -persistent CSMA protocol the p values are adjusted according to the offered load and channel conditions. The channel conditions can be obtained in the same way as done in the link adaption mechanisms in 802.11. The probability of successful packet transmission in the PHY layer denoted $P_s^{(d)}$ is given by (4-50). The index d refers to the traffic type number.

$$P_s^{(d)} = 1 - P_e^{(d)} \quad (4-50)$$

$P_e^{(d)}$ can be obtained from Figure 3-3a and b and if this probability is multiplied by p , a new dynamic p -persistent value (px) that depends on the channel conditions can also be obtained as shown in (4-51).

$$px_d = p_d(1 - P_e^{(d)}) \quad (4-51)$$

For simplicity and without loss of generality, applying this across two traffic types with s-ratio 2:1 gives expressions for px_1 and px_2 in (4-52) and (4-53) respectively.

$$px_1 = p_1(1 - P_e^{(1)}) \quad (4-52)$$

$$px_2 = \left(\frac{g_1}{g_2}\right) \left(\frac{0.5p_1}{(1-0.5p_1)}\right) (1 - P_e^{(2)}) \quad (4-53)$$

Where $P_e^{(d)}$ can be obtained from Figure 3-3a and b.

Figure 4-14 demonstrates the effectiveness of our proposed adaptive protocol for the following system parameters: In the first test, the adaptive protocol investigated for the case of heterogeneous loads only (i.e. PER=0). For simplicity, 2 traffic types [AC1, AC2], $p = [0.1, 0.05]$, $G_r = [0.25, 0.75]$ and PER= 0 are investigated. The results are shown for two access categories with 5 stations each and the target is $S_1=2S_2$. The results show that this target cannot be achieved due to offered load ratios. However, the adaptive protocol improves the performance of AC1 towards meeting the target. As the offered load increases the throughput performance of AC1 is improved by 54% compared to normal protocol and meets the target at $G = 6$. At high offered load values ($G >10$) the throughput of AC1 exceeds the target that because the system performance reaches the saturation region. Figure 4-15 shows the results of our proposed protocol for the case of an error-prone channel. In this scenario the stations of AC2 with lower priority incur poor channel conditions with PER= 0.3. In this case most of the time will be spent on unsuccessful transmissions due to channel errors which waste the system capacity. The results show that the adaptive protocol improves the throughput performance of the stations of AC1 with higher priority by 81% compared to the normal protocol and the total the system throughput is improved by 16.5%.

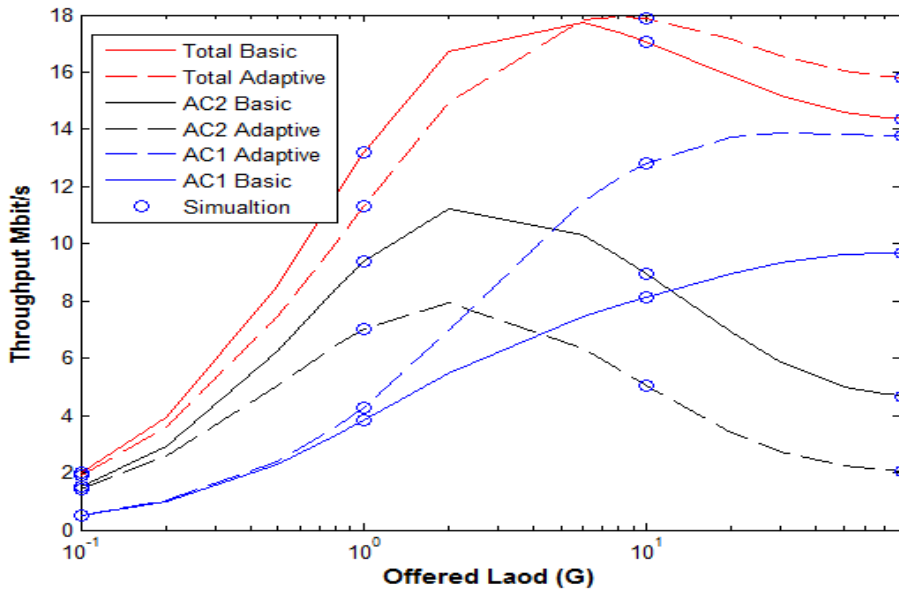


Figure 4-14: Throughput performance of the adaptive protocol with heterogenous loads $Gr=[0.25, 0.75]$, $p=[0.1, 0.05]$ and $PER=0$.

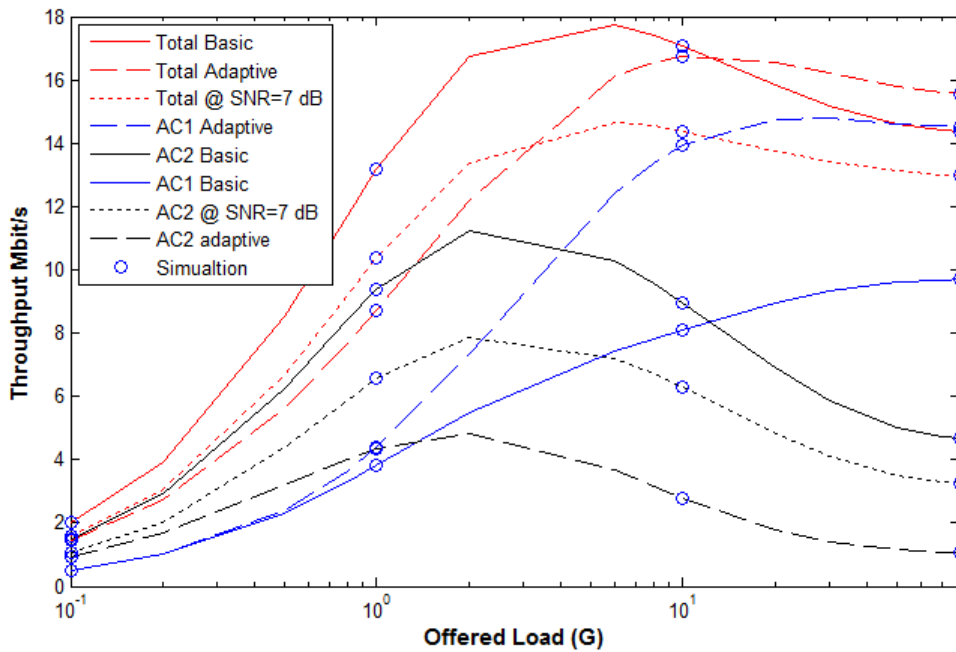


Figure 4-15: Throughput performance of the adaptive protocol with heterogenous loads $Gr=[0.25, 0.75]$, $p=[0.1, 0.05]$ and $PER=0.3$.

4.6.1 Limitations and Complexity of the Adaptive Protocol

This proposed algorithm can be implemented practically as it only needs the PER information which can be obtained in the same way as in link adaptation mechanisms. This PER value clearly reflects the quality of the channel and hence the SNR values. The default p values will be set by the station on the basis of an ideal channel. As the link degrades the p value changes dynamically according to equations (4-54) and (4-55), and as the channel improves the p value is returned to its default value. The limitation of this protocol is that it does not support a link-adaptation mechanism which is our topic for future research. The proposed protocol can be easily implemented as it does not require any hardware modifications.

4.7 WLAN Planning

In the following experiment, the benefit from accurate modeling for the throughput in terms of network planning is demonstrated. In this case study, two access categories, AC1 and AC2, are considered with $p_1 = 0.1$ and $p_2 = 0.05$, respectively. The offered load ratios are $G_r = [0.5, 0.5]$ with capture threshold, $z = 2$ dB and the normalized offered load, $G = 10$. The throughput per traffic type per station is calculated using the same way as in section 3.7. Figure 4-16 shows the throughput per station versus the number of stations in the system. The results show that the throughput per station is decreased as the number of station stations increases until reaches 6 stations afterword the throughput starts to increases as the number of station increases. The results shows that when the capture included the AP can serve up to 18 stations with no less than 500 kbit/s for AC1 and 250 kbit/s for the AC2 compared to case when the capture is not included the QoS required falls down below the targets when the number of station is between 1 and 16.

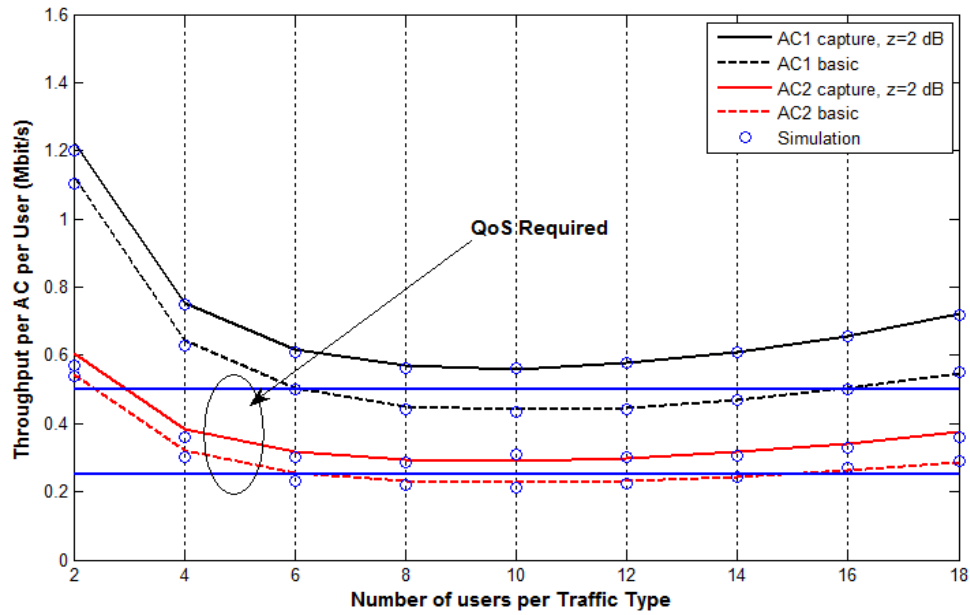


Figure 4-16: Non-saturated throughput per user as a function of number of users per traffic type with capture effect

4.8 Conclusions

In this chapter, we have developed a cross layer approach for the non-saturated throughput/delay performance. A comprehensive analytical model was presented to calculate the non-saturated throughput/ delay of a QoS differentiated p -persistent CSMA protocol in multipath fading channel. The results showed that the capture effect included in this new model offers much higher non-saturated throughput performance than the model that assumes a perfect channel. The results showed that at low offered load the capture effect has little effect on the system performance, and as the offered load increases the capture effect enhances the throughput and delay performance. The results demonstrated the importance of developing this accurate model by including the channel errors and capture effect. The results showed that when the capture effect is included the throughput performance for some cases is increased by 21% compared to the basic model. In addition, the results demonstrated that the throughput/delay performance when the channel errors and capture are included is highly

dependent on the traffic loads. This realistic model leads to efficient network planning and design for the case of non-saturated stations. The closed form expressions allow derivation of the throughput as a function of a large number of system level parameters, including capture threshold and effects of channel errors for a variety of applications. Other key system parameters include the absolute and relative p -persistent values, the total system offered load and the relative offered loads per traffic type. We have developed an adaptive p -persistent CSMA protocol with heterogeneous traffic that mitigates the effects of channel errors and improves the high priority access categories at low offered load values. The results showed that our proposed protocol can improve the high priority access category throughput by 81% and the overall throughput performance by 16.5% compared with the normal protocol.

Chapter 5

Modeling of p -Persistent CSMA protocol with Multirate Capability

The throughput/delay performance of high-rate 802.11 stations is significantly degraded by low-rate stations even though the former instantaneously transmit with a high link data rate. This phenomena is often called the "*performance anomaly*" of IEEE 802.11 whereby an unexpected drop in the throughput performance of the stations with high bit-rates is observed. Most of the recent analytical work for the existing IEEE 802.11 DCF and the IEEE 802.11e EDCA use the Markov chain which requires a very high degree of complexity. As the parameters increase, in order to make the model close to the real environment, the complexity exponentially increases. This complexity makes these models limited to a few parameters that can be included for the evaluation of service differentiation mechanisms supported in 802.11e. In this chapter, a comprehensive and closed form analytical approach to calculate the saturated throughput and delay for differentiated p -persistent CSMA with multirate is developed. This model also takes into account the induced channel errors and the capture effects in a Rayleigh fading environment. Also, a new adaptive p -persistent CSMA protocol is introduced to alleviate the *performance anomaly* of the 802.11a/g and 802.11n. This new p -persistent model can be applied to 802.11e EDCA WLANs, thus providing a new analysis that extends the modelling capability without having a large degree of complexity.

5.1 System Model for p -persistent CSMA with Multirate

Similar model to that was considered in [56] that was explained in chapter 3 with a modification to include the multirate capability is investigated as shown in Figure 5-1. The model chapter 3 investigates the case where all stations the network transmit as at the same rate (i.e. single rate) while in this chapter stations with different traffic types can transmit at different bit rates. This model allows the *performance anomaly* of WLANs to be evaluated and solutions can be then proposed. The main difference between this model and the old model is that the transmission time (T_d) is variable depending on the rate of transmission and whether it is a successful transmission or a collision. The second modification of the model is the incorporation of the PHY layer effects in terms of the packet error rate and capture effect. A transmission will be successful only if one station commences a transmission at the start of the timeslot which corresponds to the vulnerable period with a good channel, or the received power of the concerned packet that experiences a collision is higher than a threshold z as explained in the section 3-2.

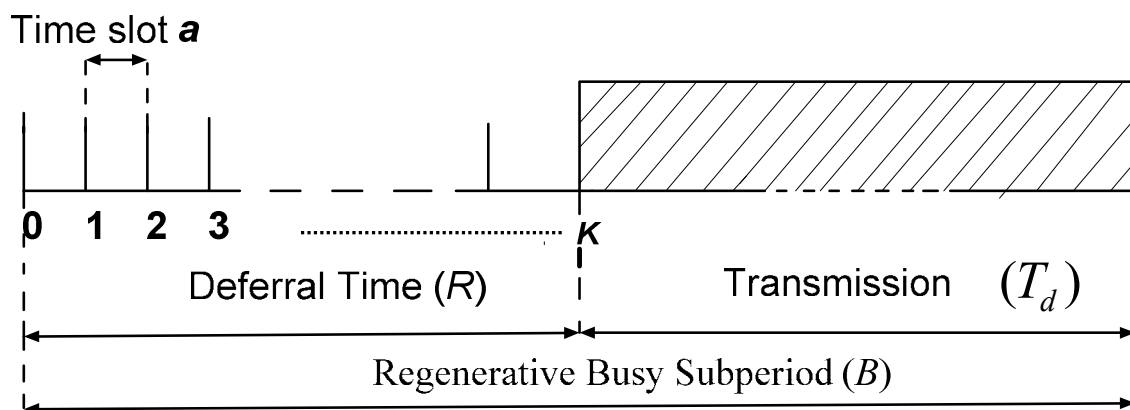


Figure 5-1: Channel state cycle for saturated case with multirate

5.2 Throughput analysis of p -persistent CSMA with multirate

An analytical approach for the throughput of p -persistent CSMA with multirate is provided in this section for the basic case and subsequently with PHY layer effects.

5.2.1 Basic p -persistent CSMA with Multirate

In this analysis the word "basic" refers to the multirate model with ideal channel conditions, and the term "single rate" refers to the model in [56]. In [56] the throughput S of p -persistent CSMA for traffic type d was calculated using (5-1). The next few equations are similar to those in chapter 3 and we restate them here just to keep the logical development of the analysis.

$$S_d = \frac{E[U_d]}{E[B]} \quad (5-1)$$

Where $E[U_d]$ is the expected time of useful transmission of traffic type- d , so the total system throughput can be calculated as in (5-2).

$$S = \sum_{d=1}^{d_{max}} S_d \quad (5-2)$$

The probability that only a type 1 station commences transmission at timeslot boundary k and that no transmissions have started before this for $k=0, 1, 2, \dots, \infty$ is given by (5-3).

$$P(1tx_1) = M_1 p_1 (1 - p_1)^k [(1 - p_1)^{k+1}]^{M_1 - 1} \quad (5-3)$$

The probability that no transmission, defined by $P(0tx_d)$ has occurred before time slot boundary $k+1$ for each other traffic type d is calculated from (5-4).

$$P(0tx_d) = [(1 - p_d)^{k+1}]^{M_d} \quad (5-4)$$

The probability of successful transmission of traffic type 1 is calculated as shown in (5-5) then an expression for $E[U_1]$ is given by (5-6).

$$P(S_d) = \left(P(1tx_d) \prod_{d \neq 1} P(0tx_d) \right) \quad (5-5)$$

$$E[U_d] = T_d \times b_d \times \sum_{k=0}^{\infty} P(S_d) \quad (5-6)$$

The value b_d represents the percentage of a successful transmission that contains useful data for traffic type d , allowing MAC and PHY overheads to be accounted and T_d is the packet transmission time.

The expected busy period ($E[B]$) is the sum of the expected deferral and expected transmission times as in (5-7).

$$E[B] = E[R] + E[T_c] \quad (5-7)$$

The timeslot boundaries are numbered as $k = 0, 1, 2, \dots, \infty$. The expected length of the deferral time $E[R]$ can be calculated as shown in (5-8).

$$E[R] = a \sum_{k=1}^{\infty} \left(\prod_{d=1}^{d_{max}} (1 - p_d)^{M_d k} \right) \quad (5-8)$$

The expected length of the transmission time can be calculated by (5-9).

$$E[T] = E[T_s] + E[T_c] \quad (5-9)$$

Where $E[T_s]$ and $E[T_c]$ are the expected successful and collision times respectively. Up to this point the model considers only the single rate case where $E[T]$ equals 1 as originally stated in [56]. However, in order to modify the model to include a multirate capability, $E[T]$ should be calculated differently as follows: firstly the successful transmission time for each traffic type, $E(T_{s_d})$, should be calculated; for example, the expected successful transmission time of traffic type 1, $E(T_{s_1})$, is given by (5-10).

$$E(T_{s_1}) = \sum_{k=0}^{\infty} \left(P(1tx_d) \prod_{d \neq 1}^{d_{max}} P(0tx_d) \right) \times T_1 \quad (5-10)$$

Then, the total expected successful transmission time $E(T_s)$ is given by (5-11)

$$E[T_s] = \sum_{d=1}^{d_{max}} E[T_{s_d}] \quad (5-11)$$

$E[T_c]$ is due to two types of collision, internal collisions which result in a collision between two or more packets from stations within the same traffic type, and external collision which is

due to a collision between two or more packets from stations with different traffic types. In order to calculate $E[T_c]$ the probability of more than one station (i.e. $\beta_d \geq 2$) transmitting at the same time (P_d) must be calculated first, as shown in (5-12). The probability of an internal collision of traffic type 1 (P_{i1}) is given by (5-13).

$$P_d = \binom{M_d}{\beta_d} (p_d(1-p_d)^k)^{\beta_d} [(1-p_d)^{k+1}]^{M_d-\beta_d} \quad (5-12)$$

$$P_{i1} = \binom{M_1}{\beta_1} (p_1(1-p_1)^k)^{\beta_1} [(1-p_1)^{k+1}]^{M_1-\beta_1} \times \prod_{d \neq 1} [(1-p_d)^{k+1}]^{M_d} \quad (5-13)$$

The probability of an external collision (P_{e1}) for traffic type 1 can be calculated as shown in (5-14)

$$P_{e1} = \sum_{\beta_1=1}^{M_1} \sum_{\beta_2=0}^{M_2} \dots \sum_{\beta_{d_{max}}=x}^{M_{d_{max}}} \left(\prod_{d=1}^{d_{max}} P_d \right) \quad (5-14)$$

Where $x = 0$ if any other traffic type has a packet to transmit and $x=1$ if all other traffic types have no packets to send. When calculating the external collision of the traffic type 2 the external collision between the traffic type 1 and type 2 should be excluded as it is already included in the case of traffic type 1 and so on. The total collision time of traffic type 1, $E[T_{c,1}]$, can be calculated using (5-13) and 5-14) as shown in (5-15).

$$E[T_{c,1}] = \sum_{k=0}^{\infty} \sum_{\beta_1=1}^{M_1} \sum_{\beta_2=0}^{M_2} \dots \sum_{\beta_{d_{max}}=x}^{M_{d_{max}}} \left(\prod_{d=1}^{d_{max}} P_d \right) \times T_{max} + \quad (5-15)$$

$$\binom{M_1}{\beta_1} (p_1(1-p_1)^k)^{\beta_1} [(1-p_1)^{k+1}]^{M_1-\beta_1} \times \prod_{d \neq 1} [(1-p_d)^{k+1}]^{M_d} \times T_1$$

Where T_{max} is the maximum collision time of a transmitted packet in the network and the total collision time $E[T_c]$ can be calculated as in (5-16)

$$E[T_c] = \sum_{d=1}^{d_{max}} E[T_{c,d}] \quad (5-16)$$

The total transmission time $E[T]$ of the QoS differentiated p -persistent CSMA protocol with multirate capability is given by (5-17).

$$E[T] = \sum_{d=0}^{d_{max}} E[T_{s,d}] + \sum_{d=1}^{d_{max}} E[T_{c,d}] \quad (5-17)$$

Then, the throughput of traffic type 1 is given by (5-18).

$$S_1 = \frac{b_1 \times T_1 \times \sum_{k=0}^{\infty} (P(1tx_d) \prod_{d \neq 1}^{d_{max}} P(0tx_d))}{a \sum_{k=1}^{\infty} (\prod_{d=1}^{d_{max}} (1-p_d)^{M_d k}) + E[T]} \quad (5-18)$$

Finally, the total system throughput is given by (5-19).

$$S = \sum_{d=1}^{d_{max}} S_d \quad (5-19)$$

5.2.2 Multirate p -persistent CSMA with PHY layers effects

In this subsection the throughput of multirate p -persistent CSMA with PHY layer effects will be analysed. This section presents the interaction between PHY and MAC layers for a QoS

differentiated p -persistent CSMA protocol with multirate capability. The interaction between the two layers can be established by replacing the probability of successful traffic type d , $P(S_d)$, in the pure MAC layer by the probability of successful traffic type d , $P(S_dphy)$, with PHY layer effects in terms of packet error rate and capture effect. This probability is the sum of the probability of success of traffic type d , $P(S_dpe)$, when only one packet is received in the presence of packet errors, and the probability of success of traffic type d , $P(S_dcap)$, when the packet is involved in a collision but still can be received successfully by the receiver. For M stations in the system with traffic type d , we can write:

$$P(S_dphy) = P(S_dpe) + P(S_dcap) \quad (5-20)$$

The analysis is exactly the same as in chapter 3, so we just write the final equation for traffic type 1 as shown in (5-21).

$$P(S_1phy) = P(1tx_1) \prod_{d \neq 1} P(0tx_d) \times (1 - P_e^1) + \sum_{\beta_1=2}^{M_1} \sum_{\beta_2=0}^{M_2} \dots \sum_{\beta_{d_{max}}=0}^{M_{d_{max}}} \left(\prod_{d=1}^{d_{max}} P(\beta_d tx_d) \right) (\beta_1) q((\beta - 1)|z_1) \quad (5-21)$$

Now the expected time per busy subperiod, $E[U_{1phy}]$, spent on successful transmissions can be calculated by evaluating equation (5-21) over range of $k=1, 2, \dots, \infty$ as shown in (5-22).

$$E[U_{1_phy}] = T_1 \times b_1 \times \sum_{k=0}^{\infty} P(S_{1_phy}) \quad (5-22)$$

Where b_1 is the fraction of time spent on useful transmission of traffic type1 and T_1 is the packet transmission time.

The expected busy period in the presence of PHY layer effects ($E[B_{phy}]$) is the sum of the expected deferral and expected transmission times, as in (5-23).

$$E[B_{phy}] = E[R] + E[T_{phy}] \quad (5-23)$$

The expected transmission time in the presence of PHY layer effects ($E[T_{phy}]$) can be calculated by (5-24)

$$E[T_{phy}] = E[T_{s_phy}] + E[T_f] + E[T_{c_cap}] \quad (5-24)$$

Where $E[T_{s_phy}]$ is the successful transmission time with PHY layer effects as shown in (5-25) and $E[T_f]$ is the transmission time when the packet is not received due to packet error rates, which can be calculated by (5-26).

$$E[T_{s_phy}] = \sum_{d=1}^{d_{max}} T_d \times \left[\sum_{k=0}^{\infty} P(s_{d_phy}) \right] \quad (5-25)$$

$$E[T_f] = \sum_{d=1}^{d_{max}} \left[T_d \times P_e^{(d)} \times \sum_{k=0}^{\infty} P(s_d) \right] \quad (5-26)$$

$E[T_{c_cap}]$ is the collision time when the capture effect is taken into account and can be calculated by (5-27).

$$E[T_{c_cap}] = \sum_{d=1}^{d_{max}} E[T_{c_d}] \times (1 - \beta_d q((\beta - 1)|z_1)) \times T_{max} \quad (5-27)$$

Now $E[T_{phy}]$ can be calculated using equations (5- 25), (5-26) and (5-27). By substituting equation (5-28) in (5-23) and then substituting (5-23) and (5-22) in (5-1) a cross-layer (PHY/MAC) throughput of traffic type 1, S_{1-phy} , with multirate can be calculated as shown in (5-28).

$$S_{1-phy} = \frac{E[U_{1-phy}]}{E[B_{phy}]} \quad (5-28)$$

5.3 Delay analysis of p -persistent CSMA with Multirate

The delay is defined as the time from when a packet becomes head of the line at a station until it is successfully received as explained in chapter 3. In p -persistent CSMA the delay begins at the start of R following the station's previous successful transmission, and ends once the station's next successful transmission has completed. The analytical approach for the delay of p -persistent CSMA with multirate will be provided for the basic case and then for a cross-layer approach

5.3.1 Basic p -persistent CSMA with Multirate

In this delay analysis expected transmission time ($E[T]$) is calculated differently from the analysis described in [56], as shown in equation (5-9) to model the multirate. The main difference between this analysis and that in [85] is the calculation of the collision time $E[T_c]$ as in equation (5-16). The delay is calculated for a station with traffic type $d = 1$, however this analysis can be applied to stations of any of the traffic types in the system by simple substitution. In order to calculate the average delay, the probability that a particular type 1 station is successful should be calculated. The analysis is similar to that in chapter 3 except that the collision time is calculated differently as in equation (5-16) and we just write the final equation.

The overall delay for a type 1 packet, \bar{D}_1 with multirate capability can be calculated as shown in (5-29).

$$\bar{D}_1 = \frac{E[R] + \sum_{d=0}^{d_{max}} E[T_{s,d}] + \sum_{d=1}^{d_{max}} [E[T_{c,d}]]}{P_1} \quad (5-29)$$

Where

$$P_1 = \frac{P(s_1)}{M_1} \quad (5-30)$$

5.3.2 Multirate p -persistent CSMA with PHY Layer Effects

This model also matches the model presented in chapter 3 except that the transmission time is calculated according to equation (5-29). The main difference is the calculation of failure time due to packet error rates and the collision time. The probability that a particular type 1 station successful (P_{1_phy}) in the presence of PHY layer effects can be calculated as in (5-31).

$$P_{1_phy} = \frac{P(s_1phy)}{M_1} \quad (5-31)$$

The overall average delay for a type 1 packet in the case of multirate and PHY layer effects can then be calculated as shown in (5-32).

$$\bar{D}_{1_phy} = \frac{E[R] + E[T_{phy}]}{P_1} \quad (5-32)$$

5.4 Adaptive Multirate p -persistent CSMA Protocol

A key design requirement of the p -persistent CSMA protocol is to calculate the value of p that provides a maximum throughput. In [56] p -persistent CSMA with service differentiation used different p values for different access categories according to QoS requirements. In [56] the service differentiation was based on throughput ratios of the access categories according to Hui's ratio [84] for the case of ideal channel conditions. An adaptive p -persistent CSMA protocol that can change the p value dynamically according to the channel condition was proposed in chapter 4. In the adaptive protocol, the link adaptation mechanism was not taken into account while here in this chapter the link adaptation mechanism is included. In the proposed algorithm the new p value should be calculated based on the PER before changing to a lower data rate. This new p value will be used when the station starts transmitting at a lower bit rate and as soon as the link conditions are improved the p value should be set back to its default value. This algorithm alleviates the anomaly issue as it improves the QoS of the high priority stations when affected by low priority stations transmitting at a lower bit rate by reducing their probability of accessing the channel. The adaptive p -persistent CSMA protocol

that can dynamically change p values according to the physical link conditions to mitigate the anomaly performance of WLANs is proposed here.

Hui's ratio defines the throughput or s-ratio between stations of different traffic types when the contention window (CW) setting provides service differentiation and is given by (5-33) when p is used to model the CW [84].

$$S_1 : S_2 : \dots : S_{d_{max}} = (p_1)/(1 - p_1) : (p_2)/(1 - p_2) : \dots : (p_{d_{max}})/(1 - p_{d_{max}}) \quad (5-33)$$

This trend was proved in [84] and can be used for calculating the p -persistent values to achieve service differentiations. For simplicity only two traffic types are considered, an expression for S_2 in terms of S_1 is given by (5-34).

$$S_2 = S_1 (p_2(1 - p_1)) / (p_1(1 - p_2)) \quad (5-34)$$

If the s-ratio is 2:1 then p_2 can be calculated from equation (5-34) as shown in (5-35).

$$p_2 = 0.5p_1 / (1 - 0.5p_1) \quad (5-35)$$

From (5-40), p_2 will be changed to satisfy the s-ratio 2:1. This trend works effectively in ideal channel conditions. In adaptive p -persistent CSMA, p values are adjusted according to the channel conditions. The channel conditions can be obtained in the same way used in the link adaption mechanisms in 802.11. The probability of successful packet transmission denoted P_s is given by (5-36), which is the same equation as in chapter 4.

$$P_s = 1 - P_e^{(d)} \quad (5-36)$$

$P_e^{(d)}$ can be obtained from Figure 3-3a and b as explained in chapter 4. If this probability (P_s) is multiplied by p_d , a new dynamic p -persistent value (px_d) that depends on the channel conditions can be obtained as shown in (5-37).

$$px_d = p_d(1 - \varphi \times P_e^{(d)}) \quad (5-37)$$

Where φ is a scaling factor that depends on the QoS needed and the range of φ is defined in (5-38). By applying this across two traffic types with s-ratio 2:1 gives expressions for px_1 and px_2 in (5-39) and (5-40) respectively.

$$0 \leq \varphi < \frac{1}{P_e^d} \quad (5-38)$$

$$px_1 = p_1(1 - \varphi \times P_e^{(1)}) \quad (5-39)$$

$$px_2 = \left(\frac{0.5p_1}{(1 - 0.5p_1)}\right)(1 - \varphi \times P_e^{(2)}) \quad (5-40)$$

This proposed algorithm can be implemented practically in a very simple way as PER information can be obtained through the link adaptation mechanisms. The default value of p will be set by the station on the basis of an ideal channel and as the link degrades the p value changes dynamically according to equations (5-39) and (5-40) as explained in section 4.6.1. This protocol is similar to that was presented section 4.6 with a modification to work with link-adaption mechanisms (i.e. changing the data rate according to the link quality). Also, this protocol does not require any information from the base station or any other stations in the system other than measure of PER. The proposed protocol can be easily implemented as it does not require any hardware modifications and can benefit from link-adaption mechanisms for calculating the PER values.

5.5 Simulation Setup

The simulator that was developed in chapter 3 was modified to model the system described in section 5-2. The main modification was in the Transmit Function. In this Function, the station that commences a successful transmission should be classified according to its category type. Based on this classification the packet will be transmitted at this category data rate. In the case of unsuccessful transmission, the collided packets should be classified based on their access categories and the transmission time will be considered based on the lowest data rate of the collided packets. In this simulator all throughput and delay values should be absolute, not normalized as in the case of a single data rate. The rest of the simulator is the same to that explained in chapter 3.

5.6 Results and Discussions

In this section, several experiments were investigated to illustrate the anomaly effect in WLANs. The throughput and delay results of these experiments demonstrate the accuracy of our multirate mathematical models provided in the previous sections. The throughput results are presented first followed by the delay results. In addition, experiments that demonstrate the effectiveness of the new adaptive protocol in alleviating the anomaly effect are provided.

5.6.1 Throughput Results

In this section, the results are divided into two sets. The first set provides the results for the multirate basic model and the second set provides the results for the cross-layer approach with multirate.

A- Basic multirate model results

In order to illustrate the anomaly effect three experiments were carried out. In the first experiment, the 802.11b DCF modelled for two traffic groups. Simultaneously, the p -persistent CSMA with 2 traffic types of the same priority is investigated to reflect the same behaviour. In the second experiment, the first experiment is repeated for 802.11n and a corresponding p -persistent CSMA protocol. In the third experiment, the QoS differentiated p -persistent CSMA protocol with multirate is investigated.

In the first experiment, a similar DCF network topology was considered to that in [71] based on 802.11b, with the topology composed of two stations in Group 1 (G1) transmitting at 11 Mbit/s while varying the number of stations from 2 to 14 in Group 2 (G2) transmitting at 1Mbit/s. In order to do a fair comparison, the topology in [71] was used for the p -persistent CSMA protocol evaluated here. Access Category 1 (AC1) corresponds to G1 while Access Category 2 (AC2) corresponds to G2. The same experiment was repeated for 802.11n with data rates 26 and 6.5 Mbit/s for DCF and p -persistent CSMA with a multirate capability. The simulation parameters are shown in Table 5-1. For the case of p -persistent CSMA protocol, the p value was to 0.03 for both access categories which corresponds to the homogeneous case of protocol. The p -values in our model can be modelled in an 802.11 DCF simulator by fixing the size of the contention window (CW) such that $CW_{\min} = CW_{\max}$. The relationship between p and CW is $p = 2/(CW + 2)$ as calculated in [86]. The results for p -persistent CSMA were obtained both analytically and by simulations, while the results for DCF with multirate capability were obtained by simulations only. Figure 5-2a shows graphs of throughput versus number of stations for the 802.11b DCF and p -persistent CSMA. The results show that the throughput of both G1 and G2 are less than 1Mbit/s even though stations in G1 transmit at 11 Mbit/s. The same throughput trend was obtained for AC1 and AC2. Figure 5-2b shows the results for 802.11n and similar trends are obtained as for the results in

Figure 5-2a. The results illustrate the behaviour of the performance anomaly. The results show very close agreement between 802.11 DCF with a fixed size of contention window and the homogeneous case of p -persistent CSMA. The results demonstrate that the throughput is severely degraded die to the anomaly effect.

Table 5-1: system simulation parameters of 802.11b/n

Parameters	802.11b	802.11n
Packet size	2324 byte	1500 byte
ACK	192 μ s	32 μ s
SIFS	10 μ s	16 μ s
DIFS	50 μ s	34 μ s
Slot	20 μ s	9 μ s

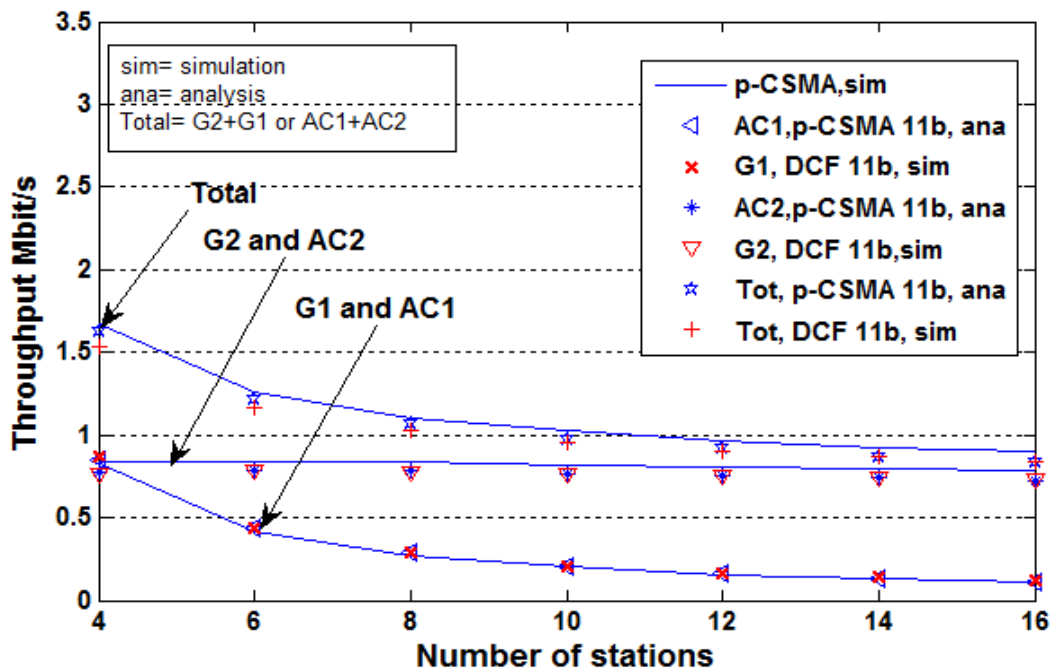


Figure 5-2a: Saturated throughput per group and traffic type of 802.11 DCF and p -persistent CSMA respectively for 802.11b stations

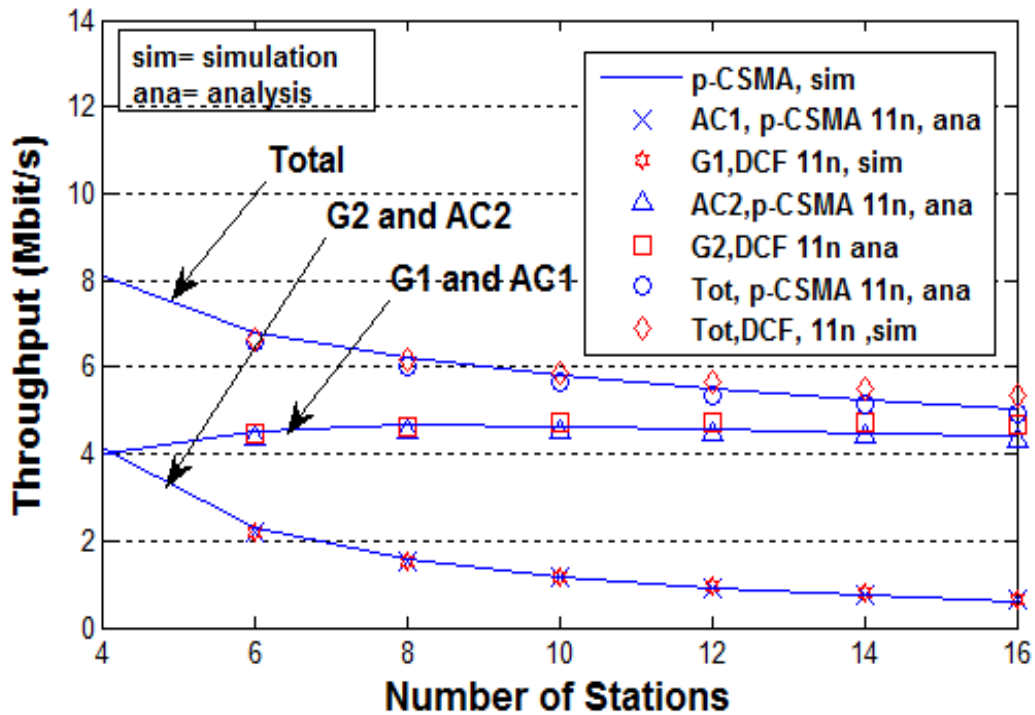


Figure 5-2b: Saturated throughput per group and traffic type of 802.11 DCF and p-persistent CSMA respectively for 802.11n stations

Figure 5-3 shows the throughput performance per traffic type of a *p*-persistent CSMA protocol with QoS differentiation for 4 traffic types (5 stations per traffic type) when transmitting at different data rates. A p_1 value equal to 0.03 was used while p_2 , p_3 and p_4 were calculated in order to achieve throughput ratios $S_1=2S_2$, $S_2=2S_3$ and $S_3=2S_4$ according to Hui's ratio [84]. In order to show the capability of our model (i.e. multirate), two scenarios were investigated. In the first scenario (i.e. single rate), all station of all traffic types transmit at data rate of 58.5 Mbit/s. Each Station of traffic type 1 achieves an average throughput of 3.23 Mbit/s. In the second scenario (i.e. multirate), stations of traffic type 2 to type 4 drop their channel rates to 39, 26 and 6.5 Mbit/s, respectively, due to adverse channel conditions. In this scenario, each station of traffic type 1 can only achieve an average throughput of 2.07

Mbit/s, even though its channel rate is 58.5 Mbit/s which corresponds to a 36.4% drop in the throughput due to the *performance anomaly* effect.

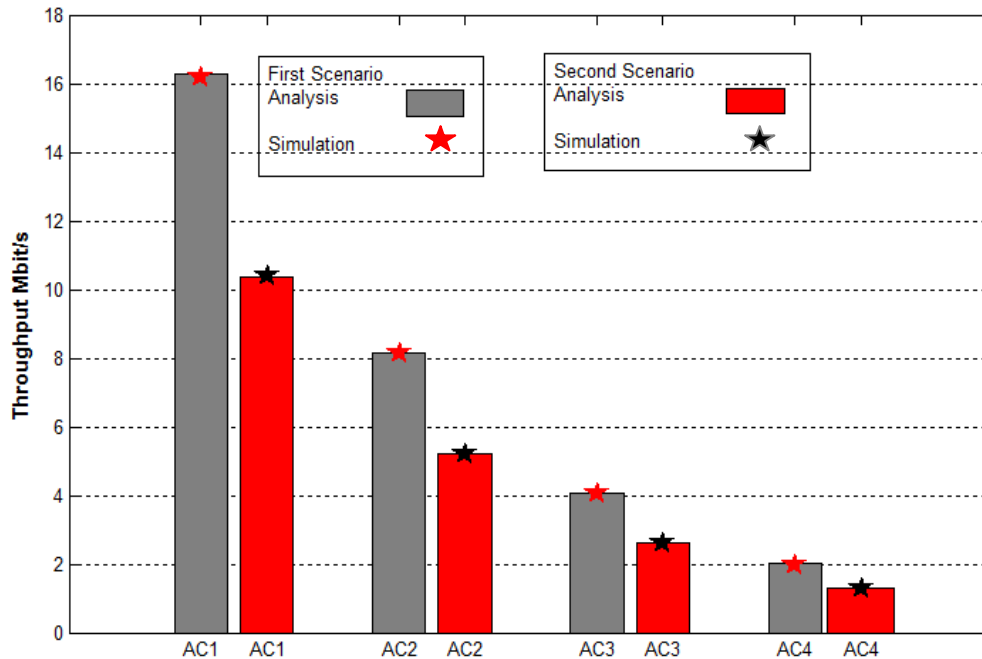


Figure 5-3: Throughput of stations transmitting at different data rates for 802.11n with different priorities

B- Cross-layer results

In this set of results, the effect of the PHY layer was investigated in terms of packet error rate and capture effect. The same scenarios as in the first set of results were investigated. In Figure 5-4, the effect of packet error rate on the throughput performance was investigated in the two scenarios. The first scenario demonstrates the case where all stations of the four traffic types transmit at 58.5 Mbit/s with two channel conditions (SNR = 8 dB and 9 dB). The "single rate" in the legend in Figure 5-4 refers to the model with single data rate and ideal channel conditions while the "multirate" refers to the model with multirate capability and ideal channel conditions. Also, in Figure 5-4 stations from 1 to 5 belong to AC1, stations from 6 to 10 belong to AC2, stations from 11 to 15 belong to AC3 and stations from 16 to 20

belong to AC4. As expected the throughput degrades due to channel errors by 10% and 6% for SNR values 8 dB and 9 dB respectively in the case of the old model. The same result was obtained for the multirate. However, the packet error rate was the same for the 4 access categories but the SNR values are different according to the data rate for each traffic type.

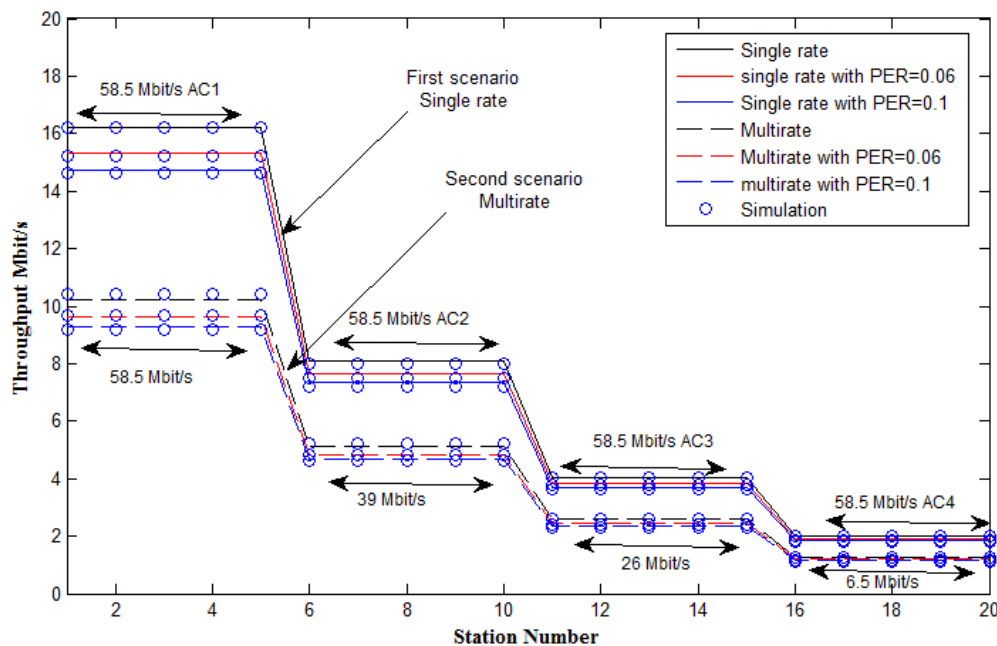


Figure 5-4 Throughput for stations of 4 traffic types with single rate and multirate scenarios and channel errors effect

Figure 5-5 shows the throughput versus number of stations when the capture effect is taken into account. In this experiment traffic type 1 transmits at 58.5 Mbit/s and $p_1 = 0.05$. Traffic type 2, type 3 and type 4 transmit at 39 Mbit/s, 26 Mbit/s and 6.5 Mbit/s respectively. Their priorities were chosen to achieve throughput ratios $S_1=2S_2$, $S_2=2S_3$ and $S_3=2S_4$. Comparing the two cases without capture and with capture in Figure 5-5, the results show that as the number of stations increases the throughput with capture effect improves due to the increase in number of collisions in the network. For example, when the number of stations is equal to 28 the improvement in the throughput is 18.5 % compared to the case when the capture effect

is not included. This shows the total system throughput for the same experiment and the results show the same trend as the total system throughput is improved by 19% when the capture is included and number of stations is equal to 28. These results confirm that modelling the capture effect is important in order to obtain a more accurate network characterisation. However, the throughput of the higher data rates is degraded due to performance anomaly but including the capture effect shows alleviation of the issue. Comparing this result to that obtained in Figure 3-5b, it can be seen that the results in Figure 3-5b show that the capture effect can improve the throughput by 26% when the number of stations is equal to 28 whereas in the multirate model the capture effect can only improve the throughput by 19%. This is because in the case of a multirate model, the network is less congested, even though there is the same number of stations, as stations with low data rates take longer time to transmit which reduces the probability of collision.

Figure 5-5a shows the results for throughput of 4 traffic types at capture threshold, $z=5\text{dB}$ with the number of stations as a parameter. This scenario is similar to that in Figure 5-3 except that $p_1=0.05$ and the number of station is a variable. A similar trend to that in Figure 3-5 is obtained. The results show that although the traffic types transmit at a different data rates, a station still can benefit from the capture effect. For example, when the number of stations is equal to 28 the throughput is increased by 20% compared to the case of without capture. Figure 5-5b shows the total throughput of the experiment presented in Figure 5-5a. The term "single rate" in the legend of Figure 5-5b refers to the basic model without considering multirate. Again, the results show that including the capture effect in a more accurate characterization of network. The results show that total throughput is increased from 15.2 Mbit/s to 18.4 Mbit/s when the number of stations is equal to 28. This experiment demonstrates that when a station transmits at a different data rate the throughput performance is better than it appears in the basic case analysis due to the capture effect phenomena.

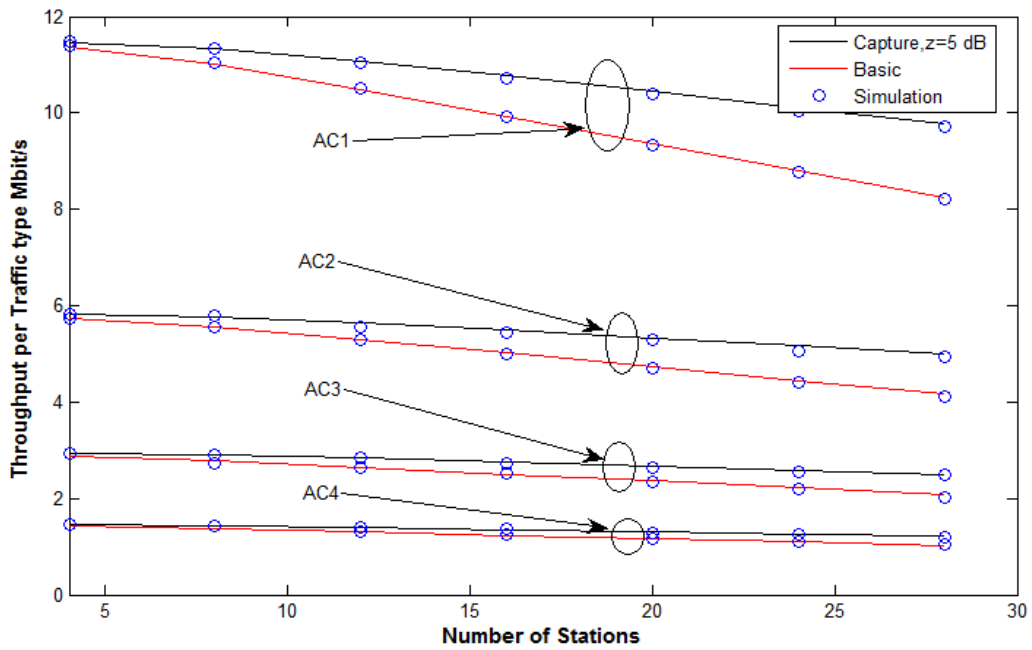


Figure 5-5a: Throughput versus number of stations for 4 traffic types with single rate and multirate scenarios, $p_1=0.5$ and $z=5$ dB

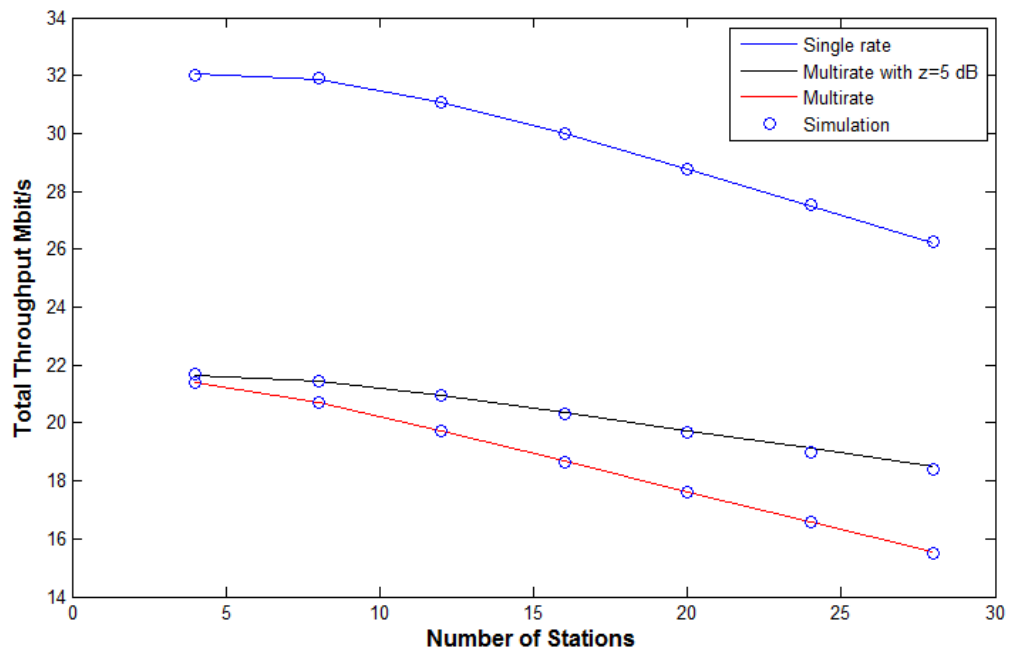


Figure 5-5b: Total throughput versus number of stations for 4 traffic types with single rate and multirate scenarios, $p_1=0.5$ and $z=5$ dB

Figure 5-6 demonstrate the PHY layer effects where $PER = 0.06$ and threshold z as a parameter. In this experiment all stations are considered to have the same PER but at different SNR values due to transmitting at different data rates. The results in Figure 5-6 show when the number of stations is less than 12 the benefit from the capture effect is negligible, as there are no collisions and the failed packets are due to the link quality. As the number of stations increase the capture effect becomes clearer in the throughput performance. This improvement in the throughput depends also on the capture threshold z . For example, when the number of stations is equal to 28, the throughput with $z=2, 5, 10$ dB is higher than the basic single rate model by 14.6, 19.6 and 12% respectively.

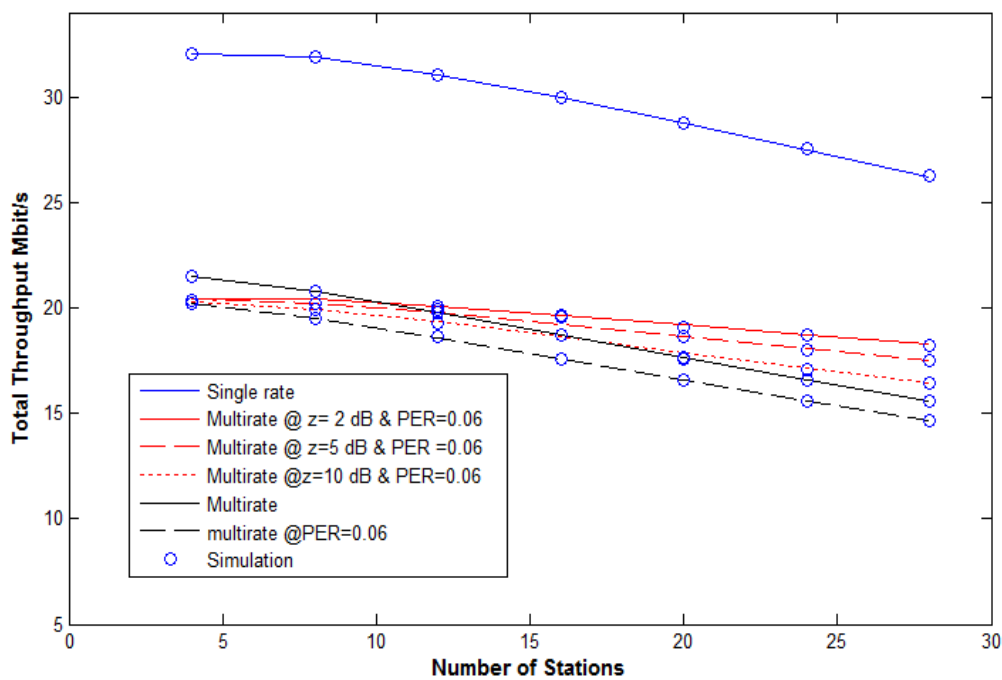


Figure 5-6: Total throughput versus number of stations for 4 traffic types with $p_1=0.5$, $PER = 0.06$ and capture threshold z as parameter at different data rates

5.6.2 Delay Results

Figure 5-7 shows the delay performance per traffic type of the two scenarios that were investigated in Figure 5-3. The results show that the average delay is increased due to the anomaly effect. For example, in the first scenario the average delay of traffic type 1 is 3.6 ms while in the second scenario it is increased to 5.7 ms, corresponding to a 58% increase in the average delay. Figure 5-8 shows the effect of packet error rates on the average delay for the two scenarios in Figure 5-4. The results are shown, as a line graph for clarification. The packet error rates have a similar effect on the system; average delay performances were similar as in the throughput case. As expected, the results show that as the packet errors degrade the delay performance for all traffic types.

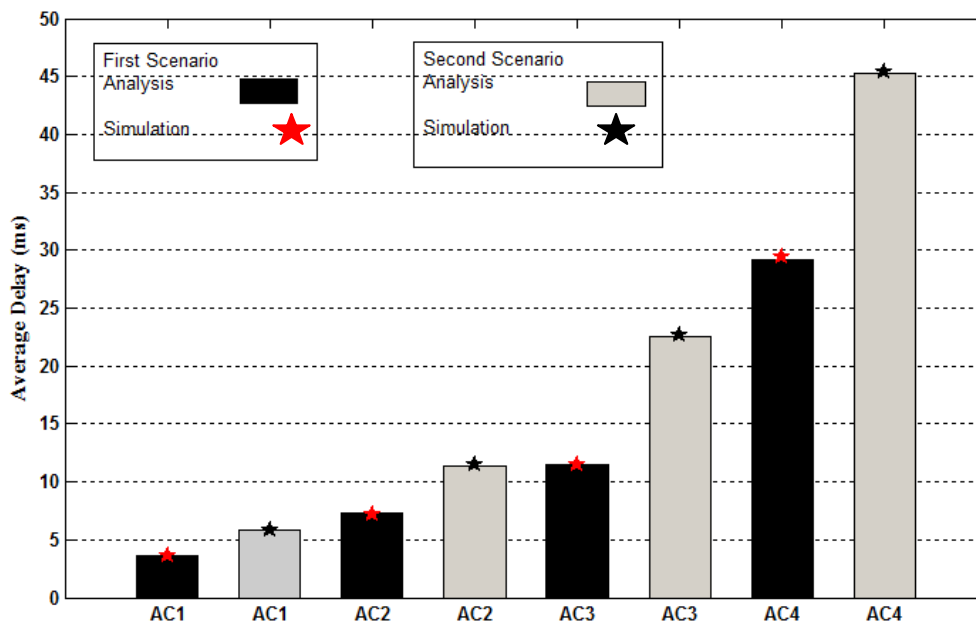


Figure 5-7 : Delay of stations for 4 ACs with single rate and multirate scenarios, $p_1=0.5$

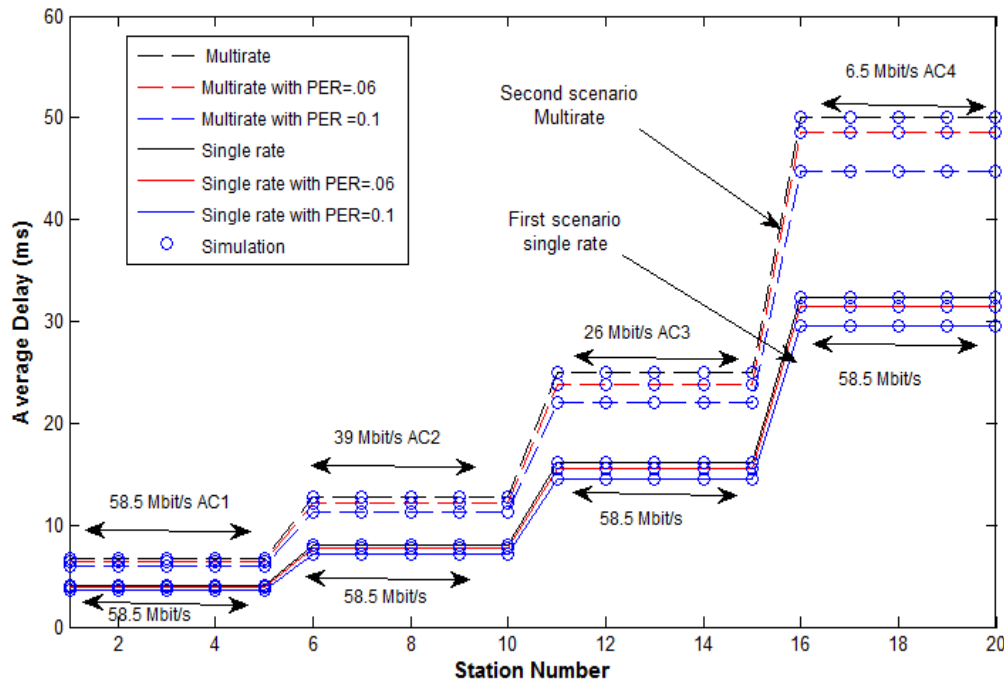


Figure 5-8 Average delay of stations of 4 traffic types transmitting at different data rates for 802.11n with channel errors effect

Figure 5-9 and Figure 5-10 show the results of the average delay per traffic type for the same throughput experiments in Figure 5-5 and Figure 5-6 respectively. Figure 5-9 shows that the capture effect reduces the average delay for all traffic types and the lowest priority benefits more than the highest priority. For example, the average delay of AC 4 is reduced from 80.4 ms when the capture is not included to 67.77 ms when $z = 5$ dB. Figure 5-10 shows the case when packet error rates and different values of capture threshold are investigated. The results show the same trend as in the throughput performances. When $PER = 0.06$ average delay per traffic type is increased and as the capture threshold decreases the average delay is reduced.

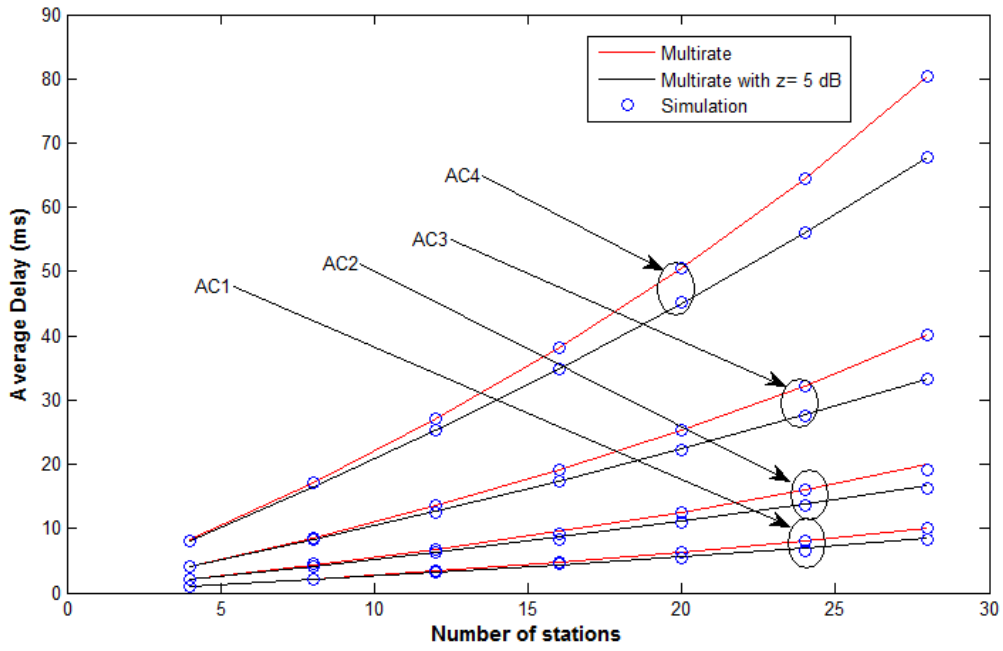


Figure 5-9 Average delay versus number of stations for 4 traffic types with $p_1=0.05$ and $z=5$ dB at different data rates

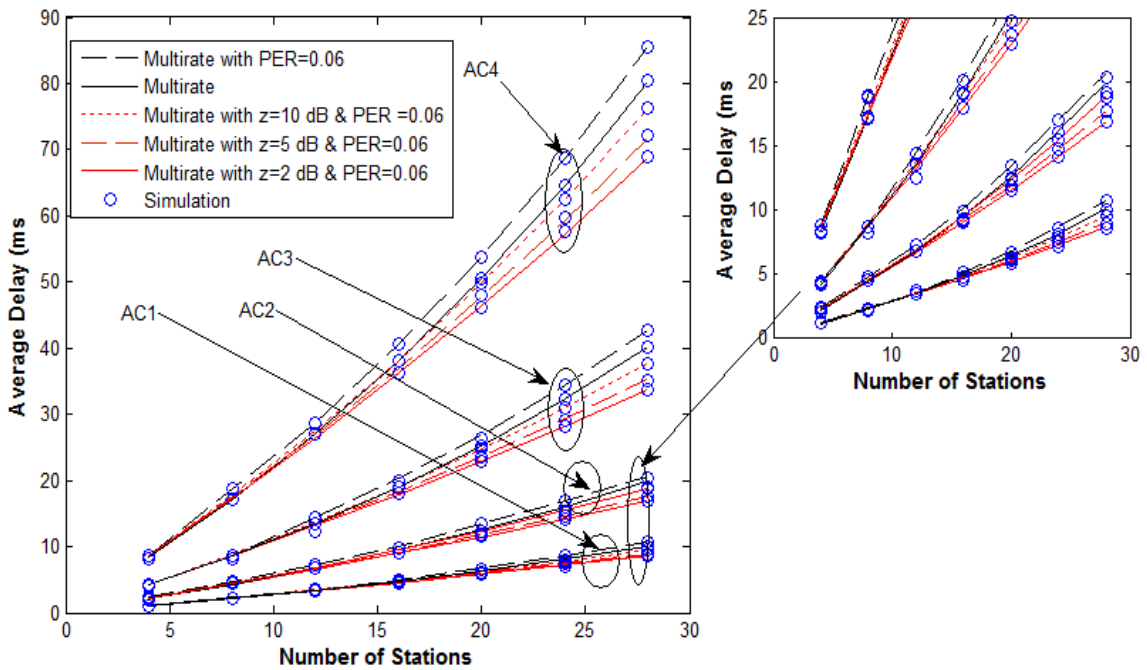


Figure 5-10: Average delay versus number of stations for 4 traffic types with $p_1=0.5$, $PER=0.06$ and capture threshold z as parameter at different data rates

5.6.3 Adaptive Protocol Results

In order to demonstrate the effectiveness of the new adaptive protocol, two scenarios were investigated. In the first scenario, two access categories were considered (AC1 and AC2) with 5 stations each. Their priorities were chosen to achieve throughput ratios $S_1=2S_2$ and $p_1=0.03$. Stations of traffic type 1 always transmit at 58.5 Mbit/s, while stations of traffic type 2 changed their data rate according to channel conditions. Here, we consider PER =0.1 which makes the station drop its data rate to a lower one. For example when PER=0.2, the station drops its data rate from 58.5 Mbit/s to 39 Mbit/s. The results of the first scenario for the throughput and delay are depicted in Figure 5-11 and Figure 5-12, respectively. Firstly, stations of traffic type 2 drop their data rate from 58.5 Mbit/s to 39 Mbit/s which makes the average throughput of traffic type 1 degrades from 20.53 Mbit/s to 18.49 Mbit/s as shown in Figure 5-11. When the adaptive protocol is used and p_2 is changed to a new value according to equation (5-40) where PER=0.2 the throughput of traffic type 1 is only degraded to 20.19 Mbit/s. Secondly, when the stations of traffic type 2 dropped their data rate to 26 Mbit/s, the throughput for stations of traffic type 1 is decreased to 16.17 Mbit/s and when the adaptive protocol is applied the throughput only degraded to 19 Mbit/s, which corresponds to 17.5% increase in the throughput compared to the non-adaptive protocol. Finally, when stations of traffic type 2 transmit at 6.5 Mbit/s, the throughput of traffic type 1 stations degrades to 7.5 Mbit/s, while with the adaptive protocol they degrade to 12.23 Mbit/s which corresponds to a 63% increase in the throughput compared to the normal protocol. The results in Figure 5-11 demonstrate that the adaptive protocol alleviates the anomaly issue in WLANs Figure 5-12 shows the results of the average delay. The results demonstrate that the adaptive protocol also improves the average delay performance of traffic type 1. For example, when stations of traffic type 2 transmit at 6.5 Mbit/s the delay increased from 2.8

ms to 7.8 ms, while when the adaptation protocol is applied the delay is increased only to 4.8 ms.

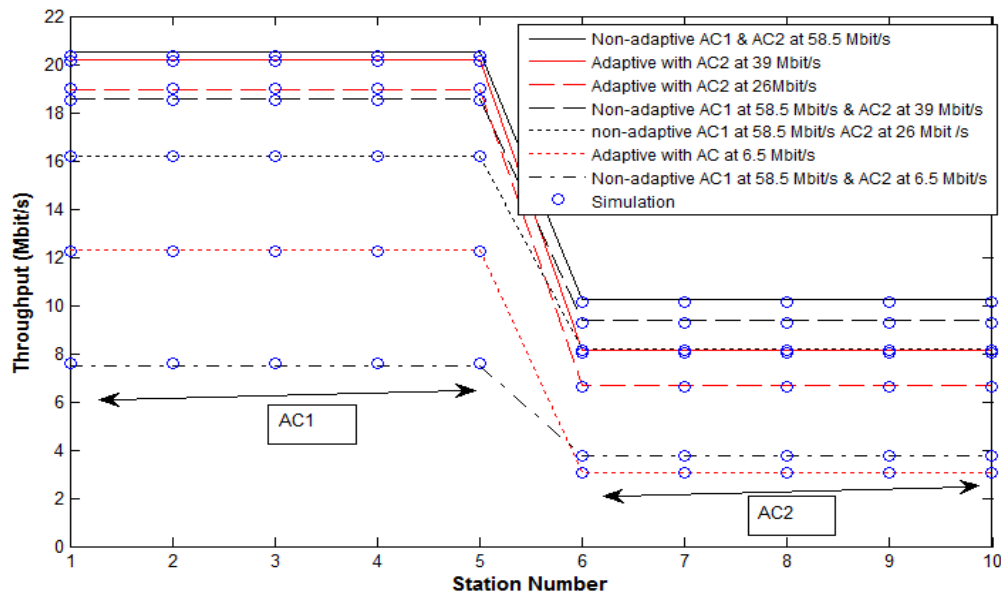


Figure 5-11: Throughput performance of the adaptive protocol for 2 access categories with 5 stations each and $p_1=0.03$ at different data rates

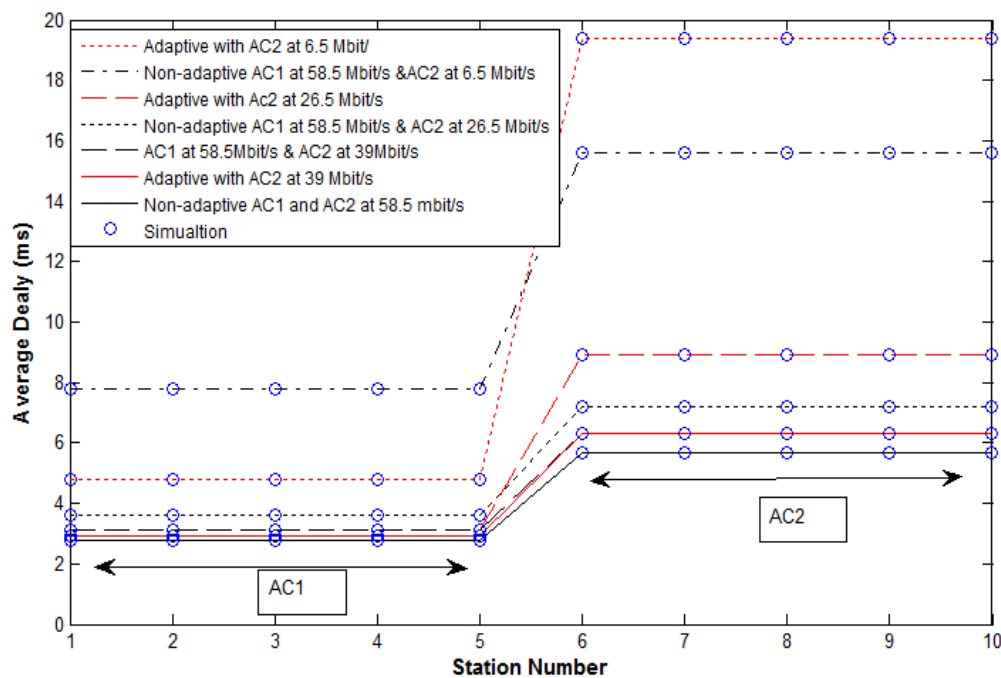


Figure 5-12: Average delay performance of the adaptive protocol for 2 access categories with 5 stations each and $p_1=0.03$ at different data rates

Figure 5-13 and Figure 5-14 show the results of the second scenario of the throughput and delay respectively. In this scenario, again two access categories were considered with 5 stations per traffic type. Their priorities were also chosen to achieve throughput ratios $S_1=2S_2$ and $p_1=0.03$. Stations of traffic type 1 always transmit at 58.5 Mbit/s, while stations of traffic type 2 transmit at 6.5 Mbit/s. This experiment investigates the benefits from including the scaling factor φ (i.e. scaling the value of PER before multiplied with p value). The term "Phi" in the legend refers to the scaling factor φ . The PER =0.5 and the range of possible values of scaling factor, φ are ($0 < \varphi < 1.8$). When $\varphi = 0$ the protocol non-adaptive and when $\varphi = 1$ the obtained result is similar to that in previous scenario. As φ increases the throughput is improved, for example, when $\varphi = 1.2$ the throughput of traffic type 1 stations is improved by 83.7% compared to the non-adaptive. By proper selection of the scaling factor, the throughput can be restored back to the value where there is no anomaly issue. In this experiment when $\varphi = 1.6$ the throughput is 19.0 Mbit/s, which was very close to the case before the anomaly happened. Proper selection of the scaling factor is also very important to maintain a good level of fairness between the two traffic types.

The results in Figure 5-14 demonstrate that including the scaling factor in adaptive protocol can improve the average delay performance of the traffic type 1 to reach the point before the anomaly occurred. For example, when stations $\varphi = 1.6$ the average delay is 3.07 ms while before the anomaly occurred it was 2.8 ms, which confirms the effectiveness of the new protocol. The above results in the two scenario demonstrate that the p -persistent CSMA can be used adaptively to mitigate the anomaly issue in the WLANs. The improvement of performance of the affected traffic type can be enhanced by introducing the scaling factor. However, the scaling factor should be selected properly in order to maintain a good level of fairness among the traffic types. By using the adaptive protocol the QoS required for a certain

traffic type with specific applications can be maintained by this new adaptive p -persistent CSMA protocol.

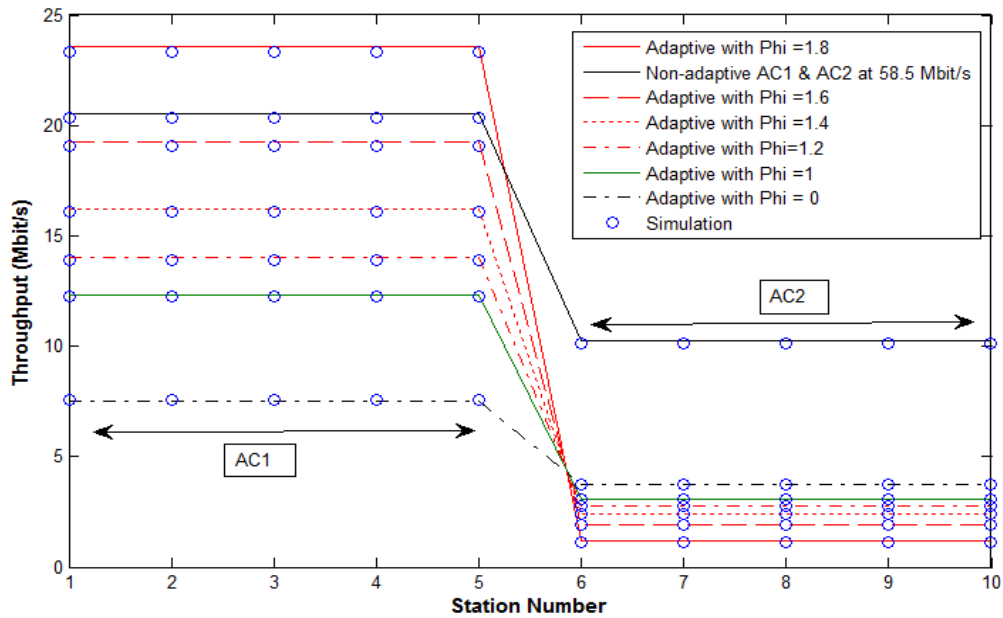


Figure 5-13: Throughput performance of the adaptive protocol for 5 station per 2 access with $p_1=0.03$ and φ as a parameter

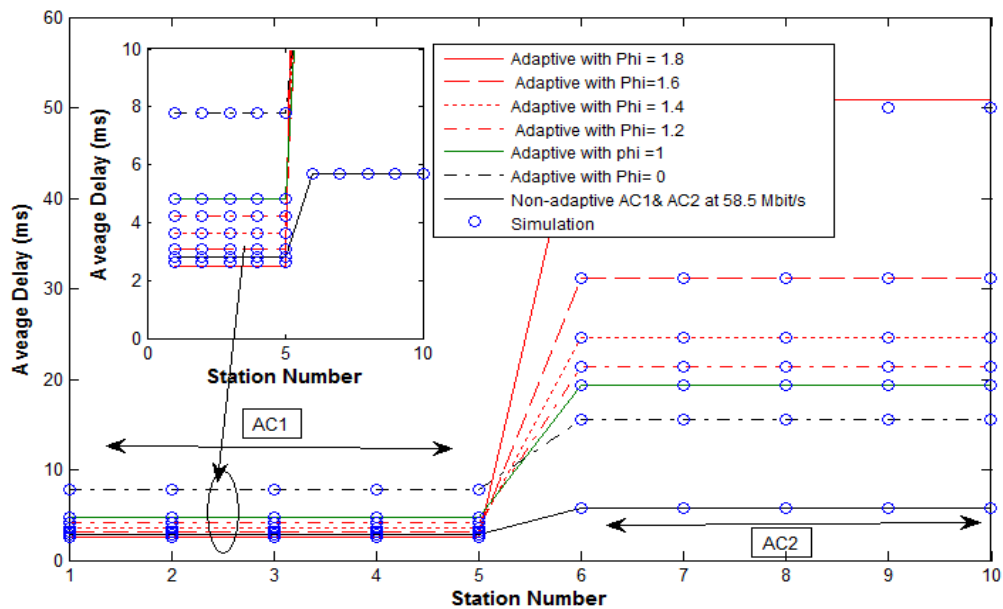


Figure 5-14: Average delay performance of the adaptive protocol for 5 stations per access category with $p_1=0.03$ and φ as a parameter

5.7 Enhanced Multirate Model

In this model, our previous multirate model is generalised to model the multirate capability for each station in the system regardless of its traffic type.

5.7.1 Model Description

The main differences between this model and the previous model is that the transmission time, $T_{d,\vartheta}$, (ϑ is the group number) is variable depending on the rate of transmission of the station regardless of its traffic type and whether there is a successful transmission or collision. This means stations with the same traffic type could have different transmission rates as shown in Figure 5-15. The system contains M stations, where $M=M_1+M_2+\dots+M_{d_{max}}$, M_d represents the number of stations with type d traffic, and d_{max} is the total number of traffic types in the system. Each station has only one traffic type. In our model, we classify the stations within the same traffic type into different groups (ϑ) according to their rate of the transmission, where stations belonging to a particular group have the same data rate. The number of stations in group ϑ is denoted as $M_{d,\vartheta}$ where $\vartheta = 1, 2, \dots, \vartheta_{max}$ is the group number, and the total number of stations within each traffic type is M_d as shown in (5-41).

$$M_d = \sum_{\vartheta=1}^{\vartheta_{max}} M_{d,\vartheta} \quad (5-41)$$

Hence the total number of stations in the system is given by (5-42).

$$M = \sum_{d=1}^{d_{max}} \sum_{\vartheta=1}^{\vartheta_{max}} M_{d,\vartheta} \quad (5-42)$$

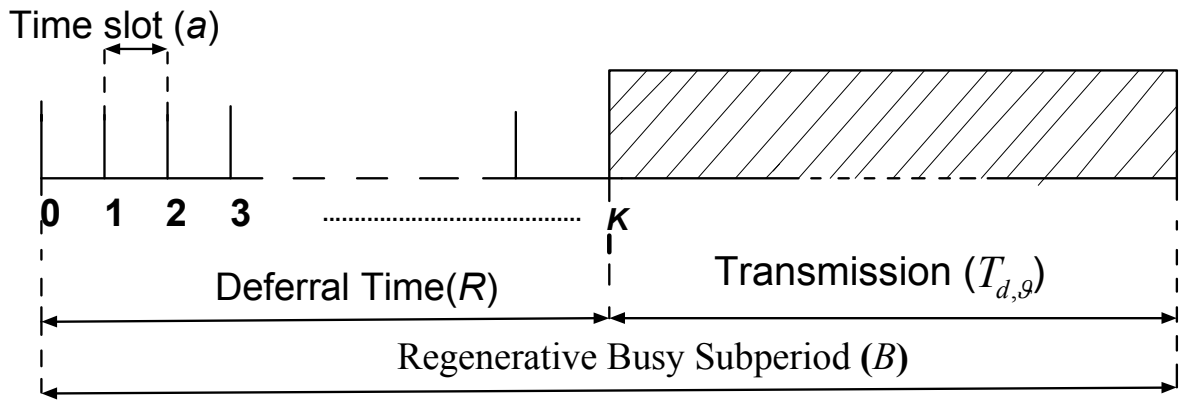


Figure 5-15: Channel state cycle for saturated case with multirate per station

5.7.2 Basic Throughput Analysis

In this model, a more realistic approach is considered where each station in the network has its own data rate. In order to include this approach into our model, equation (5-1) must be modified as in (5-43) to calculate the throughput of group 1 ($S_{1,1}$) and equation (5-3) must be modified to calculate the probability of a successful transmission for group 1 within traffic type 1 as shown in (5-43).

$$S_{1,1} = \frac{E[U_{1,1}]}{E[B]} \quad (5-43)$$

$$P(1tx_{1,1}) = M_{1,1}p_1(1 - p_1)^k[(1 - p_1)^{k+1}]^{M_{1,1}-1} \quad (5-44)$$

$$k = 0, 1, 2, \dots, \infty$$

The probability that no transmission has occurred before time slot boundary $k+1$ for stations of each other traffic type and for stations of each other group within traffic type 1 (i.e. $\vartheta \neq 1$) is obtained by modifying equation (5-4) as shown in (5-46).

(5-45)

$$P(0tx_{d,\vartheta}) = [(1 - p_d)^{k+1}]^{M_d} [(1 - p_1)^{k+1}]^{M_{1,\vartheta}}$$

Using equations (5-44) and (5-45) the probability of a successful packet transmission, $P(S_{1,1})$, of stations of group 1 within traffic type 1 commencing transmission at time slot boundary k for $k=0, 1, 2, \dots, \infty$ is given by (5-46).

$$P(S_{1,1}) = P(1tx_{1,1}) \prod_{d \neq 1, \vartheta \neq 1}^{d_{max}, \vartheta_{max}} P(0tx_{d,\vartheta}) \quad (5-46)$$

If (5-46) is evaluated over the full range of k , then $E[U_{1,1}]$ can be obtained as shown in (5-47).

$$E[U_{1,1}] = b_{1,1} \sum_{k=0}^{\infty} P(S_{1,1}) \quad (5-47)$$

The expected busy period ($E[B]$) is the sum of the expected deferral time $E[R]$ and expected transmission times $E[T]$ as in (5-7). The expected length of the deferral time, $E[R]$, can be calculated as shown in (5-48).

$$E[R] = a \sum_{k=1}^{\infty} \left(\prod_{d=1, \vartheta=1}^{d_{max}, \vartheta_{max}} [(1 - p_d)^{k+1}]^{M_{d,\vartheta}} \right) \quad (5-48)$$

$E[T]$ is calculated differently as follows: Firstly the successful transmission time for each group within traffic type d , $E[T_{s,d,\vartheta}]$ should be calculated, for example, the expected successful transmission time of traffic group 1 within type 1, $E(T_{s,1,1})$, is given by (5-49).

$$E[T_{s_{-1,1}}] = \sum_{k=0}^{\infty} \left(P(1tx_{1,1}) \prod_{d \neq 1, \vartheta \neq 1}^{d_{max}, \vartheta_{max}} P(0tx_{d,\vartheta}) \right) \times T_{1,1} \quad (5-49)$$

Then, the total expected successful transmission time $E(T_s)$ is given by (5-50)

$$E[T_s] = \sum_{d=1}^{d_{max}} \sum_{\vartheta=1}^{\vartheta_{max}} E[T_{s_{-1,\vartheta}}] \quad (5-50)$$

$E[T_c]$ is the collision time and is due to two types of collisions, internal collision which result from a collision between two or more packets from stations in the same group with same traffic type and external collisions which are due to a collision between two or more packets from stations of other groups with the same and different traffic types. In order to calculate $E[T_c]$ the probability of more than one station (i.e. $\beta_{d,\vartheta} \geq 2$) transmitting at the same time ($P_{d,\vartheta}$) is calculated first as shown in (5-51). The probability of an internal collision of traffic type 1 ($P_{i1,1}$) is given by (5-52).

$$P_{d,\vartheta} = \binom{M_{d,\vartheta}}{\beta_{d,\vartheta}} (p_d(1-p_d))^{\beta_{d,\vartheta}} [(1-p_d)^{k+1}]^{M_{d,\vartheta}-\beta_{d,\vartheta}} \quad (5-51)$$

$$P_{i1,1} = \binom{M_{1,1}}{\beta_{1,1}} (p_1(1-p_1))^{\beta_{1,1}} [(1-p_1)^{k+1}]^{M_{1,1}-\beta_{1,1}} \\ \times \prod_{d \neq 1, \vartheta \neq 1}^{d_{max}, \vartheta_{max}} [(1-p_d)^{k+1}]^{M_d} [(1-p_1)^{k+1}]^{M_{1,\vartheta}} \quad (5-52)$$

The probability of an external collision ($P_{e1,1}$) for group1 within traffic type 1 can be calculated as shown in (5-53)

$$P_{e1,1} = \sum_{\beta_{1,1}=1}^{M_{1,1}} \dots \sum_{\beta_{1,\vartheta_{max}}=0}^{M_{1,\vartheta_{max}}} \sum_{\beta_{2,\vartheta}=0}^{M_{2,1}} \dots \sum_{\beta_{1,\vartheta_{max}}=0}^{M_{2,\vartheta_{max}}} \dots \sum_{\beta_{d_{max},\vartheta_{max}}=x}^{M_{d_{max},\vartheta_{max}}} \left(\prod_{d=1, \vartheta=1}^{d_{max}, \vartheta_{max}} P_{d,\vartheta} \right) \quad (5-53)$$

Where $x = 0$ if any other traffic type has a packet to transmit and $x=1$ if all other traffic types have no packets to transmit. When calculating the external collision of group 2 with traffic type 1 the external collision between group 1 and group 2 should be excluded as it is already included in the case of traffic type 1 and so on for other groups. The total collision time of group 1 with traffic type 1, $E[T_{c_{-1,1}}]$, can be calculated using (5-52) and (5-53) as shown in (5-54).

$$E[T_{c_{-1,1}}] = \sum_{k=0}^{\infty} P_{e1,1} \times T_{max} + \sum_{k=0}^{\infty} P_{i1,1} \times T_{1,1} \quad (5-54)$$

Where T_{max} is maximum collision time of a transmitted packet and the total collision time $E[T_c]$ can be calculated as in (5-55).

$$E[T_c] = \sum_{d=1}^{d_{max}} \sum_{\vartheta=1}^{\vartheta_{max}} E[T_{c_{-1,\vartheta}}] \quad (5-55)$$

The throughput of group 1 within traffic type 1 can be calculated by substituting equations (5-50) and (5-55) into equation (5-7) and then substituting equation (5-7) and (5-48) into (5-43). The total system throughput can be calculated as shown in (5-57).

$$S = \sum_{d=1}^{d_{max}} \sum_{\vartheta=1}^{\vartheta_{max}} s_{1,\vartheta} \quad (5-56)$$

5.7.3 Basic Delay Analysis

The delay is calculated for a station in group 1 with traffic type $d = 1$, however this analysis can be applied to stations of any of the traffic types in the system by simple substitution. The overall delay for a group 1 with station traffic type 1 packet, $\bar{D}_{1,1}$, with multirate capability can then be calculated as shown in (5-57).

$$\bar{D}_{1,1} = \frac{E[R] + \sum_{d=1}^{d_{max}} \sum_{\vartheta=1}^{\vartheta_{max}} E[T_{c_{-1,1}}] + \sum_{d=1}^{d_{max}} \sum_{\vartheta=1}^{\vartheta_{max}} E[T_{s_{-1,1}}]}{P_{1,1}} \quad (5-57)$$

Where $P_{1,1}$ is shown in (5-58).

$$P_{1,1} = \frac{P(s_{1,1})}{M_{1,1}} \quad (5-58)$$

Now the average delay of stations of traffic type 1 can be calculated as shown in (5-59).

$$\bar{D}_1 = \sum_{\vartheta=1}^{\vartheta_{max}} \bar{D}_{1,\vartheta} \quad (5-59)$$

5.7.4 Throughput Analysis with PHY Effects

This analysis is similar to that in model 1 except that the packet error rates effect and capture are added to the analysis using groups instead of traffic type. In this analysis, only the key equations are presented. Equations (5-43) and (5-20) are written for groups as shown in (5-60) and (5-61).

$$S_{1,1_phy} = \frac{E[U_{1,1_phy}]}{E[B_{phy}]} \quad (5-60)$$

(5-61)

$$P(S_{d,\vartheta}phy) = P(S_{d,\vartheta}pe) + P(S_{d,\vartheta}cap)$$

For this model, equation (5-21) can be written for groups as shown (5-62).

$$\begin{aligned}
P(S_{1,1}phy) &= P(1tx_{1,1}) \prod_{d \neq 1, \vartheta \neq 1} P(0tx_{d,\vartheta}) \times (1 - P_e^{1,1}) \\
&+ \sum_{\beta_{1,1}=2}^{M_{1,1}} \dots \sum_{\beta_{1,\vartheta_{max}}=0}^{M_{1,\vartheta_{max}}} \dots \sum_{\beta_{d_{max},\vartheta_{max}}=0}^{M_{d_{max},\vartheta_{max}}} \left(\prod_{d=1}^{d_{max}} P(\beta_{d,\vartheta}tx_{d,\vartheta}) \right) (\beta_{1,1})q((\beta - 1)|z_{1,1})
\end{aligned} \tag{5-62}$$

Then an expression for $E[U_{1,1,phy}]$ given by (5-64).

$$E[U_{1,1,phy}] = T_{1,1} \times b_{1,1} \times \sum_{k=0}^{\infty} P(S_{1,1}phy) \tag{5-63}$$

The expected busy period in the presence of PHY layer effects ($E[B_{phy}]$) is the sum of the expected deferral and expected transmission times as in (5-64)

$$E[B_{phy}] = E[R] + E[T_{phy}] \tag{5-64}$$

The expected transmission time in the presence of PHY layer effects ($E[T_{phy}]$) can be calculated by (5-24). $E[T_{s,phy}]$ is the successful transmission time with PHY layer effects for the case of group basis as shown in (5-65), and $E[T_f]$ is the transmission time when the packet is not received due to channel errors and can be calculated by (5-66).

$$E[T_{s_phy}] = \sum_{d=1}^{d_{max}} \sum_{\vartheta=1}^{\vartheta_{max}} \left[T_{d,\vartheta} \times \sum_{k=0}^{\infty} P(s_{d,\vartheta}phy) \right] \quad (5-65)$$

$$E[T_f] = \sum_{d=1}^{d_{max}} \sum_{\vartheta=1}^{\vartheta_{max}} \left[T_{d,\vartheta} \times P_e^{(d,\vartheta)} \times \sum_{k=0}^{\infty} P(s_{d,\vartheta}) \right] \quad (5-66)$$

$E[T_{c_cap}]$ is the collision time when the capture effect is considered in the system and can be calculated by (5-67).

$$E[T_{c_cap}] = \sum_{d=1}^{d_{max}} \sum_{\vartheta=1}^{\vartheta_{max}} E[T_{c_d,\vartheta}] \times (1 - \beta_{d,\vartheta}(\beta - 1)|z_{d,\vartheta}) \times T_{max} \quad (5-67)$$

In order to calculate the throughput of group 1 equations (5-65), (5-66) and (5-67) should be substituted into equation (5-24) and then substituting equation (5-24) and (5-8) into (5-65). Substituting (5-64) and (5-63) into (5-60) gives the throughput of group 1 with traffic type 1 with PHY layer effects. The throughput of traffic type 1 can be calculated as shown in (5-68) and the total system throughput can be calculated as shown in (5-69).

$$S_{1_phy} = \sum_{\vartheta=1}^{\vartheta_{max}} S_{1,\vartheta} \quad (5-68)$$

$$S_{phy} = \sum_{d=1}^{d_{max}} S_{d_phy} \quad (5-69)$$

5.7.5 Delay analysis with PHY Effects

In this model all calculations are made using groups. The probability that a particular group 1 within a traffic type 1 station is successful ($P_{1,1_phy}$) in the presence of PHY layer effects can be calculated as in (5-71).

$$P_{1,1_phy} = \frac{P(s_{1,1_phy})}{M_{1,1}} \quad (5-71)$$

The overall average delay for a group 1 with type 1 packet in the case of multirate and PHY layer effects can then be calculated as shown in (5-72).

$$\bar{D}_{1,1_phy} = \frac{E[R] + E[T_{phy}]}{P_{1,1}} \quad (5-72)$$

5.7.6 Results and Discussions

In order to demonstrate the accuracy of our enhanced multirate model, we consider the following two scenarios as shown in Figure 5-16. In the first scenario, two traffic types were considered with 10 stations each. The value of p_1 was set to 0.03 and p_2 was calculated to achieve $S_1=2S_2$. Each traffic type was divided into 2 groups, G11 and G12 for traffic type 1 and G21 G22 for traffic type 2. Stations of all groups transmit at 58.5 Mbit/s. The results show that the throughput of G11=G12=9.6 Mbit/s due to the same p value while the throughput of G21 and G22 is equal to 4.8 Mbit/s, which corresponds to half of the throughput of traffic type 1. In the second scenario, stations of G12 transmit at 39 Mbit/s, stations of G21 transmit 26 Mbit/s and stations of G22 transmit at 6.5 Mbit/s. Figure 5-16 shows that the throughput of G11 stations decreased by 55% compared to the case where all stations in the network transmit at the same data rate. The main effect is due to the stations of G12 as they have the same priority which results in both groups having similar throughput

even though G11 transmits at 58.5Mbits. A similar trend is obtained for G21 and G22 where the throughput of G12 is degraded to the same value as G22's throughput, which is equal to 2.15 Mbit/s. This scenario demonstrates that the anomaly effect is more significant when stations with the same traffic type transmit at a different data rate than the case in our previous model where stations with same traffic type transmit at the same data rate.

Figure 5-17 shows the delay results for the same scenarios and a corresponding trend to the throughput results is obtained. The delay in the G11 group is degraded due to the anomaly issue in the network. The main factor in the delay degradation of G11 comes from stations of G12 and is due to having a similar priority. This scenario clearly demonstrate that when the stations within the same traffic type transmit at different data rates, the stations with higher data rate see their throughput and delay performances degraded to the same performance of stations with lower data rates.

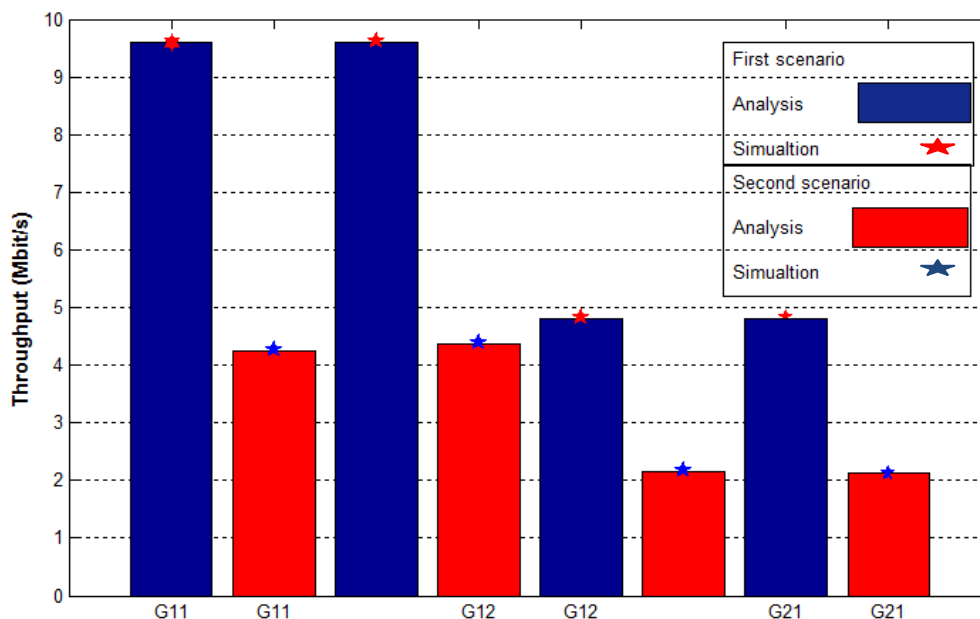


Figure 5-16: Throughput of stations of 2 traffic types with 2 groups each transmitting at different data rates for 802.11n with different priorities and $p_1=0.03$

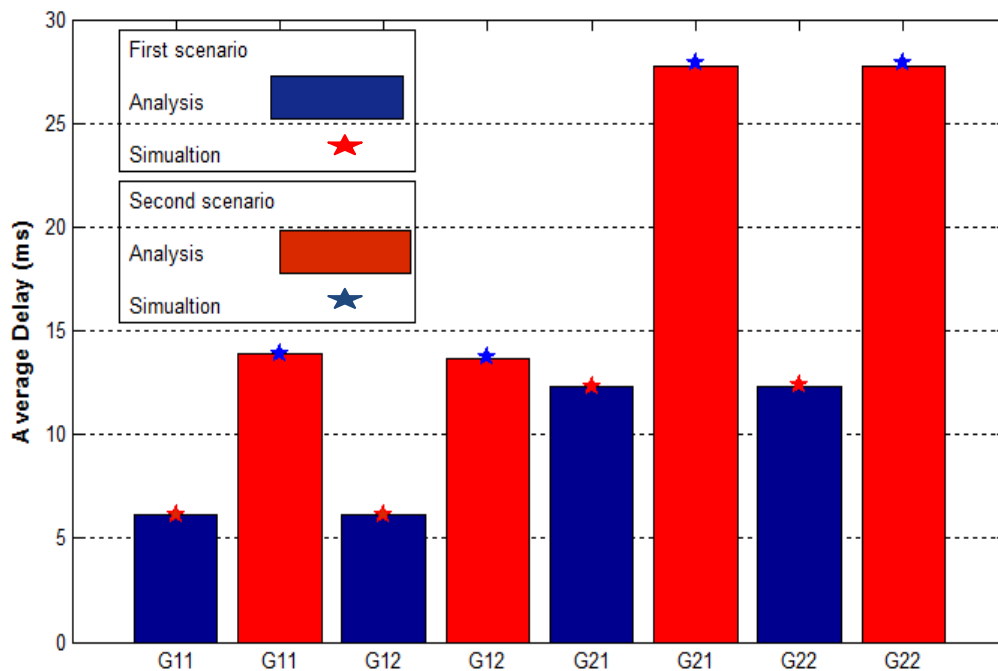


Figure 5-17: Average delay of stations of 2 traffic types with 2 groups each transmitting at different data rates for 802.11n with different priorities and $p_1=0.03$

The following set of results illustrate the PHY layer effects in terms of packet error rates and capture effect when the enhanced model of multirate is considered.

Figure 5-18

shows the total throughput versus number of stations with PHY layer effects. Again four groups (G11, G12, G21 and G22) are used and the throughput ratio is $S_1=2S_2$ with $p_1=0.05$. When the capture effect is included with $z=5$ dB, the throughput is improved by 39 % compared to the case where the capture is not considered. The results also show that the anomaly issue has a significant effect on the throughput performance. By comparing the results of the throughput with capture and the results for single rate even without considering the capture, the total throughput degraded by 49% when the number of stations is 28. Figure 5-19 shows the delay results for the same experiment. Here also the capture improves the

delay performance for traffic types 1 and 2 compared to the case where the capture is not included, a similar trend to that was obtained in the case of the throughput.

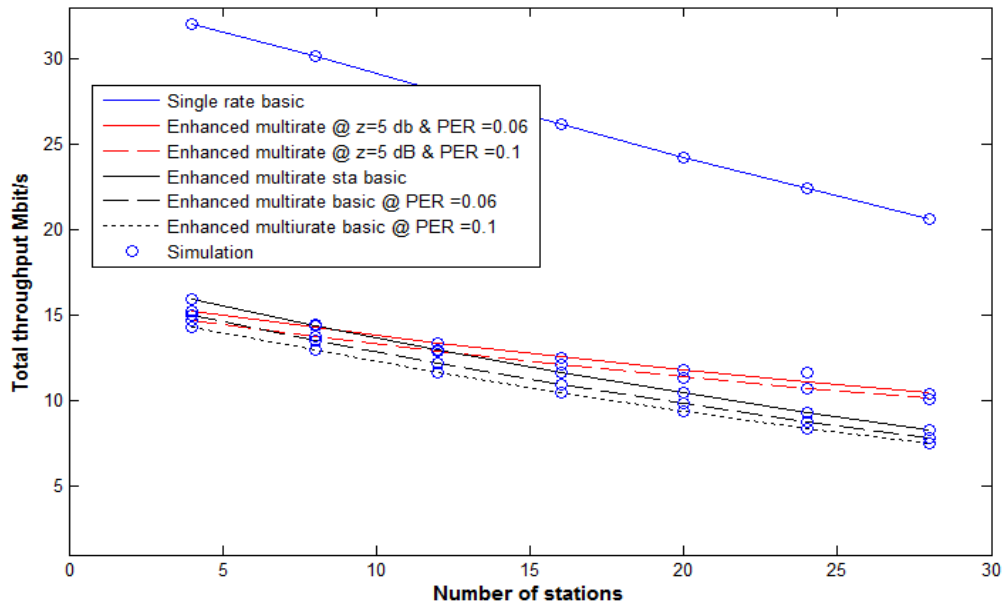


Figure 5-18: Total throughput versus number of stations for 2 traffic types with 2 groups each and $p_1=0.5$, $z=5\text{dB}$ and PER as parameter at different data rates

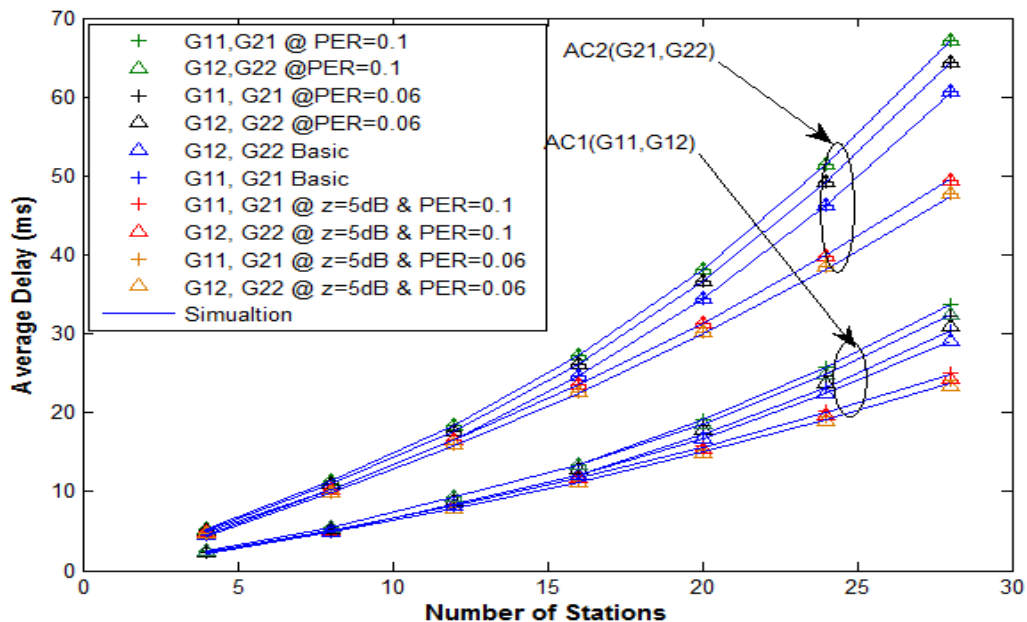


Figure 5-19: Average delay versus number of stations for 2 traffic types with 2 groups each and $p_1=0.5$, $z=5\text{dB}$ and PER as parameter at different data rates

5.7.7 Adaptive Protocol Results for Enhanced Protocol

In this section the adapting protocol is investigated for the same experiment in Figure 5-17. The same two scenarios that were investigated in figure are adopted here to show the effectiveness of the adaptive protocol. Here also, in first scenario (single rate) all stations transmit at 58.5 Mbit/s. In the second scenario (multiarte), stations of G11 transmit at 58.5 Mbit/s, stations of G11 transmit at 39 Mbit/s, stations of G21 transmit 26Mbit/s and stations of G22 transmit at 6.5 Mbit/s. Figure 5-20 shows that the adaptive protocol improves the throughput of G11 and G12 by 59% and 27% respectively compared to the non adaptive protocol. The throughput of G21 is also improved by 11% while the throughput of G22 is degraded by 21% compared to the non-adaptive protocol. The results clearly show that the adaptive protocol improves the throughput performance of groups with high priority and transmit at high data rate. There is a small tradeoff where the low priority groups that transmit at low data rates their throughput is slightly degraded due the adaptation protocol. However, the advantage of the adaptive protocol in terms of improving the high priority stations transmitting at high data rates is significant compared with its disadvantage, which the small degradation of the throughput performance of low priority group which already transmit at low data rate. These results demonstrate the effectiveness of the adaptive protocol for improving the throughput performance of stations with high priory and transmit at high data rate when their throughput performance is affect by low priory station that transit at low data rates.

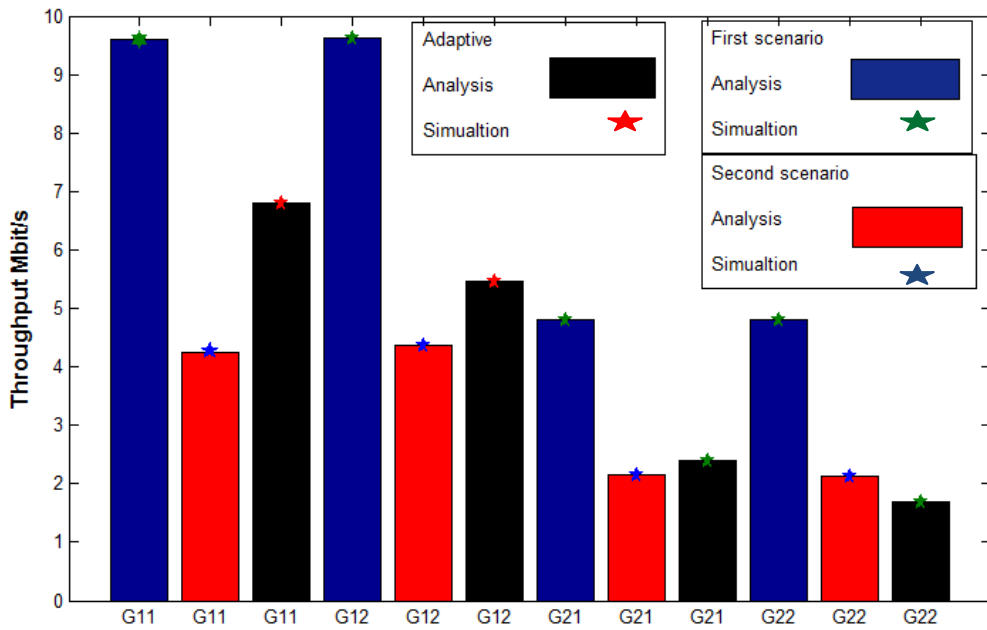


Figure 5-20: Throughput performance of the adaptive protocol for 2 AC with 5 station per group with $p_1=0.03$.

5.8 WLAN Planning

In this set of results, the benefit of the adaptive protocol in network panning is demonstrated. In this case study, two traffic types were considered with p_1 set to 0.03, and p_2 set to provide throughput ratio $S_1:S_2=2:1$. The throughput per user per traffic type, S_{du} , is calculated by $S_{du} = \frac{S_d}{M_d}$ is explained in section 3-7. Number of stations per traffic type is 18 and traffic type 1 stations transmit at 58.5 Mbit/s, while stations of traffic type 2 transmit at 6.5 Mbit/s. The results in Figure 5-21 show that when the non adaptive protocol is adopted, the AP can serve 7 users of traffic type 1 with QoS requirements of 1 Mbit/s, and 7 users of traffic type 2 with QoS requirements of 500kbit/s. For adaptive protocol, the AP can serve 11 users of traffic type 1 with QoS requirements of 1 Mbit/s, and 7 users of traffic type 2 with QoS requirements of 500Kbit/s. In total, when the non adaptive protocol is used the AP can serve

14 users while in the adaptive protocol is adopted the AP can serve 18 users. This is equivalent to a 28% improvement in the capacity of the system meaning fewer APs should be deployed. When the scaling factor is used (i.e. scaling the value of PER before multispeed it with p value), the adaptive protocol improves the number of user that the AP can serve by 35%. These results demonstrate that more efficient network planning can be achieved with the use of the adaptive protocol when the WLAN suffers from the *performance anomaly*.

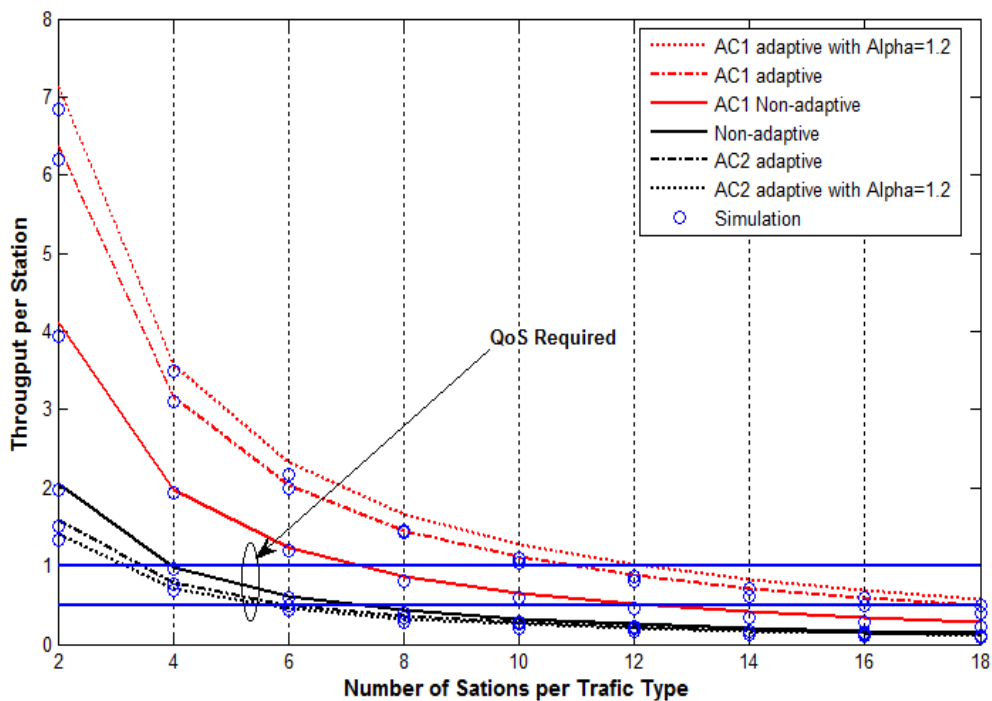


Figure 5-21: Saturated throughput per user as a function of number of user per traffic type with adaptive protocol

5.9 Conclusions

In this chapter, we have developed a new throughput and delay analysis for a QoS differentiated p -persistent CSMA protocol with multirate capability by modifying the model in [56]. However, the previous studies based on Markovian analysis could only access fewer

configurations, limited to a single traffic type. This new analysis is an effective way of modeling 802.11 DCF and EDCA in the case of the *performance anomaly*. The results showed that due to the *performance anomaly*, the throughput performance of stations with a high priority is degraded by 36.4 % even though they transmit at 58 Mbit/s. Results have been produced to validate the analysis by comparing it to the single traffic type model in [71] and through simulations. We have modelled a more practical and realistic scenario by including the PHY layer effects. The results showed that including the capture effect improves the performance by 19.6%. An adaptive p -persistent CSMA protocol is proposed to mitigate the anomaly issue and the results show that this adaptive protocol can improve the system performance by 83% when the scaling factor $\varphi = 1.2$. The model was further enhanced whereby each station in the network can transmit at any data rate regardless of its traffic type. The results of this model showed that when stations with the same traffic type transmit at different data rates the throughput performance and delay are dominated by the stations with lowest data rate. The results demonstrated that when stations transmit at 58.5 Mbit/s their throughput performance is degraded by 55%. Finally, this improved model was modified to include the PHY layer effects in terms of packet error rate and capture. The delay performance is also investigated and the results showed corroborating trends to those obtained in the case of throughput. The results showed that the adaptive protocol improves the network capacity which leads to fewer APs that being deployed. The size of these changes demonstrate the need to model the multirate scenario in order to obtain an accurate characterization of the network performance and more efficient network planning.

Chapter 6

Conclusions and Future work

Due to the high demand for QoS differentiated WLANs, the improvement of the throughput and delay performance for CSMA/CA-based WLANs has become more important than ever. Two main research directions have focused on the improvement and the accuracy of calculating the throughput and delay. The first direction was from the pure MAC protocol perspective. The second direction was from the PHY/MAC perspective, where the PHY layer effects are included in the analytical models for more accurate evaluation of the throughput and delay performance of WLANs. This direction was one of our main topics in this thesis. After Bianchi's landmark work in [5], where he provided an analysis for the saturated throughput of the basic 802.11 protocol based on a two dimensional Markov model of the MAC layer, developing an accurate closed form solution of the throughput and delay has received significant attention by researchers due its importance in network planning and design. In fact, a large number of works have investigated almost every aspect of the behaviour of DCF under different traffic loads and channel transmission conditions. In a wireless channel, a packet may not be received correctly for two main reasons. Firstly, when the SNR value is too low this makes a single packet experience bit errors after decoding at the receiver. Secondly, when there is a collision between two or more packets from different stations, the SIR typically degrades significantly and packets are destroyed. However, in wireless networks, a packet collision does not necessarily mean all the simultaneously

transmitted packets are being lost. One of these packets can be received correctly if the received power ratio is greater than a certain value, called the SIR threshold. This phenomenon is called the capture effect and has a significant impact on the network capacity. The other key parameters that determine the capacity is the minimum association rate between the AP and the stations. Stations transmitting at low data rates occupy the channel for a longer time, which causes the overall system throughput to be significantly reduced. Therefore, the throughput of a station that transmits at a high data rate may be degraded to the throughput value of a station that transmits at the lowest data rate. This phenomenon is known as the *performance anomaly*. In this thesis the first aim was to develop more accurate models to calculate the throughput and average delay of a QoS differentiated p -persistent CSMA protocol. A summary and discussion of the main outcomes obtained throughout the thesis is presented. The areas of novelty and originality developed from this research are also stated. Finally, the areas of work that require further investigation are discussed.

6.1 Summary and Discussion

In this thesis, an analytical expression for the saturated throughput/delay of the QoS differentiated p -persistent CSMA protocol in the presence of a multipath Rayleigh fading channel was developed. This analysis validates the accuracy of our developed simulation model of the PHY/MAC cross-layer. This approach offers an accurate characterisation of the performance of a QoS differentiated systems such as 802.11e EDCA in a more realistic environment, with less complexity compared to the Markovian analytical models. In order to show the effectiveness of our model and the benefit from developing a more accurate model, many scenarios were investigated. The results showed that benefit from the capture effect depends on the number of stations in the network, capture threshold and the number of traffic types in the system. The results demonstrated that as the number of stations increase the throughput and delay performance are improved, for example, when the number of stations is

36 the throughput is increased by 47% with threshold $z=2$ dB compared to the basic case. The delay results demonstrate that without capture and p_1 between 0.01 and 0.02 minimises delay across all ACs and maximises throughput. However, this gives a restrictive range on p_1 when managing the overall network loads in differential mode. By including capture effect, the operating range of p_1 is seen to increase from 0.01 to 0.05 in order to keep delays across ACs low and the throughput high. This is important for the lower priority traffic types which are more sensitive to the capture effect. It can be concluded that including the capture effect in the analysis results in accurate estimation of the capacity of the system. Compared to the case where the capture is excluded, there is an increase of 33% in network capacity which means fewer APs should be deployed. More efficient network planning can be achieved with the use of more accurate throughput/delay calculations and excluding the capture effect from the analysis underestimates the throughput/delay performance of the network.

In chapter 4, a cross layer approach for the non-saturated throughput/delay performance was developed. A closed form analytical model was presented to calculate the non-saturated throughput and delay of a QoS differentiated p -persistent CSMA protocol in fading and shadowing channels. The developed model expresses the throughput/delay performance as a function of the number of stations, packet error rates and capture threshold. This was developed from on the analysis of the saturation case in chapter 3 by allowing the stations to be non-saturated. The offered load of the stations was varied, enabling them to have heterogeneous loads as well as heterogeneous priorities. The results demonstrated that when the offered load, G , is less than 1 there is no noticeable benefit from including the capture effect and the packet error rates have very little effect on the throughput performance. This is due to the low chance of collisions, as there is not much traffic in the network. As G increases, the benefit from the capture effect becomes more pronounced and the packet error rate has a clear degrading effect on the throughput performance. The results also showed that

when comparing the performance of this new model with PHY layer effects to the basic model, the total throughput is increased by 28 % at $G=10$ and $\text{SNR} > 12.5$ dB, while at $\text{SNR} = 7$ dB the total throughput is only improved by 7% compared to the basic model. The delay results illustrated that including the capture effect in the analysis results in reducing the delay while the packet error rates increase the delay. An adaptive p -persistent CSMA protocol with heterogeneous traffic that mitigates the throughput degradation due to the packet error rates and improves the high priority access categories at low offered load values was developed.

In chapter 5, a new saturated throughput/delay model for a QoS differentiated p -persistent CSMA protocol with multirate capability was developed. This new analysis is an effective way of modelling 802.11 DCF and EDCA in the case of the *performance anomaly*. The results showed that due to the *performance anomaly*, the throughput performance of stations with a high priority is significantly degraded even though they transmit at high data rates. The model was extended to a more practical and realistic model where the PHY layer effects are incorporated. The results demonstrated that when the capture effect is taken into account the throughput is increased by 26% when the number of stations is equal to 28 with the same data rates, whereas in the multirate model including the capture effect in the analysis can only increase the throughput by 19%. This is because in the case of multirate model, the stations with low data rates take a long time to transmit which reduces the probability of collision.

An adaptive p -persistent CSMA protocol was proposed to mitigate the anomaly issue and the results show that this adaptive protocol can improve the system performance by 83% when the scaling factor $\alpha = 1.2$. The delay performance was also investigated and the results showed similar trends to those obtained for the throughput performance. The model has then been improved to a more general and realistic model, where each station in the network can transmit at any data rate regardless of its traffic type. The results of this model showed that when stations with the same traffic type transmit at different data rates, the throughput

performance and delay are dominated by the stations with the lower data rates. The results demonstrated that when stations transmit at 58.5 Mbit/s their throughput performance is degraded by 55%. These results clearly demonstrate the need for accurate modelling of the throughput/delay of a QoS differentiated p -persistent CSMA protocol. The adaptive protocol results showed that the anomaly issue can be mitigated by adjusting the p value according to the channel conditions. The results also demonstrated that the adaptive protocol enhances the network capacity which results in efficient network planning. The results showed that the capacity of the network is improved by 35% when the adaptive protocol is applied.

6.2 Areas of Novelty and Originality

The primary goal of this research work was to develop more accurate models of the throughput and delay of the 802.11e EDCA protocol using the p -persistent CSMA protocol and can be applied. The throughput and delay are the most important elements for efficient WLAN planning and design. The work in this thesis shows the QoS differentiated p -persistent CSMA can be effectively used to mitigate the anomaly performance of WLANs. To conclude this chapter, the areas of original work within this research are listed below:

1. The straightforward time-domain analysis of the new PHY/MAC cross-layer approach, which calculates the saturated throughput/delay of p -persistent CSMA allows for accurate characterisation of the network performance in a practical environment. This approach can be applied to systems with a QoS differentiation such as 802.11e EDCA networks by use of a fixed window size with less complexity than the Markovian models.
2. The new non-saturated form of p -persistent CSMA analysis with PHY layer effects enables the accurate evaluation of the throughput/delay performance of a non-

saturated network with heterogeneous priorities and heterogeneous loads accurately in a realistic environment.

3. The new saturated form of a QoS differentiated p -persistent CSMA analysis with multirate capability allows for evaluating the *performance anomaly* of WLANs.
4. An adaptive p -persistent CSMA protocol was introduced as a solution to the anomaly issue in the QoS differentiated WLANs. The protocol effectively mitigated the anomaly issue and improves the performance of the high priority traffic type.

6.3 Final conclusions

The work presented in this thesis shows that the PHY layer effects (packet error rates and capture effect) have significant impact on the throughput/delay performance of WLANs. Since the throughput and delay are main factors in the WLAN planning and design, this research develops PHY/MAC models that accurately calculate the throughput/delay of the QoS differentiated p -persistent CSMA protocol which can be applied to 802.11e. The *anomaly performance* has also a significant effect on the WLANs performance which affects the calculation of the network capacity during the network planning phase, this research develops a QoS differentiated p -persistent CSMA with multirate capability that can be used to characterises the *performance anomaly* of 802.11DCF and 802.11e EDCA. An adaptive p -persistent CSMA protocol is developed to mitigate the anomaly issue in WLANs. The developed models can be applied to the QoS differentiated systems such as 80.11e EDCA with less complexity than Markovain models. In our research, for PHY layer standards we used the IEEE 802.11a/g/n and the capture model was based on the Rayleigh fading channel, however, our models can be used with any PHY layer standard and any other capture models that may developed in the future.

6.4 Recommendations for Future Work

This section outlines some new areas of research for future work based on our finding in this thesis.

1. The thesis has aimed to analyse and characterise saturated throughput/delay of p -persistent CSMA with PHY layer effect and can be applied to 802.11e EDCA. The next logical stage would be to include the other features of the 802.11e EDCA. This includes internal collision resolution, transmit opportunity, retry limits and arbitration interframe spaces.
2. In WLAN planning, the process estimates the optimum number of APs and their placement. Many factors should be taken into account when estimating the number of APs. The main factor is the QoS required and average throughput of the network. These algorithms which are used for network planning estimate the throughput based on the MAC protocol only, without including the PHY layer effects. The next logical stage of our PHY/MAC cross-layer approaches is to be used in network planning algorithms, which will lead to more accurate estimation of the number of APs required and ensure the QoS for the users.
3. The multirate capability was only modelled for the saturated case. Modelling the multirate capability of a QoS differentiated p -persistent CSMA for the non-saturated case is a challenging task and has never been done before in any study. The thesis has aimed to analyse and characterise the non-saturated throughput/delay of p -persistent CSMA with PHY layer effect. The next logical stage would be to include the other features of the 802.11e EDCA. This includes internal collision resolution, transmit opportunity, retry limits and arbitration interframe spaces.
4. The analysis in this thesis has been validated by realistic simulations. Since our models included the PHY layer effects, these findings should be tested in a test bed

and introduce the p -persistent CSMA as an alternative to the EDCA. The adaptive protocol should also be tested in a test bed to show its effectiveness in mitigating the anomaly issue.

5. The analysis in this thesis models the channel access on the basis of the head of the line behaviour. The next logical stage would be use this analysis to develop queuing model for p -persistent CSMA protocol with PHY layer effects for both saturated and non-saturated cases.
6. Video transmission is a very challenging task over WLANs. The next step could be to investigate the video transmission over WLANs when there is an anomaly issue and investigate if our adaptive protocol could improve the video quality.

Appendix A

1- S. Abukharis, R. Makenzie and T. O'Farrell, "Improving QoS of video Transmitted over 802.11 WLANs using Fram Aggregation" in proc. Of IET London Communications Symposium 2009, September 2009.

2- S. Abukharis, R. MacKenzie and T. O'Farrell," Throughput and Delay Analysis for a Differentiated p -Persistent CSMA Protocol with the Capture Effect" VTC 2011. IEEE international conference, 15-18 May 2011, Budapest, Hungary.

3- S. Abukharis and T. O'Farrell," A new Adaptive Differentiated P -Persistent CSMA Protocol that reduces the effect of the transmission errors on the system Throughput Performance" in Proc. IWCMC 2011, IEEE international conference 4-8 Jul 2011.

4- Salim Abukharis and T. O'Farrell, " Throughput and Delay Analysis of a QoS Differentiated p -persistent CSMA Protocol with Multirate " VTC -2012 IEEE international conference, 3-6 September 2012 Québec City, Canada.

References

- [1] "IEEE Std 802.11e -2005, Part 11: Wireless LAN Medium Access Control (MAC) and Physical Layer (PHY) specifications Amendment 8: Medium Access control (MAC) Quality of Service Enhancements [S], ," 11 November 2005.
- [2] "Wireless LAN Medium Access Control (MAC) and Physical Layer (PHY) specifications," *ANSI/IEEE Std 802.11: 1999(E) Part 1, ISO/IEC 8802-11*, 1999.
- [3] ABIresearch. (2012). Available: <http://www.abiresearch.com/press/wi-fi-enabled-device-shipments-will-exceed-15-billion>
- [4] A. Raniwala and T.-c. Chiueh, "Coverage and capacity issues in enterprise wireless LAN deployment," Technical Report TR166, State University of New York, Stony Brook, NY, 2004.
- [5] G. Bianchi, "Performance analysis of the IEEE 802.11 distributed coordination function," *Selected Areas in Communications, IEEE Journal on*, vol. 18, pp. 535-547, 2000.
- [6] "Wireless LAN Medium Access Control (MAC) and Physical Layer (PHY) specifications. Amendment 4: Further Higher Data rate Extension in the 2.4 GHz band, Standard, IEEE 802.11g Part 11, 2003
- [7] "Wireless LAN Medium Access Control (MAC) and Physical Layer (PHY) specifications," *Part 11: IEEE P802.11n™/D9.0*, March, 2009 2009.
- [8] A. S. Tanenbaum, *Computer Networks*, 4 ed. New Jersey: Prentice Hall, 2003.
- [9] "Wireless LAN Medium Access Control (MAC) and Physical Layer (PHY) specifications, High-speed Physical Layer in the 5GHz Band, Supplement to IEEE 802.11 Standard, ," *IEEE 802.11a, Part 11*, September 1999.
- [10] R. P. Richard Van Nee, *OFDM For Wireless Multimedia Communications*, 1st ed. Boston, London: Artech House, 2000.
- [11] R. Prasad, *OFDM For Wireless Communications Systems* 1st ed. Boston, London: Artech House, Inc., 2004.
- [12] W. Y. Zou and Y. Wu, "COFDM: an overview," *Broadcasting, IEEE Transactions on*, vol. 41, pp. 1-8, 1995.
- [13] M. Russell and G. L. Stuber, "Interchannel interference analysis of OFDM in a mobile environment," 1995, p. 820.
- [14] B. W. J. Emmanouel C. Ifeachor, *Digital Signal Processing A practical Approach*, 2nd ed.: Prentice Hall, 2002.
- [15] S. Weinstein and P. Ebert, "Data Transmission by Frequency-Division Multiplexing Using the Discrete Fourier Transform," *Communications, IEEE Transactions on [legacy, pre - 1988]*, vol. 19, p. 628, 1971.
- [16] http://grouper.ieee.org/groups/802/11/Reports/tgn_update.htm.
- [17] S. M. Alamouti, "A simple transmit diversity technique for wireless communications," *Selected Areas in Communications, IEEE Journal on*, vol. 16, pp. 1451-1458, 1998.
- [18] I. Baig, V. Jeoti, and M. Drieberg, "A ZCMT precoding based STBC MIMO-OFDM system with reduced PAPR," in *National Postgraduate Conference (NPC), 2011*, 2011, pp. 1-5.

- [19] "Wireless LAN Medium Access Control (MAC) and Physical Layer (PHY) specifications Amendment 8:Medium Access Control (MAC) Quality of Service Enhancements," *IEEE Std. 802.11e* 2005 2005.
- [20] L. Kleinrock and F. Tobagi, "Packet Switching in Radio Channels: Part I--Carrier Sense Multiple-Access Modes and Their Throughput-Delay Characteristics," *Communications, IEEE Transactions on*, vol. 23, pp. 1400-1416, 1975.
- [21] H. Takagi and L. Kleinrock, "Throughput Analysis for Persistent CSMA Systems," *Communications, IEEE Transactions on*, vol. 33, pp. 627-638, 1985.
- [22] H. Dajiang and C. Q. Shen, "Simulation study of IEEE 802.11e EDCF," in *Vehicular Technology Conference, 2003. VTC 2003-Spring. The 57th IEEE Semiannual*, 2003, pp. 685-689 vol.1.
- [23] Q. Ni, "Performance analysis and enhancements for IEEE 802.11e wireless networks," *Network, IEEE*, vol. 19, pp. 21-27, 2005.
- [24] G. Bianchi, I. Tinnirello, and L. Scalia, "Understanding 802.11e contention-based prioritization mechanisms and their coexistence with legacy 802.11 stations," *Network, IEEE*, vol. 19, pp. 28-34, 2005.
- [25] K. Jae Hyun and L. Jong Kyu, "Capture effects of wireless CSMA/CA protocols in Rayleigh and shadow fading channels," *Vehicular Technology, IEEE Transactions on*, vol. 48, pp. 1277-1286, 1999.
- [26] Z. Q.-A. LI XIAOLONG, "Performance Analysis of the IEEE 802.11 MAC Protocol over a WLAN with Capture Effect," *Transactions of Information Processing Society of Japan*, vol. 46, pp. 2607-2613, 2005.
- [27] C. van der Plas and J. P. M. G. Linnartz, "Stability of mobile slotted ALOHA network with Rayleigh fading, shadowing, and near-far effect," *Vehicular Technology, IEEE Transactions on*, vol. 39, pp. 359-366, 1990.
- [28] Q. Ni, T. Li, T. Turletti, and Y. Xiao, "Saturation throughput analysis of error-prone 802.11 wireless networks," *Wireless Communications and Mobile Computing*, vol. 5, pp. 945-956, 2005.
- [29] J. Yin, "The Analysis of Perfomance of IEEE 802.11 MAC Protocol Using Markov Chain," *International Journal of Computer Science and Network Security*, vol. 7, pp. 27-37, December 2007 2007.
- [30] Q. Daji and C. Sunghyun, "Goodput enhancement of IEEE 802.11a wireless LAN via link adaptation," in *Communications, 2001. ICC 2001. IEEE International Conference on*, 2001, pp. 1995-2000 vol.7.
- [31] Q. Daji, C. Sunghyun, and K. G. Shin, "Goodput analysis and link adaptation for IEEE 802.11a wireless LANs," *Mobile Computing, IEEE Transactions on*, vol. 1, pp. 278-292, 2002.
- [32] J. P. Pavon and C. Sunghyun, "Link adaptation strategy for IEEE 802.11 WLAN via received signal strength measurement," in *Communications, 2003. ICC '03. IEEE International Conference on*, 2003, pp. 1108-1113 vol.2.
- [33] L. An-Chih, L. Ting-Yu, and T. Ching-Yi, "ARC: Joint Adaptation of Link Rate and Contention Window for IEEE 802.11 Multi-rate Wireless Networks," in *Sensor, Mesh and Ad Hoc Communications and Networks, 2009. SECON '09. 6th Annual IEEE Communications Society Conference on*, 2009, pp. 1-9.
- [34] L. Ting-Yu, T. Ching-Yi, and W. Kun-Ru, "EARC: Enhanced Adaptation of Link Rate and Contention Window for IEEE 802.11 Multi-Rate Wireless Networks," *Communications, IEEE Transactions on*, vol. 60, pp. 2623-2634, 2012.
- [35] M. Heusse, F. Rousseau, G. Berger-Sabbatel, and A. Duda, "Performance anomaly of 802.11b," in *INFOCOM 2003. Twenty-Second Annual Joint Conference of the IEEE Computer and Communications. IEEE Societies*, 2003, pp. 836-843 vol.2.

- [36] L. Bononi, M. Conti, and L. Donatiello, "Design and Performance Evaluation of a Distributed Contention Control (DCC) Mechanism for IEEE 802.11 Wireless Local Area Networks," *Journal of Parallel and Distributed Computing*, vol. 60, pp. 407-430, 2000.
- [37] F. Cali, M. Conti, and E. Gregori, "IEEE 802.11 protocol: design and performance evaluation of an adaptive backoff mechanism," *Selected Areas in Communications, IEEE Journal on*, vol. 18, pp. 1774-1786, 2000.
- [38] K. Younggoo, F. Yuguang, and H. Latchman, "Fast collision resolution (FCR) MAC algorithm for wireless local area networks," in *Global Telecommunications Conference, 2002. GLOBECOM '02. IEEE*, 2002, pp. 2250-2254 vol.3.
- [39] X. Yang, "Concatenation and piggyback mechanisms for the IEEE 802.11 MAC," in *Wireless Communications and Networking Conference, 2004. WCNC. 2004 IEEE*, 2004, pp. 1642-1647 Vol.3.
- [40] Z. Hadzi-Velkov and B. Spasenovski, "Saturation throughput - delay analysis of IEEE 802.11 DCF in fading channel," in *Communications, 2003. ICC '03. IEEE International Conference on*, 2003, pp. 121-126 vol.1.
- [41] P. Chatzimisios, A. C. Boucouvalas, and V. Vitsas, "Performance analysis of IEEE 802.11 DCF in presence of transmission errors," in *Communications, 2004 IEEE International Conference on*, 2004, pp. 3854-3858 Vol.7.
- [42] H. Jianhua, T. Zuoyin, Y. Zongkai, C. Wenqing, and C. Chun Tung, "Performance evaluation of distributed access scheme in error-prone channel," in *TENCON '02. Proceedings. 2002 IEEE Region 10 Conference on Computers, Communications, Control and Power Engineering*, 2002, pp. 1142-1145 vol.2.
- [43] Z. Yu, L. Kejie, W. Dapeng, and F. Yuguang, "Performance Analysis of IEEE 802.11 DCF in Imperfect Channels," *Vehicular Technology, IEEE Transactions on*, vol. 55, pp. 1648-1656, 2006.
- [44] X. Yang, "Performance analysis of priority schemes for IEEE 802.11 and IEEE 802.11e wireless LANs," *Wireless Communications, IEEE Transactions on*, vol. 4, pp. 1506-1515, 2005.
- [45] H. Ching-Ling and L. Wanjiun, "Throughput and delay performance of IEEE 802.11e enhanced distributed channel access (EDCA) under saturation condition," *Wireless Communications, IEEE Transactions on*, vol. 6, pp. 136-145, 2007.
- [46] H. Jia, M. Geyong, M. E. Woodward, and J. Weijia, "A Comprehensive Analytical Model for IEEE 802.11e QoS Differentiation Schemes under Unsaturated Traffic Loads," in *Communications, 2008. ICC '08. IEEE International Conference on*, 2008, pp. 241-245.
- [47] N. C. Taher, Y. G. Doudane, and B. El Hassan, "A complete and accurate analytical model for 802.11e EDCA under saturation conditions," in *Computer Systems and Applications, 2009. AICCSA 2009. IEEE/ACS International Conference on*, 2009, pp. 800-807.
- [48] J. del Prado Pavon and S. N. Shankar, "Impact of frame size, number of stations and mobility on the throughput performance of IEEE 802.11e," in *Wireless Communications and Networking Conference, 2004. WCNC. 2004 IEEE*, 2004, pp. 789-795 Vol.2.
- [49] F. Peng, B. Peng, and D. Qian, "Performance analysis of IEEE 802.11e enhanced distributed channel access," *Communications, IET*, vol. 4, pp. 728-738, 2010.
- [50] A. Gkelias, M. Dohler, V. Friderikos, and A. H. Aghvami, "Average packet delay of CSMA/CA with finite user population," *Communications Letters, IEEE*, vol. 9, pp. 273-275, 2005.

- [51] P. Chatzimisios, A. C. Boucouvalas, and V. Vitsas, "Influence of channel BER on IEEE 802.11 DCF," *Electronics Letters*, vol. 39, pp. 1687-9, 2003.
- [52] L. Xiaolong and Z. Qing-An, "Influence of Bit Error Rate on the Performance of IEEE 802.11 MAC Protocol," in *Wireless Communications and Networking Conference, 2007.WCNC 2007. IEEE*, 2007, pp. 367-372.
- [53] L. Xiaolong and Z. Qing-An, "Capture Effect in the IEEE 802.11 WLANs with Rayleigh Fading, Shadowing, and Path Loss," in *Wireless and Mobile Computing, Networking and Communications, 2006. (WiMob'2006). IEEE International Conference on*, 2006, pp. 110-115.
- [54] F. Daneshgaran, M. Laddomada, F. Mesiti, M. Mondin, and M. Zanolò, "Saturation throughput analysis of IEEE 802.11 in the presence of non ideal transmission channel and capture effects," *Communications, IEEE Transactions on*, vol. 56, pp. 1178-1188, 2008.
- [55] M. Geyong, H. Jia, J. Weijia, and M. E. Woodward, "Performance Analysis of the TXOP Scheme in IEEE 802.11e WLANs with Bursty Error Channels," in *Wireless Communications and Networking Conference, 2009. WCNC 2009. IEEE*, 2009, pp. 1-6.
- [56] R. MacKenzie and T. O'Farrell, "Throughput Analysis of a p-Persistent CSMA Protocol with QoS Differentiation for Multiple Traffic Types," in *Communications, 2008. ICC '08. IEEE International Conference on*, 2008, pp. 3220-3224.
- [57] R. MacKenzie and T. O'Farrell, "Achieving service differentiation in IEEE 802.11e enhanced distributed channel access systems," *Communications, IET*, vol. 6, pp. 740-750, 2012.
- [58] G. R. Cantieni, Q. Ni, C. Barakat, and T. Turletti, "Performance analysis under finite load and improvements for multirate 802.11" *Computer Communications.*, vol. 28, pp. 1095-1109, 2005.
- [59] A. N. Zaki and M. T. El-Hadidi, "Throughput analysis of IEEE 802.11 DCF under finite load traffic," in *Control, Communications and Signal Processing, 2004. First International Symposium on*, 2004, pp. 535-538.
- [60] K. Duffy, D. Malone, and D. J. Leith, "Modeling the 802.11 distributed coordination function in non-saturated conditions," *Communications Letters, IEEE*, vol. 9, pp. 715-717, 2005.
- [61] M. David, D. Ken, and L. Doug, "Modeling the 802.11 Distributed Coordination Function in Nonsaturated Heterogeneous Conditions," *Networking, IEEE/ACM Transactions on*, vol. 15, pp. 159-172, 2007.
- [62] F. Daneshgaran, M. Laddomada, F. Mesiti, and M. Mondin, "On the Linear Behaviour of the Throughput of IEEE 802.11 DCF in Non-Saturated Conditions," *Communications Letters, IEEE*, vol. 11, pp. 856-858, 2007.
- [63] F. Daneshgaran, M. Laddomada, F. Mesiti, and M. Mondin, "Unsaturated Throughput Analysis of IEEE 802.11 in Presence of Non Ideal Transmission Channel and Capture Effects," *Wireless Communications, IEEE Transactions on*, vol. 7, pp. 1276-1286, 2008.
- [64] P. E. Engelstad and O. N. Osterbo, "Delay and Throughput Analysis of IEEE 802.11e EDCA with Starvation Prediction," in *Local Computer Networks, 2005. 30th Anniversary. The IEEE Conference on*, 2005, pp. 647-655.
- [65] P. E. Engelstad and O. N. Osterbo, "Differentiation of Downlink 802.11e Traffic in the Virtual Collision Handler," presented at the Proceedings of the The IEEE Conference on Local Computer Networks 30th Anniversary, 2005.
- [66] H. Aiping, S. Lele, L. Jing, and T. Tonglan, "Modeling and Performance Evaluation of IEEE 802.11e EDCA in Error-Prone Channel Conditions," in *Global*

- Telecommunications Conference, 2007. GLOBECOM '07. IEEE, 2007, pp. 1344-1348.*
- [67] O. Abu-sharkh and A. Tewfik, "Toward accurate modeling of the IEEE 802.11e EDCA under finite load and error-prone channel," *Wireless Communications, IEEE Transactions on*, vol. 7, pp. 2560-2570, 2008.
- [68] W. Jyh-Horng, W. Chien-Erh, and C. Chiung-Hsing, "The performance study of IEEE 802.11E EDCF in channel error environments," in *Broadband Multimedia Systems and Broadcasting (BMSB), 2010 IEEE International Symposium on*, 2010, pp. 1-5.
- [69] J.-H. Wen and C.-E. Weng, "The performances study of IEEE 802.11e to support QoS in channel error environment," *Wireless Communications and Mobile Computing*, pp. n/a-n/a, 2011.
- [70] R. MacKenzie and T. O'Farrell, "Throughput and Delay Analysis for p-Persistent CSMA with Heterogeneous Traffic," *Communications, IEEE Transactions on*, vol. 58, pp. 2881-2891, 2010.
- [71] Y. Duck-Yong, L. Tae-Jin, J. Kyunghun, C. Jin-Bong, and C. Sunghyun, "Performance enhancement of multirate IEEE 802.11 WLANs with geographically scattered stations," *Mobile Computing, IEEE Transactions on*, vol. 5, pp. 906-919, 2006.
- [72] M. Ergen and P. Varaiya, "Formulation of Distributed Coordination Function of IEEE 802.11 for Asynchronous Networks: Mixed Data Rate and Packet Size," *Vehicular Technology, IEEE Transactions on*, vol. 57, pp. 436-447, 2008.
- [73] J. Byoung Hoon, K. Seong Joon, J. Hu, H. Ho Young, C. Jo Woon, and S. Dan Keun, "Performance Improvement of Error-Prone Multi-Rate WLANs through Adjustment of Access/Frame Parameters," in *Communications, 2009. ICC '09. IEEE International Conference on*, 2009, pp. 1-6.
- [74] K. Yu-Liang, L. Kun-Wei, L. Frank Yeong-Sung, W. Yean-Fu, W. Eric Hsiao-Kuang, and C. Gen-Huey, "Multi-rate throughput optimization for wireless local area network anomaly problem," in *Broadband Networks, 2005. BroadNets 2005. 2nd International Conference on*, 2005, pp. 591-601 Vol. 1.
- [75] T. Joshi, A. Mukherjee, Y. Younghwan, and D. P. Agrawal, "Airtime Fairness for IEEE 802.11 Multirate Networks," *Mobile Computing, IEEE Transactions on*, vol. 7, pp. 513-527, 2008.
- [76] H. Chih-Wei, M. Loiacono, J. Rosca, and H. Jenq-Neng, "Airtime Fair Distributed Cross-Layer Congestion Control for Real-Time Video Over WLAN," *Circuits and Systems for Video Technology, IEEE Transactions on*, vol. 19, pp. 1158-1168, 2009.
- [77] F. Daneshgaran, M. Laddomada, F. Mesiti, and M. Mondin, "On the Throughput Allocation for Proportional Fairness in Multirate IEEE 802.11 DCF," in *Consumer Communications and Networking Conference, 2009. CCNC 2009. 6th IEEE*, 2009, pp. 1-5.
- [78] K. Yu-Liang, L. Kun-Wei, F. Y. S. Lin, W. Yean-Fu, E. H. K. Wu, and C. Gen-Huey, "Multirate Throughput Optimization With Fairness Constraints in Wireless Local Area Networks," *Vehicular Technology, IEEE Transactions on*, vol. 58, pp. 2417-2425, 2009.
- [79] F. Daneshgaran, M. Laddomada, F. Mesiti, and M. Mondin, "Modelling and Analysis of the Distributed Coordination Function of IEEE 802.11 with Multirate Capability," in *Wireless Communications and Networking Conference, 2008. WCNC 2008. IEEE*, 2008, pp. 1344-1349.
- [80] M. Laddomada, F. Mesiti, M. Mondin, and F. Daneshgaran, "On the throughput performance of multirate IEEE 802.11 networks with variable-loaded stations:

- analysis, modeling, and a novel proportional fairness criterion," *Wireless Communications, IEEE Transactions on*, vol. 9, pp. 1594-1607, 2010.
- [81] K. Hyogon, Y. Sangki, K. Inhye, and B. Saewoong, "Resolving 802.11 performance anomalies through QoS differentiation," *Communications Letters, IEEE*, vol. 9, pp. 655-657, 2005.
- [82] L. Hao-Ming, N. K. Chilamkurti, S. Zeadally, and K. Chih-Heng, "QoS Support over IEEE 802.11e in Multirate Networks," in *Wireless Pervasive Computing, 2009. ISWPC 2009. 4th International Symposium on*, 2009, pp. 1-5.
- [83] M. A. a. I. A. Stgun, *Handbook of Mathematical Functions*. Newyork :Dover, 1965.
- [84] H. Jie and M. Devetsikiotis, "Designing improved MAC packet schedulers for 802.11e WLAN," in *Global Telecommunications Conference, 2003. GLOBECOM '03. IEEE*, 2003, pp. 184-189 Vol.1.
- [85] R. MacKenzie and T. O'Farrell, "Achieving service differentiation in 802.11e WLANs using persistent CSMA throughput/delay analysis," presented at the London Communications Symposium, LCS, London, 2009.
- [86] G. Bianchi, L. Fratta, and M. Oliveri, "Performance evaluation and enhancement of the CSMA/CA MAC protocol for 802.11 wireless LANs," in *Personal, Indoor and Mobile Radio Communications, 1996. PIMRC'96., Seventh IEEE International Symposium on*, 1996, pp. 392-396 vol.2.
- [87] L. Jia-Liang, K. Jaffres-Runser, J. M. Gorce, and F. Valois, "Indoor wLAN Planning with a QoS constraint based on a Markovian Performance Evaluation Model," in *Wireless and Mobile Computing, Networking and Communications, 2006. (WiMob'2006). IEEE International Conference on*, 2006, pp. 152-158.